

UCSF

UC San Francisco Electronic Theses and Dissertations

Title

Nano Technology Approaches for Cell Based Type 1 Diabetes Therapeutics

Permalink

<https://escholarship.org/uc/item/7p3448gt>

Author

Nyitray, Crystal

Publication Date

2015

Peer reviewed|Thesis/dissertation

Nano Technology Approaches for Cell Based Type 1 Diabetes Therapeutics

By
Crystal Evie Nyitray

DISSERTATION

Submitted in partial satisfaction of the requirements for the degree of

DOCTOR OF PHILOSOPHY

In

Chemistry and Chemical Biology

In the

GRADUATE DIVISION

Of the

UNIVERSITY OF CALIFORNIA, SAN FRANCISCO

Copyright 2015

By

Crystal Evie Nyitray

Dedication

Go to the places that scare you.

-Pema Chodron

To my family and friends, Na zdraví

Acknowledgements

Here I would like to acknowledge both the Suns and Moons who inspired and grounded my PhD.

Firstly I would like to thank my PhD advisor Dr. Tejal Desai for her guidance and mentorship throughout my career. Thank you for believing in me and my science. Tejal said yes to a lot of my crazy ideas, both scientific and professional and I would like to especially thank her for giving me the freedom to explore my ideas and tailor my experience.

I would also like to thank my committee members Dr. Michael German and Dr. Zev Gartner for their insightful feedback and support. It is an incredible privilege to work with and consult the leading experts in the field. I am incredibly grateful for having advisors who were always supportive of my scientific and professional development. I would also like to acknowledge honorary committee members Dr. Bo Huang, who provided big picture feedback. And Dr. Sue Miller, her mentorship and guidance both grounded and inspired my belief in the academic system.

Beyond my mentors at UCSF, I would also like to thank Dr. Sylvaine Cases and Dr. Isaac Veinbergs for their mentorship. Their belief in my ability was a key motivator for my development and success. I would also like to thank Dr. Pradip Mascharak, and Dr. Nicole Fry for helping me find my scientific identity as an undergraduate. Especially, Dr. Nancy Cox-Konopelski and Nandini Mascharak for introducing me to research and chemistry.

This research could not have succeeded without the perspective and enthusiasm of my collaborators. I would like to thank Dr. Qzihi Tang, Dr. Faleo Gateano, Dr. Natalie Wisnieski and Dr. Soya Gamsey. Thank you for helping make these ideas come to life.

My tenure at UCSF was immediately shaped by my fellow students and lab mates. I am immensely grateful for their support, advice and friendship. They gave me a home at UCSF and a family in San Francisco. From the Desai Lab I would like to especially thank: Rachel for teaching me about chemistry, nanolithography and how to design intelligent experiments. Kelly for teaching me everything I know about cellular and molecular biology. Adam for being a great source of knowledge on all topics diabetes and business. Dan for teaching me about materials chemistry, beer and music. Jessica for teaching me how to respond to unpleasant reviewers and helping me gain perspective over weekly happy hours and nonjudgmental amounts of sushi. Rob for being a source of knowledge and support in any random question. They taught me how to think, ask questions, and I am eternally grateful for their guidance, friendship and mentorship. I would especially like to thank Kelly for being my rock. Thank you for being there for me through the losses and wins, you inspired and supported me through this process, thank you.

During a PhD, the lab becomes a second home and I would like to thank all the past and present members of the Desai lab who helped along the way and became friends. Thank you for making the lab an enjoyable, fun and enlightening space. Thank you for the numerous tea and coffee breaks, happy hours, trivias and

lunches. Your company made the lab days fly by and my time in the Desai Lab memorable.

I would also like to thank my friends who encouraged and supported me along the way. I met Joel during interview weekend, and it was pretty much love at first sight. Joel, simply put, I love you and would have been lost without you. Aram, thank you for being my partner in crime, swimming, dancing, and all together foolishness. Karmela, I thank you for your sage wisdom helping make sense of this PhD life. And to Sam, thank you for helping bring a work life balance into my PhD, with hot yoga, and other activities, you are my definitely one of my strongest friends. To my girlfriend Michelle, my cupcake Lauren, and my person Robin. You are my people, my best friends, my confidants, thank you for everything, I love you.

Samuel, I wish I could write you as a co-author or second author. You were my best and biggest advisor, editor, consultant, and cheerleader. Thank you for learning about Diabetes with me.

And last but far from least I would like to thank my family. Thank you Mom and Dad for instilling me with curiosity, questions and optimism. You taught me to try and try and try, and that “nothing ventured, nothing gained”. Thank you for giving me the endurance to persevere. Kimby, thank you for always being on my side, and giving me perspective, feedback and support. I wanted to be someone you could be proud of and that motivation kept me strong in my determination to complete and succeed in this PhD, thank you. Uncle Bobby, thank you for teaching me to do whatever it takes. Aunt Cathy and Grandma Gloria, thank you for giving me inspiration and creativity. Aunt Gina for sharing in the enthusiasm and excitement.

Uncle Mark and Aunt Zoe for always only being a phone call away. And a special thank you to Grandma Vera and Grandpa Marko for being icons of courage, and supporting me along the way.

I love you all very much and dedicate this to you.

Abstract

Type 1 Diabetes (T1D) is a disease where pancreatic islet beta-cells are unable to regulate blood glucose levels, resulting in severe health issues including death.¹ 1.25 million people in the United States alone have T1D and this accounts for \$14.9 billion in healthcare cost annually (CDC, 2009). The prevalence of T1D in people under age 20 rose by 23 % between 2001 and 2009 and is projected to increase 4-6% annually (CDC & NIH), providing a strategic opportunity for therapeutic development. The gold standard of treatment requires manual correction of cellular insulin response by IM injection or by an implanted pump, however both treatments require burdensome maintenance. Although glucose homeostasis can be controlled, there is no therapy providing complete insulin independence. Here I describe a novel therapeutic technology that will lay the foreground for providing insulin independence.

Although islet transplantation has been explored, limited success has been achieved due to decreased islet function, survival and required associated immunosuppressant therapy. To address these challenges multiple encapsulation approaches have been explored.²⁻⁶ This unique technology combines the advantages of single-islet and multi-islet encapsulation approaches, providing rapid nutrient exchange of single-islet approaches and precise membrane control of multi-islet approaches. On top of providing rapid nutrient exchange, immune-isolation and minimal foreign body response, this device technology, unlike others, has been

designed to provide flexible, compliant support for the encapsulated islets, recently discovered to promote cell function and survival.⁷

This technology can replace the need for burdensome therapies by restoring absent insulin secreting cells, reestablishing glucose homeostasis, effectively curing T1D. It can greatly improve diabetic treatment by having immediate glucose response, and significantly reduce associated diabetic complications. Furthermore this approach can significantly decrease reliance on patient compliance and improve patient quality of life.

Table of Contents

NANO TECHNOLOGY APPROACHES FOR CELL BASED TYPE 1 DIABETES

THERAPEUTICS	I
<i>DEDICATION</i>	III
ACKNOWLEDGEMENTS	IV
ABSTRACT	VIII
LIST OF FIGURES.....	XIV
CHAPTER 1: INTRODUCTION	1
TYPE 1 AND 2 DIABETES.....	1
PHYSIOLOGY	2
CURRENT TREATMENT FOR TYPE 1 DIABETES	3
<i>Exogenous Insulin Injections.....</i>	<i>3</i>
<i>Pancreas Transplantation</i>	<i>4</i>
<i>Islet Transplantation.....</i>	<i>5</i>
POTENTIAL CELL SOURCES FOR ISLET TRANSPLANTATION.....	7
TISSUE ENGINEERING	8
IMMUNOISOLATION AND BIOLOGICAL BARRIERS FOR ENCAPSULATED ISLETS.....	10
<i>Innate Immune Response.....</i>	<i>11</i>
<i>Adaptive Immune Response.....</i>	<i>12</i>
<i>Biological Barriers.....</i>	<i>13</i>
DEVICE BIOCOMPATIBILITY	15
CONCLUSION	17
DISCLOSURE.....	18

CHAPTER 2: 3D TISSUE ENGINEERING – 3D MICROENVIRONMENT STIFFNESS AFFECTS

ISLETS INSULIN PROCESSING AND SENSITIVITY 19

ABSTRACT 19

INTRODUCTION 20

RESULTS AND DISCUSSION 23

CONCLUSION 35

MATERIALS AND METHODS 36

Polyacrylamide (PA) micro-well scaffold fabrication.....36

Hydrogel stiffness measurements37

Cell culture37

Glucose Stimulation Insulin Secretion (GSIS) Assays38

Fluorescent Microscopy.....38

Quantitative real-time polymerase chain reaction.....39

ACKNOWLEDGEMENTS 40

DISCLOSURE STATEMENT 40

CHAPTER 3: CELL ENCAPSULATION – POLYCAPROLACTONE THIN-FILM MICRO- AND NANOPOROUS CELL ENCAPSULATION DEVICES 41

ABSTRACT: 41

INTRODUCTION 42

RESULTS AND DISCUSSION 45

CONCLUSION: 59

MATERIALS AND METHODS: 61

Microporous thin-film fabrication..... 61

Nanoporous thin-film fabrication..... 61

Non-porous membrane fabrication 62

<i>Assembly of thin-film devices</i>	62
<i>Characterization using scanning electron microscopy of films and devices</i>	63
<i>Cell culture</i>	63
<i>Glucose stimulated insulin secretion</i>	64
<i>Cytokine assay</i>	64
<i>Bioluminescent imaging</i>	64
<i>Histology</i>	65
<i>Vasculature</i>	66
ACKNOWLEDGEMENTS	66
DISCLOSURE	67
 CHAPTER 3: NANO PARTICLE DIAGNOSTICS – PORPHYRIN-BASED NANOPARTICLES	
FOR LUMINESCENT OXYGEN DETECTION	68
ABSTRACT:	68
INTRODUCTION:	69
RESULTS AND DISCUSSION	70
CONCLUSION	78
MATERIALS AND METHODS:	79
<i>Synthesis of MABP Nanoparticle</i>	79
<i>Dye-hydrogel composite formation</i>	80
<i>UV Dye Stability Study</i>	80
<i>Oxygen sensing study</i>	80
<i>Plate reading setup</i>	81
<i>Size analysis:</i>	81
ACKNOWLEDGEMENTS	81
DISCLOSURE	81

CHAPTER 4: CONCLUSION AND FUTURE DIRECTIONS.....	82
CONCLUDING THOUGHTS ON CELL BASED THERAPEUTICS	82
FUTURE DIRECTIONS	84
APPENDIX A	86
APPENDIX B	94
REFERENCES:	146
PUBLISHING AGREEMENT	173

List of Figures

Figure 1 Polyacrylamide (PA) can be used to construct primary islet-derived and Min6-derived 3D β -cell clusters.....	24
Figure 2 Insulin expression and secretion is affected by cluster size.....	25
Figure 3 Figure 2: β -cell insulin expression is regulated by micro-well stiffness.	26
Figure 4 Min6-derived β -cell clusters in compliant 0.1 kPa micro-wells have increased glucose sensitivity.....	27
Figure 5 Min6-derived β -cell clusters maintain a circular nuclear shape in compliant PA microwells.	29
Figure 6 Erk signaling is not required for stiffness-sensitive insulin expression.....	30
Figure 7 MLCK and ROCK signaling are required for stiffness-sensitive insulin expression.	31
Figure 8 Stiffness-sensitive insulin expression is mediated by β -catenin signaling..	32
Figure 9 Compliant thin-film cell encapsulation technology overview.....	42
Figure 10 PCL micro- and nanoporous thin-film fabrication for cell encapsulating devices.....	47
Figure 11 <i>In vitro</i> device function.....	49
Figure 12 <i>In vivo</i> device image and tracking	51
Figure 13 Microporous barrier inhibits cell-invasion.....	52
Figure 14 Device exterior SEM.....	53
Figure 15 Cytokines affect cell viability.	54
Figure 16 Cytokine protection.	56

Figure 17 Device vascularization.	57
Figure 18 Cell-free device controls for device vascularization.	58
Figure 19 Histology of devices.	59
Figure 20 Nano particle synthesis.	71
Figure 21 Spectroscopy of MAPB-free dye, MAPB-nanoparticles, MAPB-hydrogel and MAPB-composite.	73
Figure 22 Size characterization.	75
Figure 23 MAPB-hydrogel and MAPB-composite hypoxia detection.	76
Figure 24 MABP detection.	77
Figure 25. Hydrogel and composite degradation profile.	78

Chapter 1: Introduction

Type 1 and 2 Diabetes

Diabetes is a chronic disease where blood glucose goes unregulated.¹ The disease is typically due to either an insufficient production of insulin by the pancreas to control blood sugar as in Type 1 Diabetes (T1D), or to an improper response to insulin by the patient's cells as in Type 2 Diabetes. If untreated, diabetes can induce devastating complications such as heart disease, stroke, loss of vision, retinopathy, kidney failure, nervous system damage, and even death.⁸ Type 2 diabetes accounts for approximately 90% of all diabetes and is often linked to obesity. It can be generally combated with appropriate diet, exercise and oral medications but may still require exogenous insulin in some extreme cases.

On the other hand, Type 1 Diabetes accounts for approximately 10% of all diabetes. The prevalence of T1D in people under age 20 rose by 23 % between 2001 and 2009 and is projected to increase 4-6% annually (CDC & NIH). In 2009, 1.25 million people in the United States alone had T1D and this accounted for \$14.9 billion in healthcare cost annually (CDC, 2009).

Type 1 Diabetes, also known as Juvenile Diabetes because it is usually discovered during adolescence, is an autoimmune disease where the pancreatic islet beta-cells responsible for secreting insulin are selectively destroyed.⁹ This results in decreased production of insulin that decreases continuously with the destruction of

the insulin producing beta-cells. Additionally, diabetes is linked to many health complications, such as heart disease, stroke, high blood pressure, blindness, kidney disease, neuropathy and amputation. These complications underscore the urgency of better understanding how treatment strategies may help reduce the effect of this disease.

Physiology

The pancreas contains both exocrine and endocrine cells and is chiefly responsible for the digestion and metabolism of fats, proteins and glucose. The bulk mass of the pancreas is dedicated to the exocrine cells which secrete hormones signaling for the secretion of pancreatic juices, chemicals that neutralize the acidic chyme produced by the stomach, and enzymes responsible for the digestion of fats and proteins. Less than 1% of the pancreas mass is dedicated toward the endocrine cells, termed the islets of Langerhans. The islets of Langerhans consist of a cluster of α -cells, β -cells, δ -cells, γ -cells and ϵ -cells. These cells orchestrate the regulation of blood glucose levels via the secretion of hormones that signal for the increase of blood glucose in hypoglycemic states and decrease of blood glucose in hyperglycemic states. These cells aim at maintaining blood glucose levels between 3.6 mM (65 mg/dl) and 5.8 mM (105 mg/dl). Among all cells constituting the islets of Langerhans, β -cells (beta-cells) are the most important since they secrete the hormone insulin that signals for the decrease of blood glucose. Insulin binds to its receptor, which in turn translocates the glucose transporter to the surface of the

plasma membrane allowing for an influx of glucose that can be either stored or metabolized.^{10,11} Insulin is needed for glucose recognition and transport. In order to closely regulate the glucose levels a network of highly fenestrated capillaries surrounds native human islets. This results in ample blood supply and accordingly abundant nutrients that enable the cells to quickly respond to changes in blood glucose levels. When insulin-producing beta-cells are destroyed or have reduced functionality, insulin and glucose regulation is unbalanced. These defects in regulation of insulin secretion lead to several metabolic problems, including diabetes. It has been suggested that the cause of Type 1 Diabetes is linked to specific virus, micro biota and the hygiene hypothesis, however there is limited data definitively demonstrating which is the exact cause.¹²⁻¹⁷

Current Treatment for Type 1 Diabetes

Exogenous Insulin Injections

Accurate administration of insulin therapeutics that mimic the islet of Langerhans beta-cell insulin secretion is one of the largest challenges in drug delivery due to dynamic fluctuations in required insulin. The gold standard of treatment requires manual correction of cellular insulin response by IM injection or by an implanted pump, however both treatments require burdensome maintenance. This requires strict patient compliance, which is especially difficult considering type 1 diabetes onset typically starts in childhood.

Currently, the most common and effective treatment available is insulin therapy. In this therapy, subcutaneous insulin injections are administered based on the recipient's need. To maintain healthy insulin glucose dynamics, multiple daily blood glucose tests are required for the proper administration of insulin. These tests are very important because variance in diet, routine and activity can greatly affect glucose levels. Although subcutaneous insulin injection is the most effective treatment, it requires high patient compliance, expensive materials and lifelong treatment. To address these challenges there are a series of implantable insulin pumps that are gaining popularity. These devices are used to supply a sustained delivery of insulin with additional boluses when necessary. Although these devices aim to provide a less invasive treatment regime they still require additional testing and maintenance. These challenges highlight the need for a better long-term diabetes treatment plan.

Pancreas Transplantation

One option available to a limited number of type 1 diabetics is whole pancreas transplantation, which is usually performed in conjunction with a kidney transplant in patients with end-stage renal failure. With this method, long-term normal glycemia has been reached with a five-year graft survival rate of 50-70%, however recipients must strictly adhere to a lifelong immunosuppressive therapy.¹⁸ The currently used anti-rejection medications have side effects that limit the number of recipients able and interested in this treatment option. These side effects include susceptibility to infections, decreased wound healing, increased risk of lymphoma, renal dysfunction, hyperlipidemia, anemia and mouth ulcers.¹⁹ The

invasiveness of the surgery and associated lifelong therapy restrict the potential candidates to those patients with severe diabetes, who are additionally requiring another organ transplant.

Islet Transplantation

An alternative therapy is human islet transplantation. Since the majority of the pancreas is dedicated to exocrine functions and less than 1% is dedicated to endocrine functions, transplantation of only the islets greatly decreases the risk of clinical complications and increases the potential range of candidates. This less invasive procedure attempts to replace defective islets with donor islets that can detect blood glucose levels and respond appropriately with insulin, providing a controlled glycemic response in diabetic recipients without exogenous insulin.²⁰ However, a major factor preventing islet transplantation as a mainstream treatment is the recipient's requirement of lifelong immunosuppressive therapy and the subsequent dangerous side effects brought on from that treatment. It is also interesting to point out that beta-cell replacement therapy could provide a significant benefit for some type 2 diabetics where beta-cell insufficiency is a key part of the pathogenesis.²¹

Historically, transplantation of human islets to maintain glucose and insulin regulation began in the 1970s, but it was not until 1989 that the first recipient was able to cease exogenous insulin administration.^{6,22} In 2000, the success rate of the Edmonton protocol dramatically improved with the use of a steroid and glucocorticoid-free immunosuppressive plan including daclizumab, with low doses of sirolimus and tacrolimus.²³ This updated protocol resulted in seven out of seven

consecutive transplants which were still fully functional at one year. However the success rates significantly decreased with time.²⁴ The reason for long-term failure is most likely due to beta-cell loss through the innate immune response and limited nutrients.

In its 2006 annual report, the Collaborative Islet Transplant Registry presented data from 225 patients who received islet transplants. According to the report, nearly two-thirds of recipients achieved “insulin independence”—defined as being able to stop insulin injections for at least 14 days—during the year following transplantation. However, insulin independence is difficult to maintain over time and only one third of recipients maintained insulin independence at two years. Although a majority of patients did not achieve insulin independence, benefits of islet transplantation included reduced need for insulin, improved blood glucose control, and greatly reduced risk of episodes of severe hypoglycemia.

Although islet transplantation has been explored with limited success, the ability to temporarily achieve insulin delivery independence with either solid-organ pancreas or islet transplantation has increased the number of patients seeking beta-cell replacement as an alternative to practiced insulin injection therapy. Based on the potential advantages of islet transplantation as highlighted above, an encapsulated cell-based therapeutic could provide the recipient with a dynamic glucose-responsive source of insulin.

Potential Cell Sources for Islet Transplantation

It has been estimated that one million islets are needed for transplantation in a diabetic human subject, requiring at least two pancreas donors.²⁵ Each islet transplantation requires a surplus of islets due to the staggering loss of up to 80% of islets potentially destroyed in processing, culturing and transplantation.

The significant mismatch between the number of islets needed for transplantation and the islet availability highlights the need to find additional islet sources. Different cell sources are currently being evaluated to overcome this obstacle, e.g. glucose-responsive insulin producing cells derived from human embryonic stem cells (hESC).²⁶ These cells do not respond well to glucose *in vitro* but mature and function like normal beta-cells after being transplanted into mice.²⁷

Another potential cell source is from beta-cells expansion *in vivo* or *in vitro*. During normal cell growth and development the ability of differentiated β -cells to replicate is important. However, human beta-cells have shown less potential for replication compared with rodent beta-cells.²⁸ This has motivated researchers to find small molecules to encourage expansion of existing beta-cells. This search has also invigorated the hunt for small signaling molecules that can direct stem cells towards a beta-cell phenotype.²⁹

Transdifferentiation of hepatic, bile duct epithelial, and acinar cells to beta-cell like is also being currently pursued.³¹⁻³³ The hepatic and acinar cells have been reprogrammed with a recipe of transcription factors. These intrahepatic biliary epithelial cells grown in a collagen-embedded floating culture have been able to transdifferentiate into pancreatic beta-cells.

Additionally, porcine islets have been viewed as a potential source of beta-cells for transplantation due to close homology and previous success with porcine xenografts in alternative clinical endeavors.³⁰

Tissue Engineering

Based on the potential advantages of islet transplantation as highlighted above, an encapsulated cell-based therapeutic would provide the recipient with a dynamic glucose-responsive source of insulin. It has been assumed that indefinite survival would be achieved with microcapsules containing beta-cells, which elicit a minimal foreign body reaction.^{4,34} However, many factors still limit beta-cell replacement therapeutics for type 1 diabetes. An unnoticed factor that very likely affects the success is the environment surrounding the islets. Cellular contacts prior to transplantation can critically affect islet cells physiology, and consequently, the chance of success. The islet also possesses intricate connections that communicate the necessary response of the tissue. In addition, the extracellular matrix (ECM) serves as a scaffold that relays environmental cues necessary for coordinating tissue-specific responses, both chemical and physical.

Historically, a tight correlation exists in nature between structure and function of biological tissue.^{10,35,36} In vertebrates, a consistent feature of this correlation is the dependence on connexins, cadherins and integrins. Connexins, form permselective cell-to-cell channels that cluster at gap junction domains of the membrane of most cell types. Here, they mediate the diffusion-driven exchange of cytosolic molecules between adjacent cells. Another biological tool used by cells for

communication is the use of cell-cell binding proteins such as cadherins, and cell-matrix bindings such as integrins. Cadherins are one category of protein responsible for cell-cell communication. These surface binding proteins have an extracellular and intracellular domain. The extracellular domain binds the extracellular domain of a neighboring cells' cadherin. Once bound these cells can translate that binding signal to their intracellular binding domain which intraslates that signal to a variety of signalling cascades and nuclear transcription factors. Insulin regulation is a multicellular process in that the amounts of hormone necessary under most physiological conditions exceed those that can be produced by individual cells. In islets, cell-cell communication is essential to provide low-insulin release in periods of starvation and sufficient amounts of insulin after food intake.⁴⁵⁻⁵⁰

Integrins are another category of proteins responsible for cell-cell signaling, however these proteins use their external domain to bind the ECM. Cells form connections not only to other cells but also to the extracellular matrix, which provide a substratum contributing to differentiation, polarity, growth and survival.⁴³ In mature intact islets, interactions with the ECM or synthetic matrix materials regulate survival, insulin secretion, proliferation, and aid in the preservation and restoration of spherical islet morphology.⁴⁰ *In vitro* engineering of tissues that are natively exposed to mechanical cues *in vivo* has been frequently reported to enable native cellular responses.⁴⁴ Accordingly, various beta-cell-matrix interactions that closely mimic the native islet microenvironment can improve insulin output or islet longevity. This will allow for greater sensitivity when evaluating glucose stimulated insulin secretion at different cluster sizes.

Both categories of proteins are known to play a critical role in regulating cellular response, and interestingly are both known to play an integral role in glucose responsive insulin signalling.³⁷⁻⁴² Precise manipulation of physical and chemical cues through cell-cell and cell-matrix interactions promise new insight into cellular behavior and tissue function. These insights could improve clinical outcomes of islet transplantation.

Immunoisolation and Biological Barriers for Encapsulated Islets

The idea behind an encapsulated islet is that the membrane surrounding it should be permeable to small molecules such as oxygen, nutrients, glucose, and insulin but impermeable to larger molecules responsible for immune rejection. However, despite promising encapsulation studies and the development of many different encapsulation devices, the latter have yet to make an impact in the clinical setting. Some of the factors limiting the widespread application of encapsulated islets include: incomplete isolation of the islets from the immune response, and inadequate physiological interaction for the cells within the device, both of which are addressed in this dissertation in chapter 2 and 3.

Encapsulated islets that undergo transplantation have to overcome both the innate and adaptive immune response. To address these challenges multiple encapsulation approaches have been explored.²⁻⁶ Microencapsulation strategies have been used to encapsulate single islets or beta-cells with a variety of materials and technologies. These approaches focus on having a high surface area to volume ratio that supports the rapid nutrient exchange necessary for highly secretory cells

such as the islets. Where this approach is limited, macro encapsulation strategies succeed. In a macro encapsulation approach, multiple islets or beta-cells are enclosed in a large device reservoir. Although the large reservoir limits the rate of nutrient exchange, the device size improves the control of the device membrane giving nano-scale precision for the membrane.

Innate Immune Response

The activation of the innate immune response system is triggered when a donor tissue contacts the recipient's blood cells in a reaction termed the instant blood-mediated inflammatory response.⁵¹ Further loss of transplanted islets results from failure of engraftment due to ongoing immune mediated attack in the form of allograft rejection and ongoing autoimmunity.⁵²

Immune rejection of syngenic and allogenic tissue is largely dependent on direct contact with T-cells. Although a proper encapsulation system should protect against cells and antibodies, the islets are still vulnerable to smaller molecules such as chemokines/cytokines and nitric oxide. These small molecules can initiate macrophage-mediated chemotaxis and can result in transplant failure.

Placing islets within a semipermeable membrane made of an inert material which has pores that allow the passage of small molecules such as insulin (monomer: 5.8 kDa, 1.35 nm Stokes radius; hexamer: 34.2 kDa, 2.75 nm) and glucose (180 Da, 0.4 nm) but prevent the entry of macrophages and other immune cell types (~7 μm) and antibodies (~150-900 kDa, 6-50 nm) should prevent rejection by mediated T-cells although it will may not prevent contact with toxic chemokines which have a molecular weight below 30 kDa.

Adaptive Immune Response

The Immunoglobulin G (IgG) molecule (150 kDa, 5.9 nm Stokes radius) together with the IgM (910 kDa) are the most abundant immunomolecules involved in the humoral host response.⁵³ Once they are bound to the grafted tissue, their interaction with the C1q (410 kDa) component of the complement cascade activates a pathway, which will lead to the destruction of the implanted cells.⁵⁴ Binding the first component C1q to an IgM, or two or more IgG molecules, initiates a cascade that culminates in the form of the membrane attack complex, which can lyse a single cell. IgM and C1q (smallest dimension of about 30 nm) are both larger than IgG (5.9 nm Stokes radius), so if host IgM and C1q can be prevented from crossing the barrier, then a specific antibody-mediated attack on the islets should be averted. If the alternative complement pathway is activated and not inhibited by the implanted tissue, then passage of C3(200 kDa) across the membrane must also be prevented. Small complement breakdown products, such as C5a (10 kDa), may also pose a problem.⁵⁵

Since IgM and C1q have the smallest dimension of about 30 nm, they could be completely retained by a membrane with a maximum pore diameter of 30 nm. The pores of a hydrophobic membrane in contact with extracellular fluid are likely to be coated with a monolayer of protein ~10 nm thick. Thus, pores with diameters of about 50 nm would be needed to allow C1q and IgM to pass through. (see Table 1) It has also been estimated that pore diameters between 30 and 50 nm should be able to exclude the small IgG molecule although it is very likely that a smaller pore size is required to completely block it.^{56,57}

Table 1. Pores need to be smaller than	Molecular weight	Stokes radius
IgG	150 kDa	~5.9 nm
Antibodies	~100-950 kDa	~6-50 nm
Immune Cells		~4 μ m

Note: A hydrophobic monolayer of proteins is approximately 10 nm thick.

However, a tiny leak of IgG may not be so detrimental to encapsulated cells. It has been shown that components are rapidly inactivated, therefore it should be good enough to hinder IgG diffusion in the first two days after implantation rather than totally block it.^{54,56,58}

Since Type 1 Diabetes is the autoimmune destruction of beta-cells, even if the cells were identical to the recipient's previous islets they would still need to surpass both the innate and adaptive immune responses for the transplant as well as the autoimmune attack.

Biological Barriers

In order to receive nutrients, oxygen, and to perform metabolic processes appropriately, cells have to be close to a blood source, typically at a maximum distance of 150-200 μ m. If the distance is greater, hypoxic conditions can arise and result in necrosis.⁵⁹ Therefore, revascularization of encapsulated islets is critical for their long-term survival. Vascularization is not only important for preventing hypoxia, the vasculature acts as a highway allowing the cells to respond with insulin

to changes in glucose level in seconds. It is imperative that the encapsulation devices do not hinder the diffusion of these molecules, accordingly these biological requirements define the lower limits of the device pores. (Table 2)

Table 2. Pores need to be larger than	Molecular weight	Stokes radius
Insulin monomer	5.8 kDa	~1.35 nm
Insulin hexamer	34.2 kDa	~2.75 nm
Glucose	180 Da	~0.4 nm

Note: A hydrophobic monolayer of proteins is approximately 10 nm thick.

In the immediate post-transplantation period, islets are forced to depend on diffusion of oxygen and nutrients through peripheral transfusion from the surrounding tissue. This can translate in extended periods of hypoxia and nutrient deficiency, which can result in islet death.⁶⁰ It has been estimated that as much as 50-80% of islets are destroyed shortly after transplantation.⁶¹ To decrease the risk of hypoxia and nutrient deficiency, smaller islets have been used to provide easier access to oxygen and nutrients, giving them a greater chance of survival.

It has also been shown that transplanted islet aggregates fare better than individual islets in terms of histological evidence of necrosis after retrieval and cure rates in diabetic patients. Several groups have shown that clusters of beta-cells secrete insulin more effectively compared to single cells, indicating that communication between cells should be preserved in transplantation situations.^{7,62}

Device biocompatibility

As previously mentioned, immune rejection alone is not the only cause of graft failure. A fibrotic capsule can form around the encapsulated islets in the immediate post-transplantation period.^{34,63} Pericapsular fibrotic growth occurs in response to an implanted material. Immediately after implantation, fibrinogen and other proteins bind to the implanted device surface (biofouling). Macrophages then bind to receptors on the proteins and release transforming growth factor β and other inflammatory cytokines. In response to these signals, quiescent fibroblasts are transformed into myofibroblasts, which synthesize procollagen. The procollagen becomes cross-linked and then other extracellular matrix proteins gradually contribute to the formation of a dense fibrous capsule that greatly affects the diffusion of nutrients and other signaling molecules in and out of the device.

Bioincompatibility of materials can result in this fibrotic overgrowth, which in turn can be responsible for islet cell death and device failure. Lack of biocompatibility can be attributed to the purity, texture and shape of the encapsulating material. If the foreign body response induces the formation of an avascular layer adjacent to the membrane it can create a significant challenge for oxygen diffusion. The implantation of a material in the body could also lead to a neutral response, which would result in little to no fibrotic tissue and no blood vessel growth, or in the best cases it can induce neovascularization, which is the growth and proliferation of new blood vessels near the membrane interface. Neovascularization improves mass transport by bringing the microvasculature in

close proximity to the implanted cells. Neovascularization is induced by the membrane architecture in about 2-3 weeks. This means that the implanted islets experience the most severe oxygen limitations in the first few days after transplantation. Some solutions that have been explored to reduce the immediate hypoxia, post-transplantation, are to create a hydrolytically activated, oxygen-generating biomaterial.^{60,64}

On the longer time scale, it has been found that certain types of porous materials, when fabricated with specific pore sizes, cause a prolific growth of new vessels into the region adjacent to the implant.⁶⁵ There have been competing results on whether larger or smaller pore sizes are responsible for increased neovascularization.⁶⁶ However, regardless of the pore size, it is safe to conclude that in regards to biocompatibility many cells bind better to porous surfaces rather than smooth surfaces.⁶⁷ Additionally, the microgeometry of an implant has also been shown to influence the foreign body response. It has been shown that thin device implants result in thinner foreign body capsules.⁶⁸ Avoiding the foreign body response from implanted materials is very difficult and leads to many device failures.

A strategy to avoid the foreign body response is to transplant the devices into an immune-privileged site. Currently naked islets are transplanted into the liver by the portal vein. It is hypothesized that transplantation to an immune-privileged site would facilitate long-term survival of islets. Sites such as the anterior chamber of the eye in syngeneic and allogeneic mouse models, the cheek pouch in hamsters, and the testies have been examined for their immuno-privileged potential.⁶⁹⁻⁷²

Conclusion

Chapter 2 shows how addressing the physical microenvironmental cues cellular insulin response, which could improve success rates of transplantation strategies. It has been assumed that indefinite survival would be achieved with microcapsules containing beta-cells, which elicit a minimal foreign body reaction.³

In chapter 3, a unique compliant thin-film technology combines the advantages of single-islet and multi-islet encapsulation approaches, providing rapid nutrient exchange of single-islet approaches and precise membrane control of multi-islet approaches is described. On top of providing rapid nutrient exchange, immune-isolation and minimal foreign body response, this device technology, unlike others, has been designed to provide flexible, compliant support for the encapsulated islets, recently discovered to promote cell function and survival.⁷

In chapter 4, we design a nano-particle sensor imbedded in a scaffold and show how it improves the ability for oxygen sensing- an important metric for monitoring cell viability. To monitor the success of the therapy, and the nutrient availability a nano-particle diagnostic tool was developed to monitor oxygen availability. Having an oxygen sensing nanoparticle with the available chemistry for attachment affords a tool to easily add oxygen sensing functionality to a variety of materials.

All together, this technology can replace the need for burdensome therapies by restoring absent insulin secreting cells, reestablishing glucose homeostasis, effectively curing T1D. It can greatly improve diabetic treatment by having

immediate glucose response, and significantly reduce associated diabetic complications. Furthermore this approach can significantly decrease reliance on patient compliance and improve patient quality of life.

Disclosure

This chapter is a variation of the material as it appears in Schweicher, Nyitray et. Al. Fronteirs in Biosciences. It appears here with the permission from the authors.

Chapter 2: 3D Tissue Engineering – 3D Microenvironment

Stiffness Affects Islets Insulin Processing and Sensitivity

Keywords: beta-cells, islets, micro-fabrication, insulin, tissue engineering, polyacrylamide, 3D, Wnt signaling,

Abstract

Type 1 diabetes is chronic disease with numerous complications and currently no cure. Tissue engineering strategies have shown promise in providing a therapeutic solution, but maintenance of islet function and survival within these therapies represents a formidable challenge. The islet microenvironment may hold the key for proper islet maintenance. To elucidate the microenvironmental conditions necessary for improved islet function and survival, 3D polyacrylamide cell scaffolds were fabricated with stiffnesses of 0.1 kPa and 10 kPa to regulate the spatial and mechanical control of bio-signals. Specifically, we show a significant increase in insulin mRNA expression of 3D beta-cell clusters grown on compliant 0.1kPa scaffolds. Moreover, these compliant 0.1 kPa scaffolds also increase glucose sensitivity as demonstrates by the increased glucose stimulation index. Our data suggests that stiffness-specific insulin processing is regulated through the MLCK and ROCK mechanosensing pathways. Additionally, β -catenin is required for regulation of stiffness-dependent insulin expression. Through activation or inhibition of β -catenin signaling reversible control of insulin expression is achieved on the compliant 0.1 kPa and overly stiff 10 kPa substrates. Understanding the role of the

microenvironment on islet function can enhance the therapeutic approaches necessary to treat diabetes for improving insulin sensitivity and response.

Introduction

Type 1 diabetes is a disease characterized by the selective destruction of beta-cells in the islets of Langerhans, responsible for maintaining glucose and insulin homeostasis. This results in a deregulation of insulin and glucose that requires constant monitoring. The most common treatment for type 1 diabetes is insulin therapy, by insulin injection or implantation of a subcutaneous insulin pump. The clinical cell-based approaches for treating diabetes, whole pancreas transplantation and islet transplantation, have great potential for a future diabetes treatments.^{24,73} However, these treatments have not achieved long-term success. Multiple donors are necessary for each transplant, due to high loss of islet function and necrosis post transplantation. To overcome these challenges of limited cell source there have been a series of studies utilizing alternative cell sources such as stem cells to overcome the challenge of limited cell source.⁷⁴ However, much of this loss of function is due to disruption of the native cellular architecture and microenvironment and still occur with a surplus of cells. Understanding the role of the microenvironment might help overcome the challenges of limited cell survival.

In the pancreas, islets experience intricate cell-cell interactions that facilitate insulin response and viability.^{10,75-77} In native islets, cell-cell communication is essential to provide low-insulin release in periods of starvation and sufficient amounts of insulin after food intake. To produce large concentrations of insulin, β -

cells rely on multicellular processes to synergistically increase insulin production beyond what can be produced by an individual cell. Even paired beta-cells secrete more than twice the amount of insulin than a single cell.⁷⁸ Previous work has demonstrated that insulin production per cell increases with beta-cell architecture and that beta -cell survival is improved in large clusters.^{62,79,80}

Microenvironment stiffness is known to play a critical role in cellular response and differentiation, in a variety of systems.⁸¹⁻⁸⁴ Specifically, changes in microenvironment stiffness affects intercellular tension and accordingly regulates cellular and nuclear morphology through many different mechanotransduction mechanisms.⁸⁵ Matrix interactions that closely mimic the native islet microenvironment in architecture and stiffness could improve insulin output or islet viability.

Although the architecture and size of islets has been shown to be critically important little is known about the effect of microenvironmental cues, such as stiffness, on islet function and survival. In mature intact islets, interactions with the natural ECM or synthetic matrix regulate survival, insulin secretion, proliferation, and aid in the preservation and restoration of spherical islet morphology.^{75,40} Beta-cells *in vivo* are surrounded by a rich network of soft tissue (0.1 – 1 kPa) and vasculature (8-17 kPa), the two main physical interactions the islets experience.^{86,87} However, little is known about the biochemical signaling mechanisms connecting these biophysical cues to viability and insulin processing. ERK signaling through the Ras-Raf-MEK-ERK signaling pathway is a well-established mechanosensing pathway. Stiff ECM microenvironments increase the formation of complexes

between FAK and Src and Shc and the mitogen activated protein kinase (MAPK) pathway member Grb2.⁸⁸⁻⁹¹ This complex then enhances FAK-dependent activation of ERK1/2.^{40,92,93} The cell-matrix interface, which is established by the contractile response to ECM stiffness, directly regulates classical pathways of proliferation for Ras-Raf-MEK-ERK pathway. Another mechanosensing pathway that regulates cell behavior is myosin light chain kinase (MLCK) and Rho/ROCK kinase.^{41,94} Myosin II is believed to be involved in the generation of the contractile force for cell migration.⁹⁵ The activity of myosin II is mainly controlled by its light chain (MLC) phosphorylation, which is regulated by two classes of enzymes, MLCK and myosin phosphatase (Rho/ROCK).^{41,96} MLCK and Rho/ROCK kinase appear to be two major kinases that phosphorylate MLC.

The main cell-cell adhesion protein, e-cadherin, maintains beta-cells clusters formation. The adapter protein connecting to e-cadherin to the cellular cytoskeleton is β -catenin, a transcription factor for Wnt signaling. Recently cell-cell adhesion molecules have been recognized as mechanosensors.⁹⁷ Interestingly, β -catenin signaling also is a well known regulator of insulin sensitivity, possibly linking mechanotransduction to insulin processing.^{89,97}

This work utilizes standard photolithographic techniques to develop a series of polyacrylamide (PA) micro-wells scaffolds at different stiffnesses to explore the role of stiffness on insulin processing. By understanding the optimal microenvironmental cues necessary for survival and insulin response, we strive to improve long-term islet viability, which could provide a recipient with a dynamic glucose-responsive source of insulin.

Results and Discussion

Tissue engineering strategies have the power to explore the roles of architecture and microenvironment on beta-cell biology. Accordingly, research has been focused on showing importance of spherical architecture on beta-cell clusters for increased insulin production and viability.⁷⁵ They have also shown that larger beta-cell clusters secrete more insulin per cell.⁶² Additionally the importance of 3D cell clusters formation for optimal beta-cell function using a variety of different natural and synthetic materials has been demonstrated.^{60,98-105} These studies have focused on the biochemical cues initiated by surface molecule binding such as the role collagen and laminin, the two major ECM proteins of islets.^{80,106,44} Improved islet function has been demonstrated when the ECM interactions are reconstructed. Although this is useful to understand the role of architecture and ECM binding, they focus on surface chemistry mediating islet survival and function and ignore the physical and mechanical properties guiding that beta-cell response. Precise manipulation of these physical cues promise new insights into cellular behavior and tissue function, which could improve clinical outcomes of islet transplantation. In our study we have created a system in which the biomechanical properties of the material and cell can be controlled to explore their effect, a previously under acknowledged regulator of beta-cell function.

PA was chosen because it is a biocompatible hydrogel, with a tunable stiffness range. By attenuating the polymer formulation, a micro-well scaffolds ranging the physiological stiffness can be fabricated using standard

photolithographic techniques. Additionally, when hydrated and incubated at 37°C, it does not rupture due to swelling additionally if interested the acrylate handles can be exploited to covalently functionalize the surface.

To study the effect of microenvironment stiffness on islet function, standard photolithography was used to create PA square micro-wells of 100 μm by 100 μm length by width with 60 μm depth (Figure 1. A). The length and width of the micro-wells was controlled by the mask, while the depth of the micro-wells was controlled by the spin rate and subsequent thickness of the photoresist. Micro-wells with the above mentioned dimensions allowed for beta-cell clusters less than 100 μm in diameter to be created (Figure 1. D,E). beta-cell clusters 100 μm in diameter are small enough that oxygen permeability and nutrient exchange are not be significantly affected (34,35).

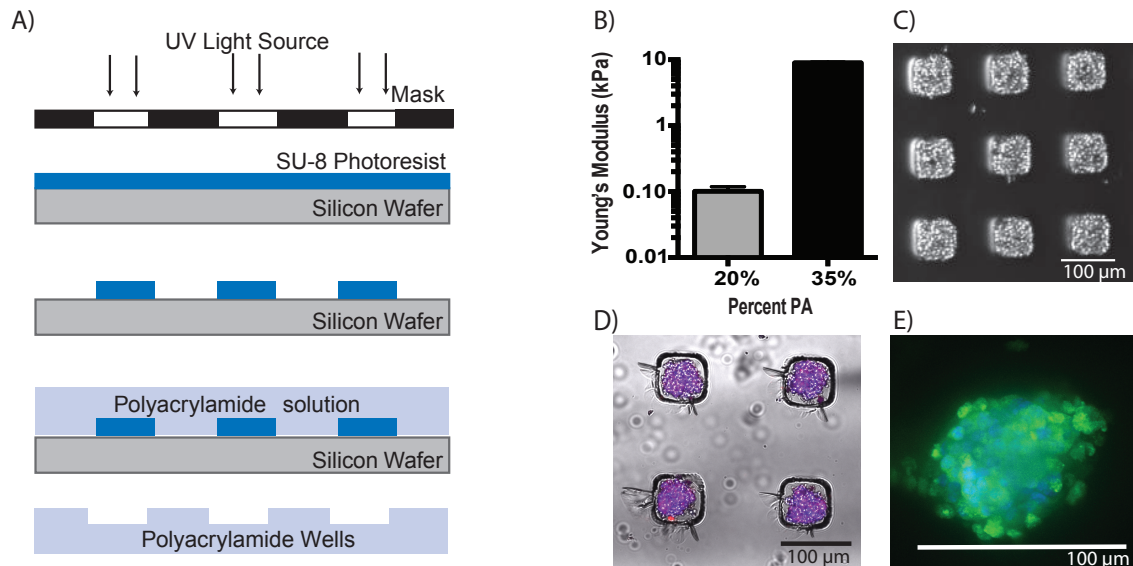


Figure 1 Polyacrylamide (PA) can be used to construct primary islet-derived and Min6-derived 3D beta-cell clusters.

A) Schematic describes PA fabrication using standard photolithography to create. B) Atomic force microscopy was used to measure substrate stiffness. C) PA micro-wells after seeding with beta-cells and D, E) culturing for 24 hours 3D beta-cell clusters are formed.

Further more this cluster size maximizes insulin expression and secretion per volume (Figure 2). The mechanical properties of PA hydrogels were altered by varying the PA concentration. The elastic modulus of the PA hydrogels was measured by atomic force microscopy (Figure 1. B). The PA stiffness was chose for this study to replicate the two common stiffnesses found in the pancreas extracellular matrix 0.1 kPa (compliant) which models the pancreatic ECM and 10 kPa (stiff) which models the surrounding vasculature.

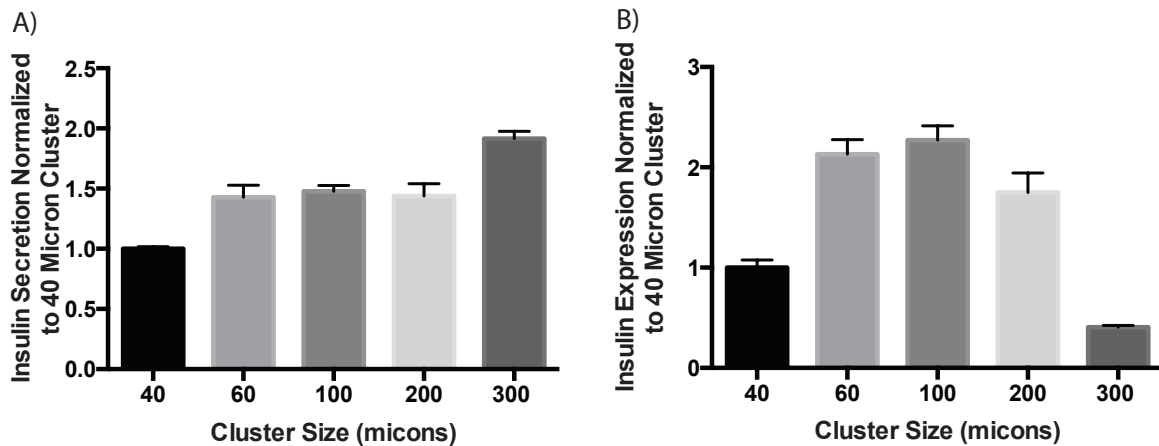


Figure 2 Insulin expression and secretion is affected by cluster size.

A) Primary islet-derived beta-cell clusters grown in microwells ranging from 40 to 300 μm demonstrate increased insulin secretion with increased size. B) beta-cells cultured in 100 μm microwells demonstrate 2-fold increase in insulin expression.

To examine the effect of substrate stiffness on beta-cell function, insulin expression and secretion was measured on compliant and stiff, flat and micro-welled substrates on both compliant, stiff, flat and micro-welled substrates (Figure 3).

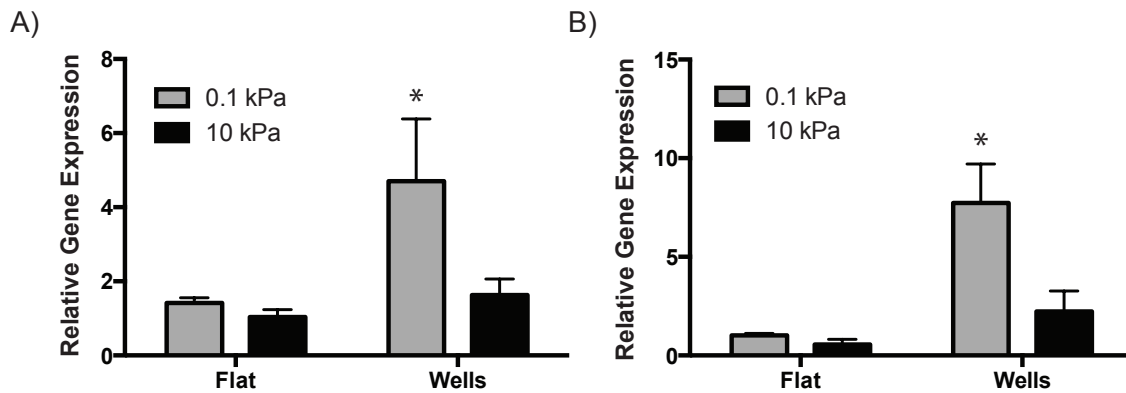


Figure 3 Figure 2: beta-cell insulin expression is regulated by micro-well stiffness.

A) Min6-derived and B) primary islets-derived clusters have increased insulin expression in 0.1 kPa micro-wells. (* Indicates $P < 0.05$)

Micro-welled substrates facilitated spherical cluster formation (Figure 1. C, D, E) known to improve insulin processing. However, only cells cultured on the compliant micro-welled substrates increased insulin expression significantly above control

levels for both MIN6 and primary islets (Figure 3. A, B). This specific response demonstrates that insulin expression is increased not only by cluster formation, but in response to stiffness of the surrounding microenvironment.

For long-term insulin secretion studies a GSIS was performed which replicates glucose levels during starvation and after eating to stimulate the phases of insulin secretion. beta-cells were cultured on both compliant and stiff micro-welled substrates and a GSIS was performed after 24, 48 and 72 hours (Figure 4).

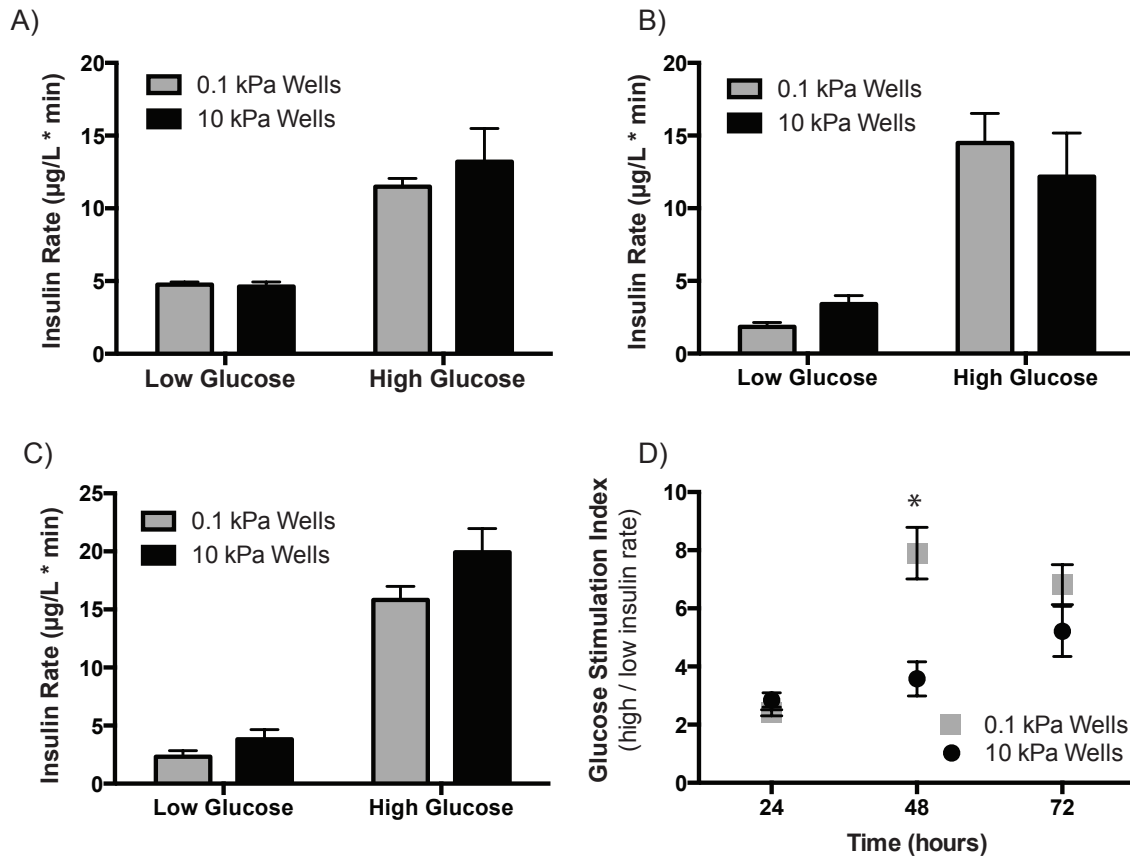


Figure 4 Min6-derived beta-cell clusters in compliant 0.1 kPa micro-wells have increased glucose sensitivity.

A) After 24 hour incubation there is no significant change in insulin secretion rate. B) After 48 hours there is a slight increase in insulin secretion on compliant micro-wells at 15 mM glucose. C) And after 72 hours there is an overall decrease in the insulin rate on compliant stiffness micro-wells. D) The Glucose Stimulation Index shows an increase in the insulin sensitivity on the 0.1 kPa substrate. (Indicates $P < 0.005$)**

Surprisingly, even though insulin expression is increased on compliant micro-wells, after 24 hours there is no significant difference in the glucose stimulation profile between the compliant and stiff micro-well substrates (Figure 4. A). Similar results are seen at the 48 hour and 72 hour time points as well (Figure 4. B,C). However, analysis of the glucose stimulation index profile shows significant improvement at the 48 hours time point (Figure 4. D). An increased glucose stimulation index demonstrates that the clusters are more efficient at secreting insulin in response to glucose, a hallmark of healthy insulin secreting clusters. Both insulin secretion rate and glucose stimulation index are important for maintaining proper insulin response.

As expected from previous research, micro-well scaffold alone improve insulin expression. However, compliant micro-well scaffolds, which combine 3D clusters with physiologically relevant stiffness greatly improves the glucose stimulation index and insulin expression. Although there is striking increase in insulin expression on compliant substrates there is only a moderate change in the insulin secretion. This could be due to the necessity of both: physical interactions

with the substrate, and biochemical signaling interactions initiated by ECM-adhesion binding proteins to further promote insulin secretion and sensitivity

Intercellular tension in response to stiff microenvironments can cause a change in nuclear morphology. Tension in cytoskeletal attachments to the nucleus can distort the circular configuration of tensionless nuclei. Thus nuclear circularity within beta-cell clusters can indicate the relative amount of internal cellular tension. As expected the beta-cell clusters cultured in stiff micro-wells, which would be expected to have higher internal cellular tension, have nuclei that are significantly less circular than those on compliant substrates (Figure 5).

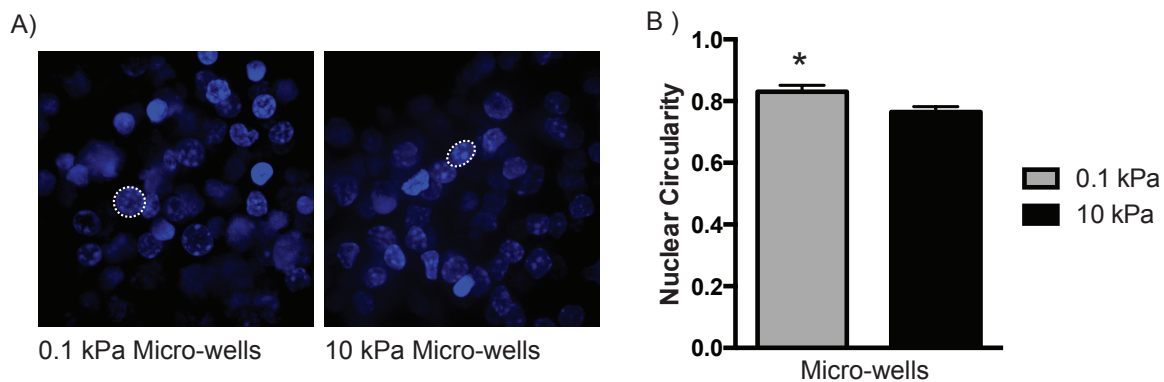


Figure 5 Min6-derived beta-cell clusters maintain a circular nuclear shape in compliant PA microwells.

A) Nuclear staining of cells cultured in compliant 0.1 kPa and stiff 10 kPa micro-wells. B) The decrease circularity of the nuclei on stiff micro-wells indicates cells experience more cellular tension.

The stiffness of the microenvironment is converted to an intercellular response through mechanosensing. Three mechanosensing signaling pathways,

ERK, MLC and ROCK signaling were explored in clustered beta-cells. To confirm the role of each signaling pathway MEK1 (ERK inhibitor), ML-7 (MLCK inhibitor) and Y27632 (ROCK inhibitor) were used. Interestingly the MEK1 inhibitor has no effect on insulin expression (Figure 6. A).

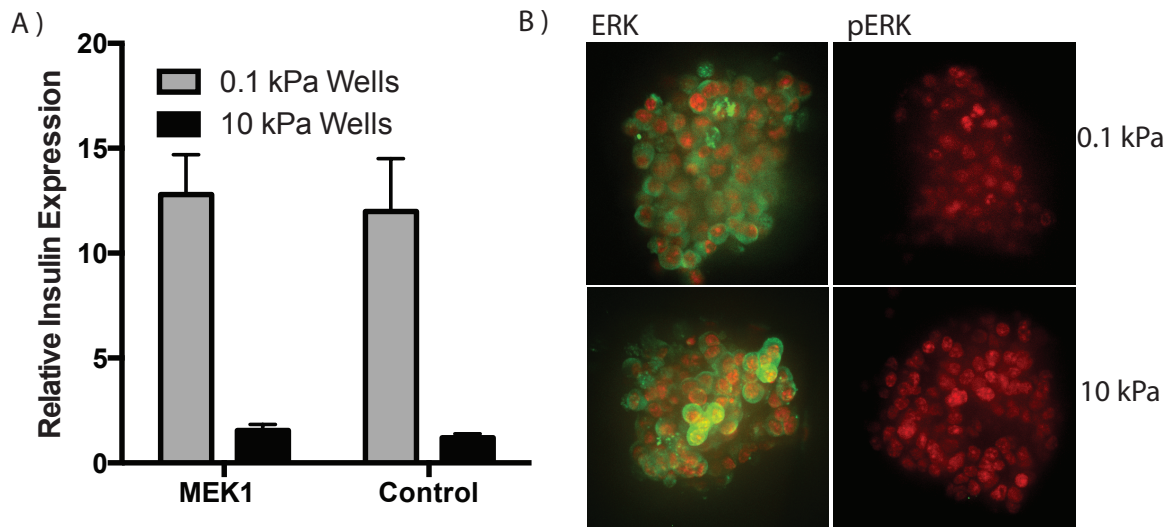


Figure 6 Erk signaling is not required for stiffness-sensitive insulin expression.

A) Incubation with a MEK1 inhibitor shows no change in insulin expression. B) Absent ERK activation is demonstrated by the lack of nuclear staining overlap between ERK (green) and the nucleus (red), and by the absent pERK (green) staining.

Furthermore the absence of ERK nuclear localization and complete absence of pERK the activated form of ERK in both substrates indicates ERK signaling is not involved (Figure 6. B). However treatment with ML-7 and Y27632 reduces insulin

expression on compliant substrates to levels achieved on the stiff substrates (Figure 7).

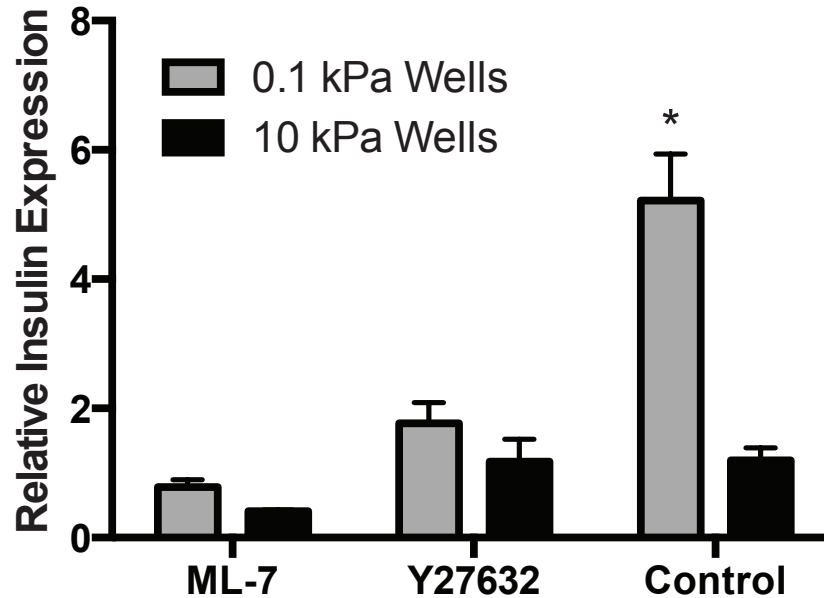


Figure 7 MLCK and ROCK signaling are required for stiffness-sensitive insulin expression.

Addition of MLCK and ROCK inhibitors significantly decrease insulin expression on compliant 0.1 kPa micro-wells to the levels in the stiff 10 kPa micro-wells.

To determine the effect of substrate stiffness on β -catenin signaling, gene expression of GSK3 β , a competitive inhibitor of β -catenin, and Lef and Tcf, binding partners of β -catenin, were analyzed. At 24 hour, gene expression for GSK3 β is decreased while Lef and Tcf expression is increased on the compliant substrates (Figure 8. A). A decreased expression of GSK3 β and increased expression of Lef and

Tcf the transcriptional binding partners for β -catenin on compliant micro-well substrates suggest canonical Wnt signaling may be upregulated to confer improved insulin sensitivity and expression. To confirm the role of β -catenin we used the β -catenin inhibitor, IRW-1 and the β -catenin activator, DCA. When β -catenin signaling is inhibited insulin expression is decreased on the compliant substrates to the level observed on the stiff substrate (Figure 8. B). However, when β -catenin signaling is activated, insulin expression is increased on the stiff substrates to the level observed on the compliant substrates (Figure 8. B). This demonstrates reversible control of insulin expression on the compliant and stiff substrates through β -catenin signaling manipulation.

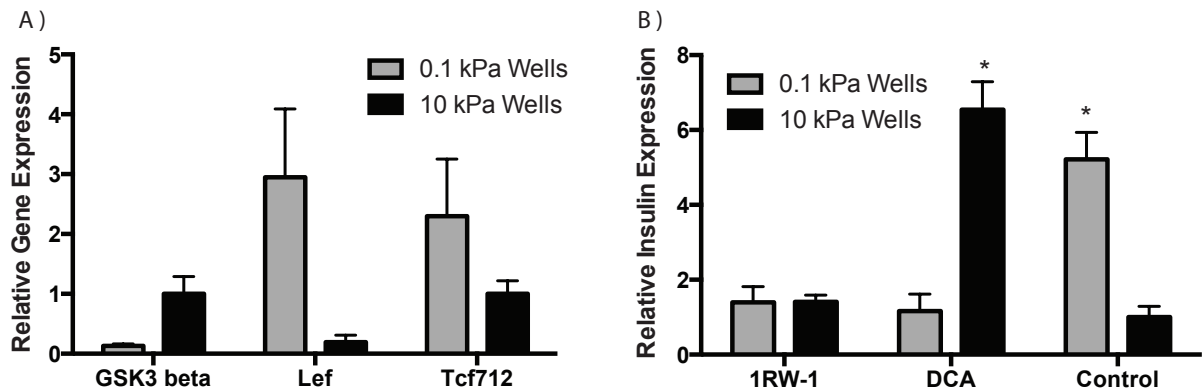


Figure 8 Stiffness-sensitive insulin expression is mediated by β -catenin signaling.

A) Decreased expression of GSK3 β and increased expression in β -catenin adaptor proteins Lef and Tcf suggest increase insulin sensitivity by β -catenin signaling. B) Incubation with IRW-1, a β -catenin inhibitor, reduces insulin expression on the compliant 0.1 kPa substrates to the level observed on the stiff 10 kPa substrates where addition of DCA, a β -catenin activator, increases

the insulin expression on the stiff 10 kPa substrate. (Indicates $P < 0.005$, *** Indicates $P < 0.0007$)**

Interestingly, increased insulin expression in beta-cells cultured on compliant substrates was down-regulated with ROCK and MLCK inhibitors, but was unaffected by ERK inhibition. This result was surprising as ERK signaling has been linked to focal adhesion formation and mechanosensing.^{40,88} The ablation of the increased insulin expression on the compliant substrates with the MLCK and ROCK inhibitor suggest a mechanosensing mechanism regulates changes in insulin, and that the MLCK inhibitor appears to have a stronger inhibitory affect. Although both the MLCK and ROCK inhibitor decrease insulin expression on the compliant substrate, the expression is never below the expression level of the stiff substrate. This suggests that these inhibitors decrease insulin expression by ablating cellular recognition of stiffness rather than the change in cellular tension of the cells regulating the changes in insulin expression.

Additionally the nucleus has been proposed to act as a cellular mechanosensor, with changes in nuclear shape causing conformational changes directly affecting transcriptional regulation^{85,107} The decreased circularity in the stiff micro-well substrates was consistent with the increased cellular tension experienced in the more rigid scaffolds. If cellular tension regulates insulin expression, inhibition of mechanosensing would be expected to increase insulin expression. However there is no increase in insulin expression with the inhibition of mechanosensing suggesting that mechanosensing not intercellular tension is necessary for stiffness controlled insulin expression. Additionally, cells cultured

with a β -catenin inhibitor, decreased insulin expression to the expression level of the stiff substrate where as cells cultured with a β -catenin activator increase the insulin expression on the stiff substrate to the levels of the compliant complaint substrate. This demonstrates that β -catenin can reversibly control insulin expression between the stiff and compliant substrate. Interesting β -catenin is an established regulator of insulin sensitivity through Wnt signaling, however had not previously been linked to mechanosensing for insulin sensitivity. These findings are consistent with the decreased expression of GSK3 β that when inactive, activates β -catenin and results in its nuclear localization. The increased expression of Tcf and Lef, the binding partners of β catenin, is also consistent with the β -catenin signaling. Furthermore indicating that β -catenin signaling is required to mediate stiffness-dependant insulin expression. This suggests that MLCK and Rock mechanosensing and β -catenin signaling through the canonical Wnt pathway modulates stiffness-dependant insulin expression and secretion.

This study demonstrates the ability of discrete biophysical cues to affect β -cell insulin expression and sensitivity in a 3D system. To our knowledge, this is the first study that investigates stiffness mediated 3D beta-cell cluster's insulin processing. The results of this study have promising implications for not only on tissue-engineering but also for diabetes treatment in transplantation and immune isolating systems. These findings can direct future islet studies, specifically improving stratagies for increased glucose sensitivity. By understanding the microenvironment responsible for improving the islet's insulin response we can

build on the current cell encapsulating technologies and improve the potential to cure diabetes.

Conclusion

To measure the role of stiffness alone on insulin processing a 3D micro-welled system that is mechanically tunable, biocompatible and fabricated using standard photolithography was designed. 3D beta-cell clusters from both MIN6 and dissociated primary cells were created and a stiffness dependent change in insulin expression and sensitivity was demonstrated. The importance of ROCK and MLCK signaling though mechanosensing was shown in stiffness dependant insulin processing. Additionally the decrease in nuclear circularity suggests increased intercellular tension. However this did not contribute to changes in insulin processing. This work demonstrated that stiffness sensitive insulin processing requires β -catenin signaling. Furthermore suggesting that β -catenin signaling through the Wnt pathway regulated by mechanosensing tunes insulin processing. Understanding the microenvironment can play a key role in future diabetes studies. This information can be directly translated to current islet transplantation methods and immune isolation devices for the long-term treatment of diabetes.

Materials and Methods

Polyacrylamide (PA) micro-well scaffold fabrication

PA micro-wells were fabricated using a two-step process. First, a micropatterned silicon wafer was created using standard photolithography techniques outlined below. A layer of SU-8 2035 negative photoresist (Microchem, Newton, MA) was spun at 1400 rpm for 30 seconds onto a 3" silicon wafer using a PMW32 spin coater (Headway Research, Garland, TX) and prebaked at 65°C for 5 minutes then 95°C for 15 minutes. An array of 100 μm micro-wells at 100 μm spacing were patterned into the photoresist using a photo mask and exposing the photoresist to UV light for 45 seconds at an intensity of 9 mW cm^{-2} using a Karl Suss MJB 3 mask aligner (SUSS MicroTech Inc., Waterbury Center, VT). The SU-8 posts were then post-baked at 65°C for 5 minutes then 95°C for 15 minutes and developed with SU-8 developer (Microchem, Newton, MA) for 10 minutes under agitation. The wafers were then hard baked at 200°C for 15 minutes. Second, a PA solution of 5mL for the 0.1 kPa substrate or 8.75 mL PA for the 10 kPa substrate (Biorad, Hercules, CA) with 4.9 mL or 1.24 mL water respectively was made. A 10% w/v solution of APS (Sigma-Aldrich, St Louis, MO) was created in 100 μL of water and added to the PA solution followed by 10 μL of TEMED (Biorad, Hercules, CA). The solution was gently inverted then poured over the SU-8 templated wafer. The PA was allowed to polymerize for 1 hour, then removed from the wafer and allowed to soak in PBS for 5 days.

Hydrogel stiffness measurements

Stiffness measurements of the hydrogel were taken by microindentation. Hydrated PA was attached to a glass slide and mounted onto the stage of an Asylum MFP-3D atomic force microscope (Asylum Research, Goleta, CA) coupled to a Nikon TE200U microscope. Force measurements were obtained using an Olympus silicon nitride cantilevers with a spring constant of 2.0 N/m. Displacement versus position data were converted to force versus indentation based on the contact position, which was fitted to a Hertzian model to obtain Young's Moduli. Force loading was applied to at least 3 samples using a 10x10 indentation matrix with a 10 μm borosilicate tip at a 0.6 N/m spring force.

Cell culture

Whole islets were isolated from Black 6 lab mice by the Islet Core at UCSF using standard islet isolating techniques. Islets were dissociated with 0.05% trypsin in PBS (Cell Culture Facility, San Francisco, CA) to a single cell suspension. The MIN6, a mouse beta-cell line, was cultured using standard cell culture techniques in DMEM High Glucose Media (Cell Culture Facility, San Francisco, CA) with 10% Fetal Bovine Serum, 1% penicillin/streptomycin (Cell Culture Facility, San Francisco). Cell cultures were maintained in a humidity controlled 5% CO₂ incubator at 37°C. The MIN6 cell line was chosen because it exhibits glucose metabolism and glucose-stimulated insulin secretion similar to normal islets. Cells were treated with the MEK1 inhibitor PD98059 at 10 μM (Cell Signaling, Danvers, MA) and Deoxycholic acid (DCA) a β -catenin activator (Sigma-Aldrich, St, MO) at 10 μM for 1 hour prior to sample collection. Cells were treated with the β -catenin inhibitor IRW-1 (Sigma-

Adrich, St Louis, MO) at 10 μ M, Rock inhibitor Y27632 (Calbiochem, Darmstadt, Germany) at 10 μ M and the MLCK inhibitor ML-7 (Calbiochem, Calbiochem, Darmstadt, Germany) at 10 μ M during seeding and samples were collected after 24 hours of culture.

Glucose Stimulation Insulin Secretion (GSIS) Assays

Before seeding, cells were trypsinized and resuspended in a complete medium. Cells were then seeded into the PA scaffold at a 10^6 cells per mL and cultured for 24 hours, 48 hours, or 72 hours. After which cells underwent a GSIS time course, cells were cultured in 5 mM glucose balanced HEPES buffer for 60 minutes, then stimulated at 15 mM glucose balanced HEPES buffer for 15 minutes and 60 minutes. The media was prepared as previously described.¹⁰⁸ The conditioned media from the MIN6 and primary islets cultured on the 0.1 kPa micro-wells and the 10 kPa micro-wells was harvested after each GSIS stimulation step. Insulin production was measured with an ELISA assay (Mercodia, Winston Salem, NC) according to the manufacturer's instructions. ANOVA followed by a Tukey Test was used to evaluate statistical significance.

Fluorescent Microscopy

Cells were fixed using 4% paraformaldehyde (Fisher Scientific, Waltham, MA) for 30 minutes at room temperature, permeabilized with 0.5% Triton X-100 (Sigma-Adrich, St Louis, MO) for 30 minutes. After 3 washes in PBS, cells were blocked with 5% goat serum for 1 hour at room temperature. Primary antibodies ERK2 (Santa Cruz, D-2) and pERK $\frac{1}{2}$ (Santa Cruz, 12D4) were added at a 1:100

dilution. Samples were incubated in primary antibody at 4°C overnight. Secondary antibodies incubated for 1 hour at room temperature. F-actin and nuclei were stained with Fluor 488 phalloidin (Life Technologies, Eugene, OR) and DAPI (Life Technologies, Eugene, OR) respectively. Cells were imaged using a spinning disk confocal (Nikon Eclipse Ti-E motorized inverted microscope with Yokogawa CS22 Spinning Disk Confocal from Solamere Technology Group, Acquisition with Micro-Manager 1.4) and analyzed using ImageJ (National Institutes of Health, Bethesda, MD).

Quantitative real-time polymerase chain reaction

mRNA was isolated using RNeasy column purification (Qiagen, Valencia, CA). The concentration and purity of RNA were determined using a Nano Drop ND-1000 Spectrophotometer (Thermo Scientific, Waltham, MA). cDNA was synthesized with iScript cDNA synthesis kit (Biorad, Hercules, CA). mRNA expression was evaluated using an Applied Biosystems Viia7 real-time polymerase chain reaction system. Forward and reverse primers and SYBR green fast mix (Life Technologies, Eugene, OR) were used to amplify each cDNA of interest. A minimum of 3 biological triplicates and one technical triplicate was run for each treatment and normalized to the house keeping gene L19 or a geometric mean of GAPDH and TBP. An ANOVA followed by a Tukey Test was used to evaluate statistical significance.

Acknowledgements

This work was supported by the Juvenile Diabetes Research Foundation (JDRF grant awards P30DK063720). The authors thank Alec Cerchiari for technical assistance, as well Jessica L. Allen and Jennifer S. Wade for critiquing the manuscript, and members of the Desai laboratories for insightful discussion and conversations. The authors would also like to thank the Tang laboratory for the MIN6 cell line, the Islet Core at UCSF for islet isolations, the Nikon Center at UCSF for Imaging and the Center for Advanced Technologies at UCSF.

Disclosure Statement

This chapter is a variation of the material as it appears in Nyitray et. Al. Tissue Engineering Part A. It appears here with the permission from the authors.

Chapter 3: Cell Encapsulation – Polycaprolactone Thin-Film Micro- And Nanoporous Cell Encapsulation Devices

KEYWORDS: Cell-encapsulation, polycaprolactone, immunoisolation, nanoporous, microporous

ABSTRACT:

Cell-encapsulating devices can play an important role in advancing the types of tissue available for transplantation and further improving transplant success rates. To have an effective device, encapsulated cells must remain viable, respond to external stimulus, be protected from immune responses, and the device itself must elicit a minimal foreign body response. To address these challenges, we developed a micro- and a nanoporous thin-film cell encapsulation device from polycaprolactone (PCL), a material previously used in FDA approved biomedical devices. The thin-film device construct allows long-term bioluminescent transfer imaging, which can be used for monitoring cell viability and device tracking. The ability to tune the microporous and nanoporous membrane allows selective protection from immune cell invasion and cytokine-mediated cell death *in vitro*, all while maintaining typical cell function as demonstrated by encapsulated cells' insulin production in response to glucose stimulation. To demonstrate the ability to track, visualize, and monitor the viability of cells encapsulated in implanted thin-film devices, luciferase positive MIN6 cells were encapsulated and implanted in allogeneic mouse models for up to 90 days. Lack of foreign body response in combination with rapid

neovascularization around the device shows promise in using this technology for cell encapsulation. These devices can help elucidate the metrics required for cell encapsulation success, and direct future immune-isolation therapies.

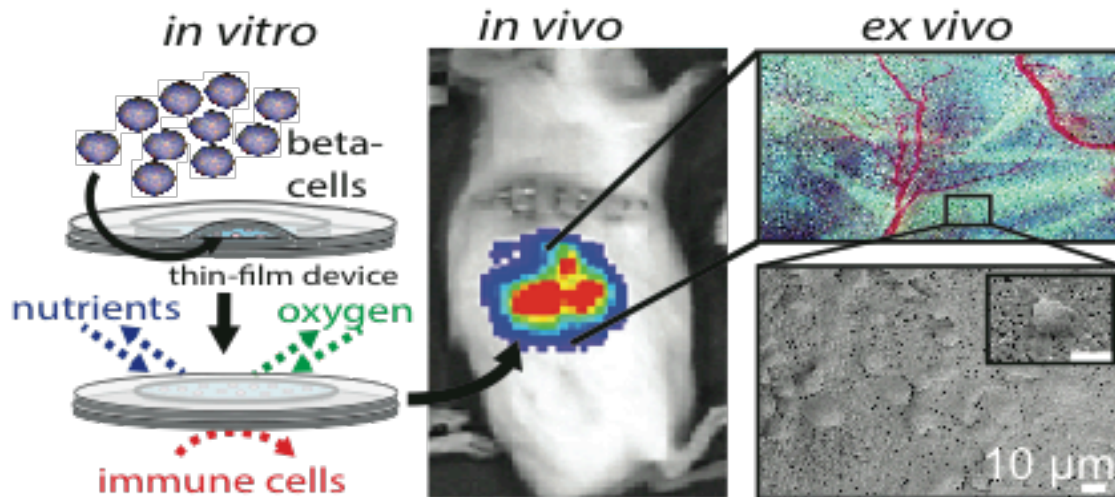


Figure 9 Compliant thin-film cell encapsulation technology overview.

Introduction

Cell replacement therapy has seen unprecedented progress in the past few years, including the ability to achieve insulin independence in humans through islet transplantation.^{1,5,109} Advancements in stem cell technology hold potential to overcome donor shortages for many patients, who can benefit from islet replacement therapy. In particular, stem-cell-derived beta-cells offer a promising new cell source for achieving insulin independence. Unfortunately, life-long systemic immunosuppression is required to protect transplanted cells from being rejected putting patients at risk of organ damage, infection and malignancies.^{23,53}

Cell encapsulation provides an alternative approach to protect transplanted cells without the complications associated with immunosuppression. While a number of strategies are being investigated,^{100,110-114} there are several challenges associated with these approaches: retrievability, control over pore dimensions, biocompatibility, scalability, and reproducible fabrication methods.

The key function of an encapsulation device is to create an environment that allows for normal insulin secretion in response to fluctuating blood glucose, while maintaining cell viability through effective nutrient exchange, effective waste exchange, and sequestration from the immune system. With the goal of creating immune-protected beta-cells, a variety of micro- and macro-encapsulating approaches have been developed over the past several decades.^{6,115-117} The fundamental distinction between micro- and macro-devices is a matter of scale: microencapsulation approaches encapsulate a single cell or islet, which maximizes surface area to volume ratios and promotes improved nutrient exchange.^{118,119} However, there is limited control of membrane thickness and pore size with microencapsulation. Additionally, since islets are individually encapsulated, thousands of micro-devices are required for each transplant, and capsule size makes live imaging and tracking a significant challenge. Conversely, macro-encapsulation devices house many cells or islets.¹²⁰ These larger devices allow for greater control over membrane parameters, such as pore size and porosity, but are plagued by limited nutrient diffusion and cell response due to the device thickness and large device reservoir. In addition to these challenges, the sharp rigid structures typically

associated with macro-encapsulation devices can lead to a foreign body response and subsequent device failure from fibrotic encapsulation.^{68,121}

In this work, we fabricate and characterize polycaprolactone (PCL) thin-film macro-encapsulation devices as an innovative strategy to address the challenges of existing micro- and macro-encapsulation approaches. A thin compliant design allows diffusion and flexibility similar to microencapsulation approaches; while the larger device surface area allows precise membrane control and retrievability, features associated with larger macro-encapsulation technologies. Encapsulated cells demonstrated viability, function, protection from immune-cell intrusion, protection from cytokine-mediated cell death, and neovascularization. PCL has been used in FDA-approved medical devices and has demonstrated long-term biocompatibility in multiple animal models.¹²²⁻¹²⁷ Additionally, PCL degradation can be tuned to match the lifetime of the encapsulated cells, eliminating the need for device removal.^{128,129} The use of porous PCL thin films allows for a thin and flexible device to be designed with either micro- or nano-scaled features, leading to better nutrient exchange, precise membrane control, and device tracking. In this study, the MIN6 cell line, a well-established mouse insulinoma cell line known to respond to glucose with insulin secretion, was used as a model for islet beta-cells. Using MIN6 cells provides a sustainable and consistent source of cells across experiments. Primary islets were also used to demonstrate long-term viability of encapsulated cells.

Results and Discussion

In this work we describe the fabrication of microporous and nanoporous PCL thin-film cell-encapsulation devices, cell behavior in these devices, and *in vivo* integration of these devices in allogeneic mouse models. To design these encapsulation devices, the geometry was engineered to combine the advantages of the precise membrane control of macro-encapsulation devices with improved nutrient exchange of microencapsulation devices. Furthermore, the choice of PCL was based on its range of molecular weights, tunable degradation profile, flexible, and use as a non-toxic material in FDA-approved medical devices. Two different methods were used to create micro- and nanoporous membranes for thin-film devices. The microporous films utilize phase separation of PEG and PCL in solution. In this method, after films are cast, the pore forming agent (PEG) is dissolved leaving a microporous film.¹²⁸ By tuning the concentration ratio and composition of the two polymers, films can be tailored for a variety of porosities and architectures.^{123,128,130-135} Nanoporous films were created from a zinc oxide nanorod template and backed with a microporous support layer. Zinc oxide nanorod dimensions can be readily tuned allowing a wide range of pores sizes, giving the ability to further refine these devices.^{136,137} **Figure 10A** schematically details the method for heat-sealing two thin-films to generate a single device. Two-step sealing decouples device shape from cell encapsulation. A first heat-sealing step controls the device size. Once the device outline is sealed, cells are inserted into the lumen of the thin-film device, and a second heat-sealing step encapsulates the cells. Device geometry can be arbitrarily selected based on the shape of the nichrome wire that defines the device seal,

typically from 1 cm to 5 cm in diameter, allowing devices to be scaled to contain more cells as necessary.

Scanning electron microscopy (SEM) was used to visualize the microporous thin films, which had approximately 2 μm sized pores and a membrane thickness of approximately 10 μm (**Figure 10B**). Similarly, a SEM image cross-section and top-down image of a nanoporous thin-film with a microporous backing showed a membrane thickness of 10 μm and nano-pores ranging from 30 nm-100 nm (**Figure 10C**). The thin design, flexibility, compliance of the material, and structure of the device as a whole creates a cell-encapsulating device that is easy to handle with precise membrane control (**Figure 10D**). Noting that oxygen diffusion in aqueous solutions is 100 μm to 200 μm , these thin-film devices with membrane thicknesses of 10 μm decrease the proximity to vasculature needed for adequate oxygen consumption.^{103,138} Given the thin-film nature of the devices, the total cell content scales with device area, while the average distance of cells from the nutrient source at the device exterior is maintained, bridging the advantages of both micro- and macro-encapsulation technologies. We expect the thin-film design of the device, coupled with rapid device vascularization, to provide sufficient oxygen for encapsulated cells.

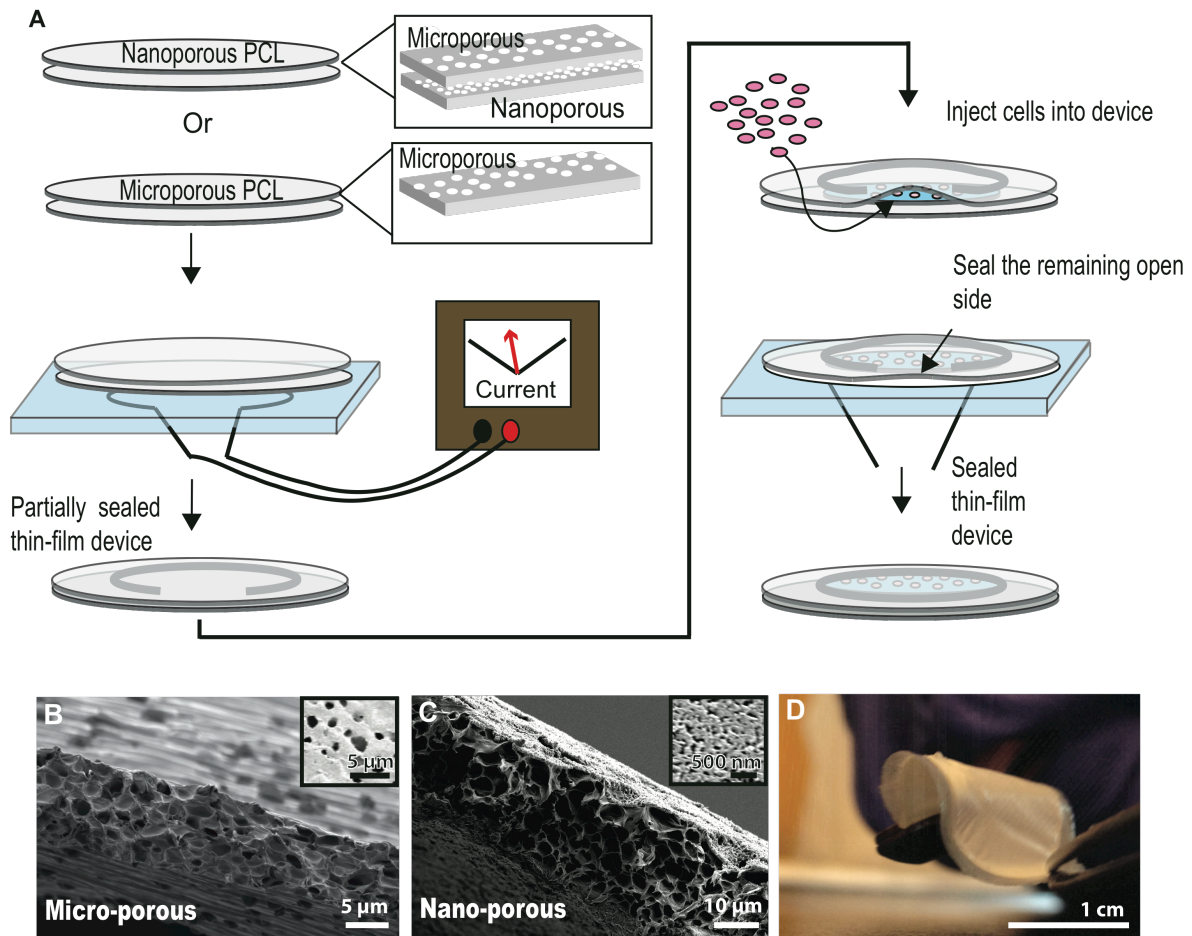


Figure 10 PCL micro- and nanoporous thin-film fabrication for cell encapsulating devices.

A) Schematic of the device two-step heat-sealing and cell encapsulation. B) Cross section SEM of the microporous thin-film and (inset) top down image of the film surface. C) Cross section SEM of the nanoporous thin-film and (inset) top down image of the nanoporous film surface. D) Image of an assembled device, demonstrating device flexibility.

mCherry-expressing MIN6 cells encapsulated in either micro- or nanoporous devices maintain viability *in vitro* through 6 days, as defined by the persistence in mCherry signal, and are able to maintain glucose stimulated insulin secretion (**Figure 11A**). The glucose stimulation index is a metric to quantify beta cell function by comparing the ratio of insulin release in a high glucose state relative to a resting state. MIN6 cells encapsulated in either micro- or nano-devices demonstrate no statistically significant changes in their glucose stimulation index (**11B**). Furthermore, freshly isolated mouse islets encapsulated in these devices maintain their glucose stimulation index over a period of 20 days *in vitro*, which is significantly improved over free islets alone which have over a 25% decrease in the glucose stimulation index from day 1 (**Figure 11C**). This demonstrates that beta-cells insulin response to glucose is maintained within both nano- and microporous thin-film devices. Additionally, glucose sensing and insulin secretion, a major function of beta-cells, is unaffected by encapsulation in either micro- or nano-devices.

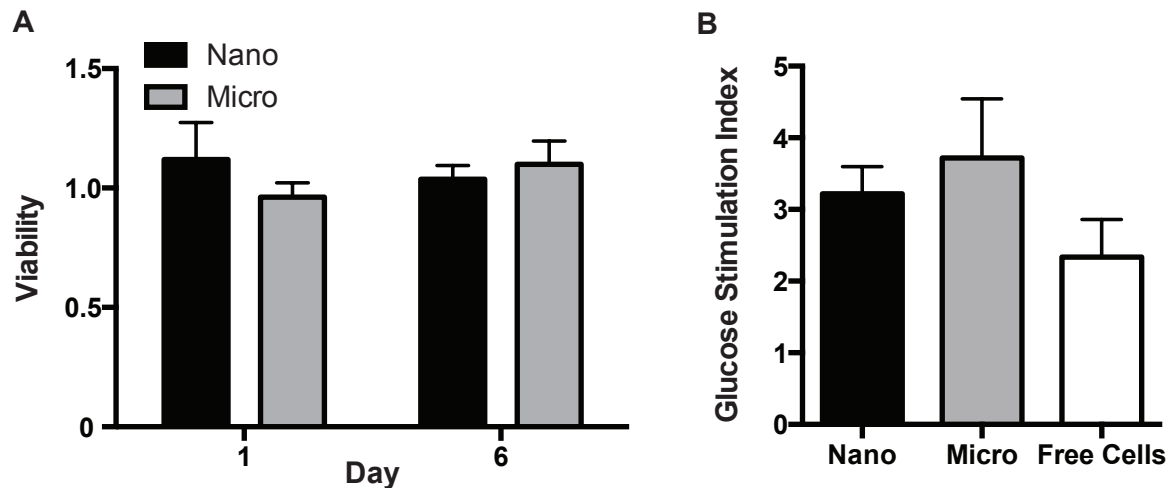


Figure 11 *In vitro* device function.

A) *In vitro* device viability of encapsulated MIN6 cells as measured with mCherry fluorescence. **B)** Glucose stimulation index of MIN6 Cells encapsulated in either micro- or nanoporous devices. **C)** Glucose stimulation of primary islets encapsulated in microporous devices. ($p \leq 0.5$, $n \geq 3$)

Viability and persistence of transplanted cells can be monitored in recipient mice in real time using bioluminescence imaging (**Figure 12**). This technique was used to monitor *in vivo* Luciferase-expressing MIN6.LUC encapsulated into thin-film devices implanted under the abdomen above the liver (**Figure 12A**), over the muscle layer in the subcutaneous space of the mouse dorsal flank (**Figure 12B**) or unencapsulated cells implanted into the kidney capsule (**Figure 12C**) of syngeneic B6 mice. Bioluminescent signal decreases with device implant depth, and both implanted device locations were visually brighter than the no device kidney capsule

control. Persistence of bioluminescent signal demonstrates maintained viability though 90 days of implantation (**Figure 12D-F**). As the bioluminescent signal tracks with device location, it also provides a non-invasive method to track device movement. Because the encapsulated cells are not fixed within the device, and the device itself is not sutured or tethered to any tissue, cellular reorganization of the encapsulated cells or daily movement of the mouse can result in the movement of the bioluminescent signal.

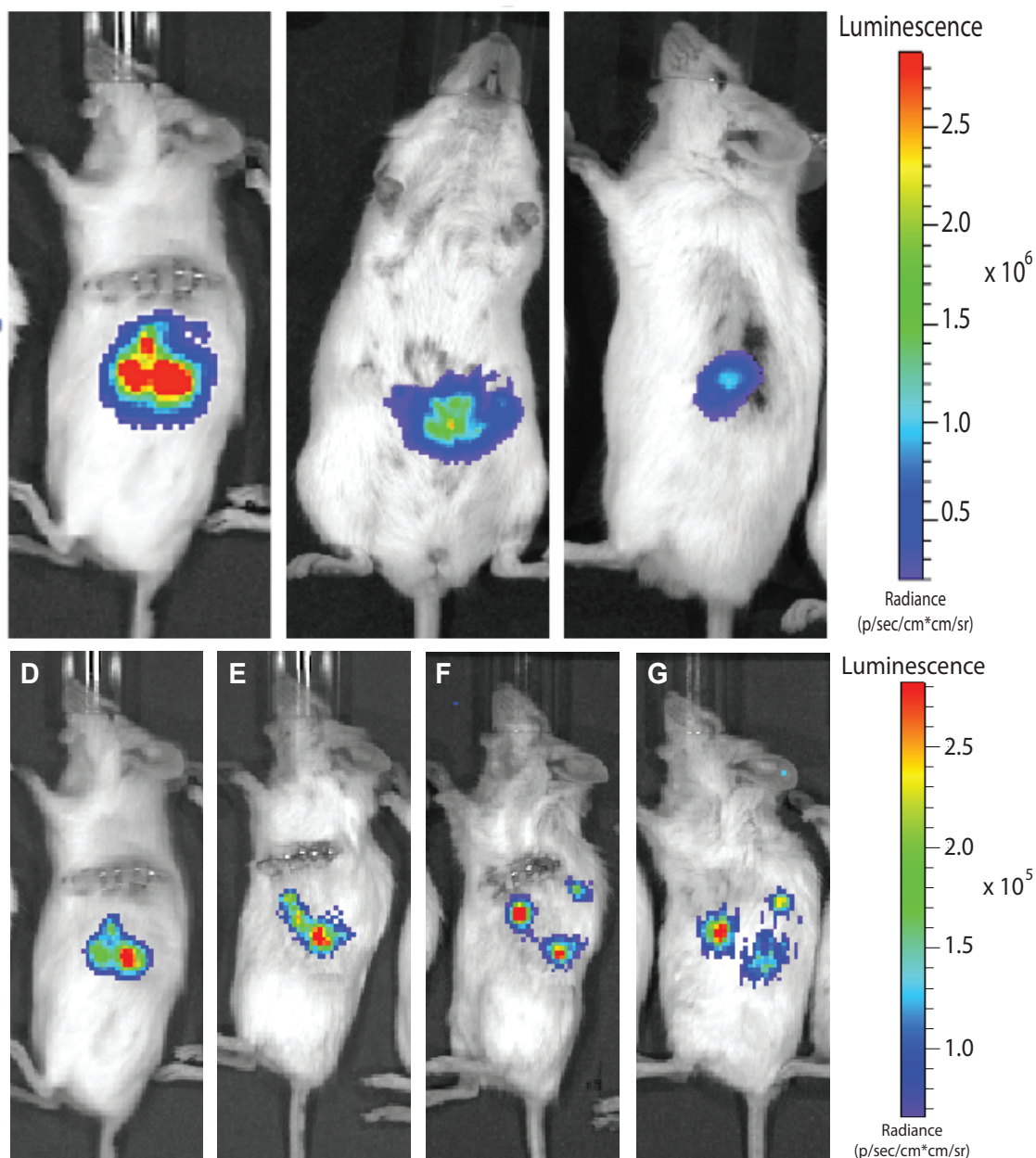


Figure 12 *In vivo* device image and tracking.

A) Device with encapsulated MIN6 cells implanted in the subcutaneous space of the mouse dorsal. **B)** Device with encapsulated MIN6 cells implanted under the mouse skin and muscle over the liver. **C)** No device control with cells

implanted directly into the kidney capsule. D) Device with encapsulated MIN6 cells implanted after 1 day, E) 30 days, F) 90 days.

Ideal immune protection requires physically excluding immune cells as well as restricting diffusion of immune mediators such as cytokines that are toxic to beta-cells. By encapsulating cells in microporous devices cell-contact-mediated immune protection may be achieved, additional cytokine-mediated immune protection may be accomplished with the nanoporous devices. Cells encapsulated in thin-film devices are physically compartmentalized from the *in vivo* environment, as clearly seen in **Figure 13A**, where cells are attached to the outer surface of the device but no infiltration into the device lumen was found.

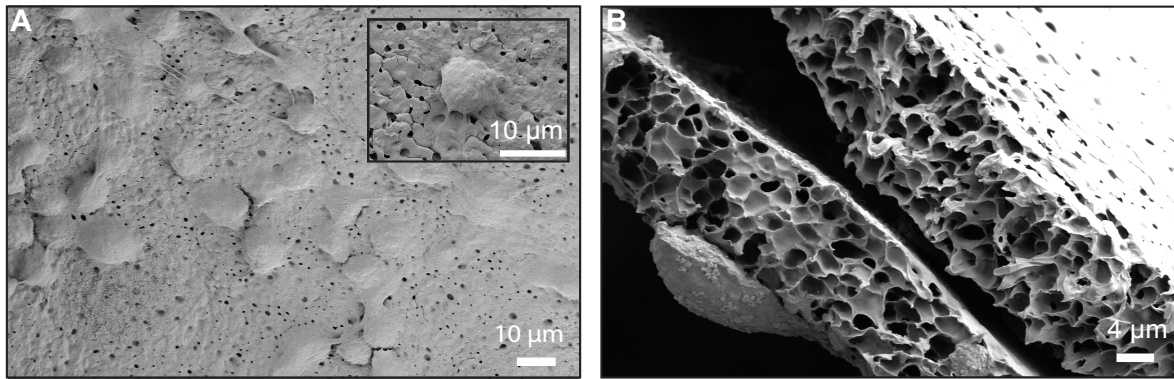


Figure 13 Microporous barrier inhibits cell-invasion.

A) Top down SEM image of cells attached to the exterior surface of the microporous thin-film device after 1 month *in vivo*. B) Cross-section SEM image of the microporous thin-film device after 1 month *in vivo*,

demonstrating membrane integrity and isolation of internal and external cells.

Despite cell adhesion on device surfaces, pores remain unclogged (**Figure 14**) most likely due to the limited fibrotic response of the surrounding tissue.

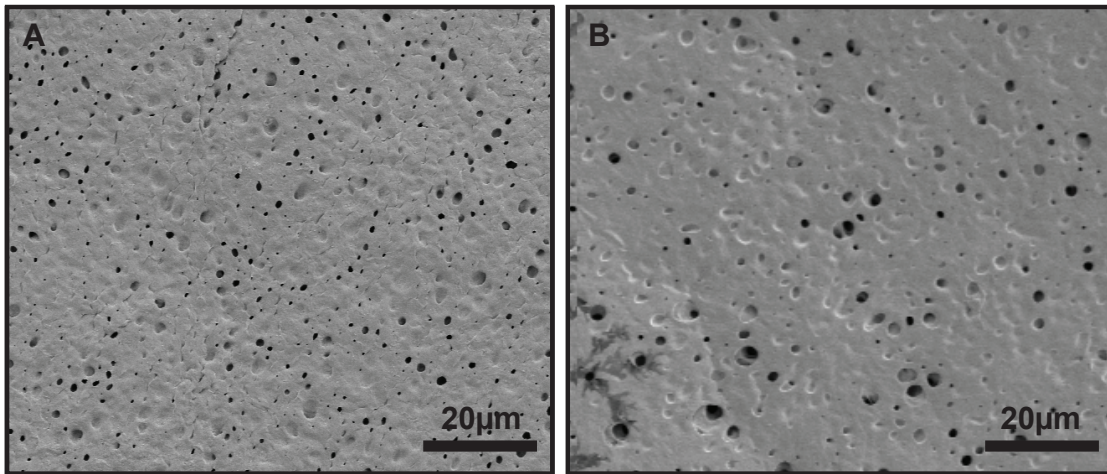


Figure 14 Device exterior SEM.

A) Device exterior prior to implantation. B) Device exterior after 2 months *in vivo*.

Figure 15B shows a SEM cross-section, with a cell attached to the external surface of a device. No cellular processes are seen extending into the device, further confirming the ability of the device to prevent cell-contact-mediated interaction by isolating the encapsulated cells from the surrounding *in vivo* tissue. By further controlling the porosity of the membrane, cytokine-mediated immune protection

may additionally be achieved. Tumor necrosis factor α (TNF α), interleukin 1 β (IL1 β), and interferon γ (IFN γ) inflammatory cytokines are known to kill beta-cells individually, and act synergistically when present in combination. They were chosen in order to test the devices' ability to protect from cytotoxic cytokines.¹³⁹⁻¹⁴² (Figure 15).¹⁴³⁻¹⁴⁵

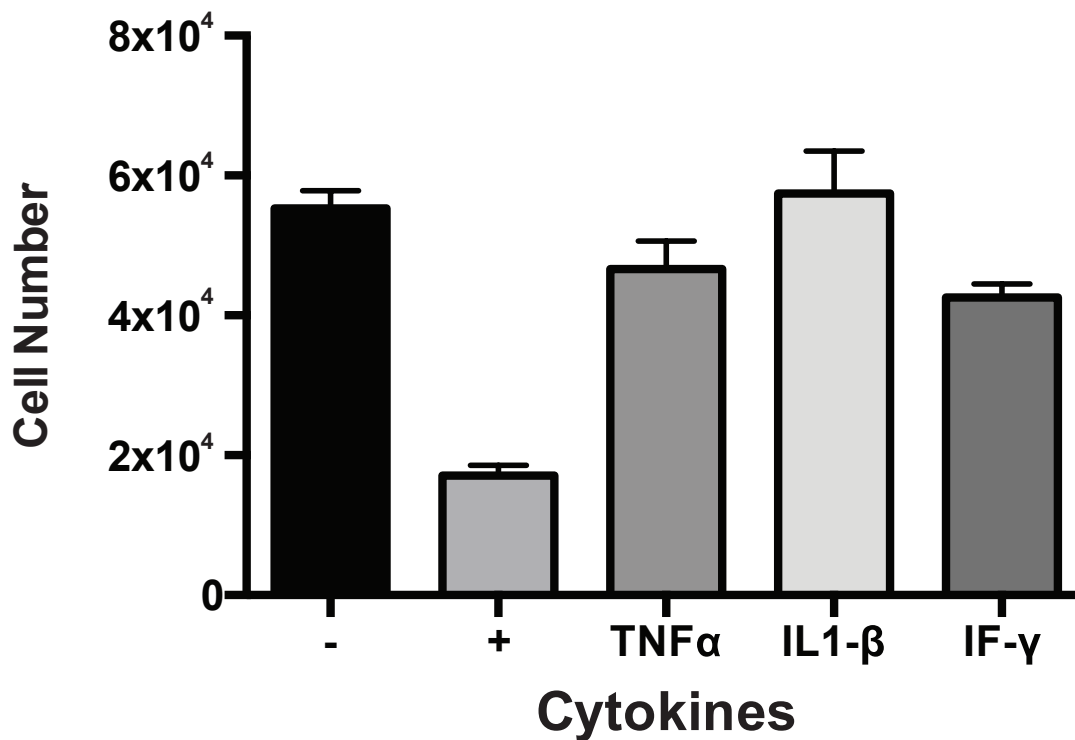


Figure 15 Cytokines affect cell viability.

Cell number was quantified by a cyquant assay (none) no cytokine control, (all) a combination of cytokines with TNF alpha, IL1 beta and IF gamma, and (TNF α), (IL1 β) and (IF γ) individually.

Interestingly, whereas microporous thin-film devices failed to maintain cell viability (**Figure 16A**), the use of a nanoporous layer in these thin-film devices mitigated the cytokine-mediated decrease in viability (**Figure 16B**). It is unclear if cytokines are completely isolated from the lumen of devices, given the size of cytokines in relation to the nano-pores a portion of cytokines are expected to pass through the membrane. The protection by nanoporous devices would result from limited transport and diffusion of cytokines through the membrane, such that the cells are unresponsive to the reduced cytokine concentrations. Considering the cytokine cocktail concentration used exceeds known cytotoxic concentrations by 10-fold, we expect the majority of the cytokines to be limited by the nanoporous barrier. This further highlights how microporous and nanoporous membranes can be used to control desired cell responses.

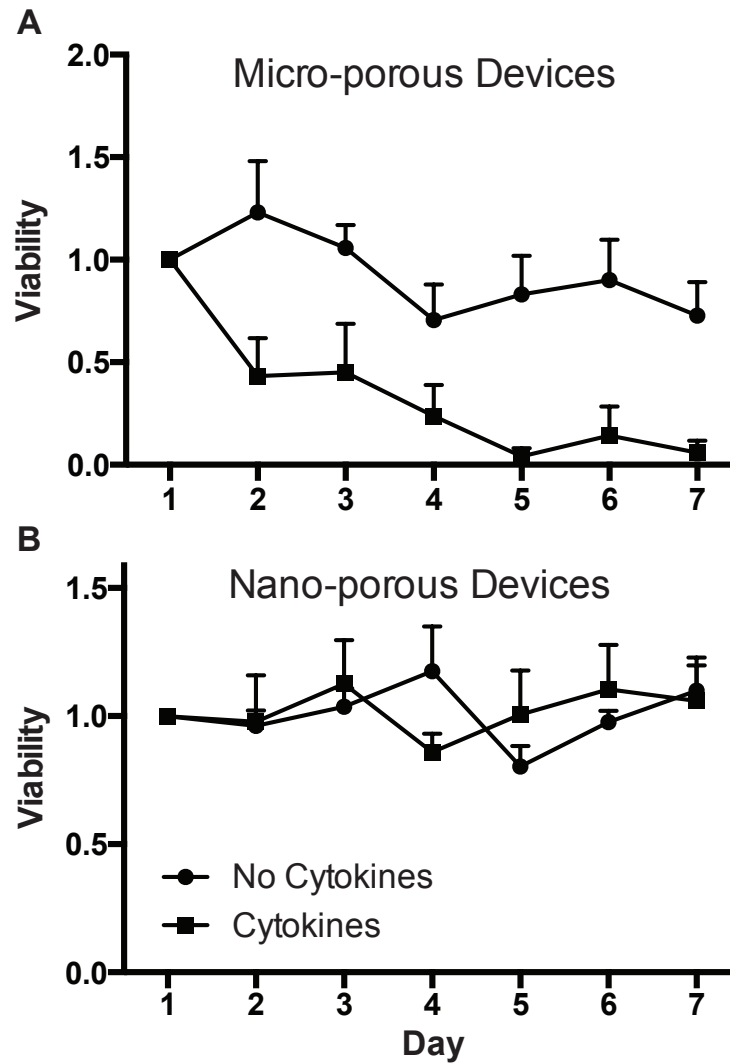


Figure 16 Cytokine protection.

A) Viability of cells within a microporous devices and B) a nanoporous devices over 1 week, with (solid line) and without (dashed lines) cytokines. (n ≥ 4)

Device vascularization *in vivo* is imperative for long-term survival of encapsulated cells. Vascularization surrounding cells encapsulated in thin-film devices is important for function and survival of encapsulated cells. To monitor the

state of device vascularization, devices were implanted, then removed and imaged at 7, 14, 30 and 90 days (**Figure 17A-D**). The first visible signs of vascularization of cell encapsulated thin-film devices, were observed 14 days after implantation (**Figure 17B**). These devices demonstrate a steady increase *in vivo* vascularization of 1.5% daily over a 2-month period (**Figure 17E**).

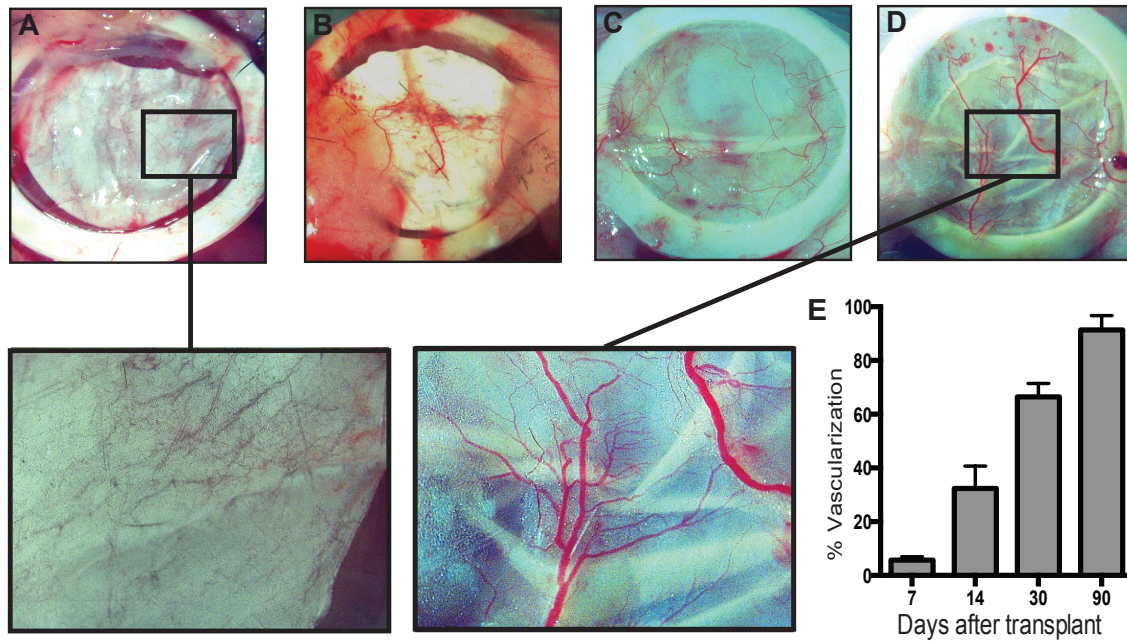


Figure 17 Device vascularization.

Bright field images of devices implanted after A) 7 days, B) 14 days, C) 30 days and D) 90 days, with magnified images at day 7 and day 90. E) Quantification of device vascularization from day 7 to day 90. (n = 3)

Vascularization of these PCL devices occurs without any supplementary additional proangiogenic factors, as shown with implanted cell-free devices with

similar vascularization (**Figure 18A, B**). When compared with common polymeric implant materials PLGA (**Figure 18C**) and PVDF (**Figure 18D**), PCL cell-free devices exhibit noticeably more developed and branched vasculature.

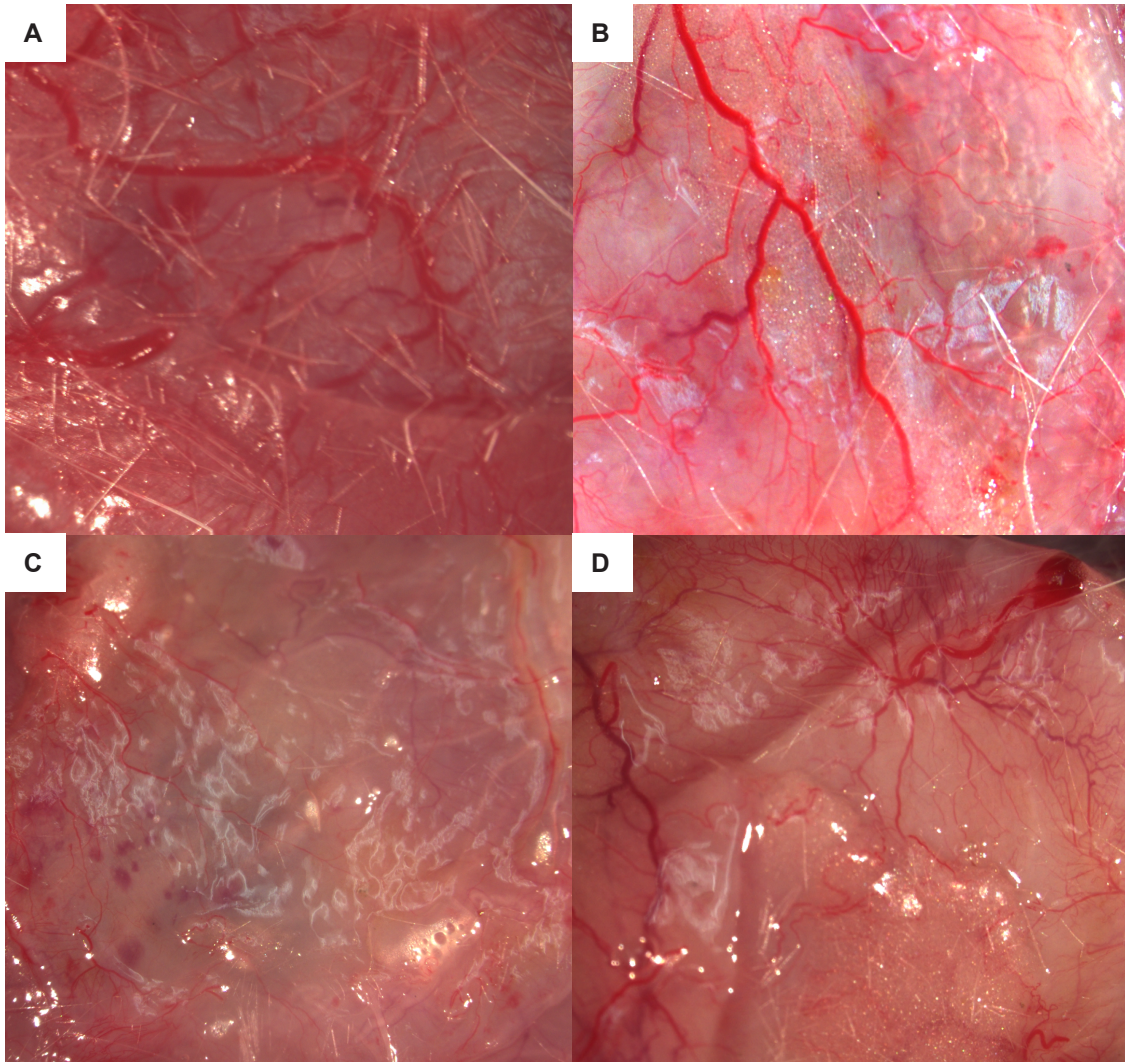


Figure 18 Cell-free device controls for device vascularization.

Bright field images of devices implanted after 50 days A) Porous-PCL, B) Non-porous PCL, C) PLGA, and D) PVDF.

Furthermore, we believe the combination of thin size of the PCL devices, their flexibility, and the structure of the devices provides a relatively minimal foreign body response (**Figure 19**).

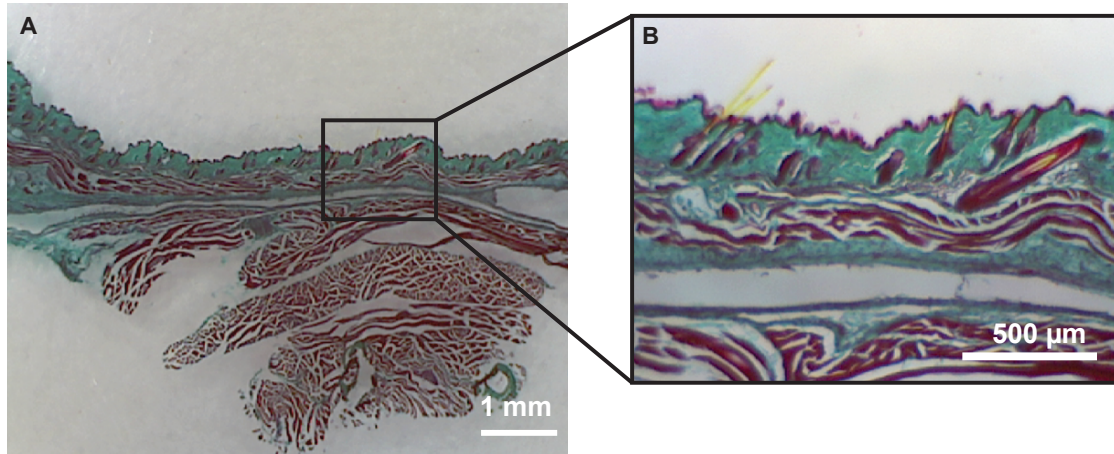


Figure 19 Histology of devices.

A) Cross section of a device after 2 months *in vivo*, with Masson trichrome staining. B) Magnification of device cross-section, demonstrating minimal fibrotic response.

Conclusion:

Here we demonstrate the successful fabrication of an innovative cell-encapsulating device that combines some of the benefits of both micro- and macro-encapsulation strategies. A flexible thin-film geometry allows precise membrane porosity selection to direct desired cellular responses and interactions, while maintaining a normal glucose response of encapsulated beta-cells. A small reservoir

volume allows a rapid response to external stimuli, limiting dilutional interference from the device reservoir. Similar to microencapsulation devices with large surface area to volume ratios, our thin-film device structure is uninhibited by device thickness. Moreover, cells encapsulated in either micro- or nano-devices demonstrate a glucose stimulation index consistent with unencapsulated cells, indicating glucose sensing and responsive insulin secretion is successfully preserved. These devices allow sufficient bioluminescence transmission through the device membrane to be measured with *in vivo* imaging systems. As demonstrated *in vivo*, these device membranes create a physical barrier between encapsulated cells and the host environment, physically preventing cell contact initiated signaling. Furthermore, incorporation of a nanoporous membrane enables these devices to obstruct cytokine passage and protect encapsulated cells from cytokine-mediated cell death. Additionally, *in vivo* studies show vascularization around the devices with limited fibrosis, which displays great promise for this device as a long-term cell encapsulation device.

This technology platform can be used to directly investigate the cell contact-dependent or soluble factor-mediated signaling by controlling pore dimensions-inhibiting specific interactions. These devices have the capacity to prevent immune cell contact with encapsulated cells, and the nanoporous device can protect encapsulated cells from cytokine-induced cell death. Future directions include using these devices *in vivo* to investigate modes of immune attack, whether contact- or soluble factor-mediated. Given the nature of these thin-film cell-encapsulation

devices, future generations could be scaled for humans, as alternative treatments for Type 1 Diabetes.

Materials and Methods:

Chemicals were purchased from Sigma Aldrich unless noted and cell culture materials were purchased from the UCSF cell culture facility. All films were spun onto silicon wafers at 1000 rpm for 30 seconds followed by 2000 rpm for 30 seconds. Devices were characterized with a Carl Zeiss Ultra 55 Field-Emission Scanning Electron Microscope using an in-lens Secondary Electron detector.

Microporous thin-film fabrication

Microporous PCL thin-films were spun from a solution of 150 mg/mL PCL (70-90 kDa Mn) and polyethylene glycol (PEG, 2kDa Mn) in 2,2,2-trifluoroethanol, which was prepared by stirring at 65 °C until dissolved. Following spin casting, the PEG was dissolved by soaking in water for 1 hour, resulting in a microporous PCL films with pores approximately 2 μm in diameter. Devices were 1 cm in diameter resulting in a surface area of 1.57 cm^2 per side, with 67.5 ± 1.3 percent porosity and 0.37 ± 0.02 density.

Nanoporous thin-film fabrication

Nanoporous PCL films were formed using an established template-based approach reported elsewhere¹²⁵. Briefly, a 0.5 M solution of zinc acetate dihydrate and ethanolamine in 2-methoxyethanol was spun onto silicon wafers and

annealed at 300 °C on a hotplate to generate a zinc oxide (ZnO) seed layer. From this seed layer, ZnO nanorods were hydrothermally grown in a 5 mM zinc acetate solution at 85-90 °C for two hours. A 150 mg/mL PCL solution was then spuncast onto the nanorods followed by a 150 mg/mL PEG:PCL solution to provide a microporous support, creating a nanoporous film with a microporous backing support layer. The film was soaked in a dilute sulfuric acid solution to etch away the ZnO nanorods and also dissolve the PEG, resulting in a nanoporous membrane with pores ranging from 30 nm to 100 nm supported by a microporous backing. Membrane characterizations and ZnO nanorod morphology were previously measured.^{124,125,128}

Non-porous membrane fabrication

Non-porous PCL films were spuncast from a solution of 150 mg/mL PCL (70-80 kDa Mn) in 2,2,2-trifluoroethanol, which was prepared by stirring at 65 °C until dissolved. Non-porous poly(lactic-co-glycolic acid) (PLGA) films were spun cast from a solution of 300 mg/mL PLGA (85:15 LA:GA 45 kDa Mn) in 2,2,2-trifluoroethanol. Polyvinylidene fluoride (PVDF) film were prefabricated from Sigma and cut to shape.

Assembly of thin-film devices

Devices consisted of two PCL thin-films heat-sealed together using resistive heating of a nichrome wire. A two-step heat-sealing method was used where 1.2 Amp current ran through a nichrome wire outlining the regions to be sealed. For the first sealing step, two films were placed over a U-shaped nichrome wire embedded

in PDMS (Sylgard 184), 1 cm in diameter. To secure the membranes a PDMS weight was placed over the films holding them flat. A 1.2 Amp current ran through the wire for 30 seconds and sealed the devices in the shape of a U, defining the device lumen shape and leaving an open side for cell injection. 1.5 Million MIN6 cells in high glucose Dulbecco's Modified Eagle's (DME) were injected into the devices through the remaining open side. Second, the remaining side of the device was sealed by placing the open edge over a straight nichrome wire embedded in PDMS and heat-sealed with a 1.2 Amp current for 30 seconds.

Characterization using scanning electron microscopy of films and devices

Micro- and nanoporous thin PCL films were mounted on a flat SEM mount with colloidal graphite (Ted Pella, Inc.). Cross sections were flash dipped in isopropanol followed by liquid nitrogen freeze fracture and then mounted. Devices from *in vivo* experiments were fixed with 3.7% formaldehyde for 30 minutes, washed in deionized water three times, then sequentially dehydrated in increasing ethanol concentrations and mounted.

Cell culture

MIN6 cells were cultured using standard media conditions.¹⁴⁶ Genes for mCherry and puromycin resistance were introduced using a lentivirus construct designed by the Lentiviral Core at UCSF. The cells were transduced using standard protocol with a multiplicity of infection of 2, and transduced cells were selected using puromycin. Genes encoding firefly luciferase and green fluorescence protein

were similarly introduced into MIN6 cells. Primary islets were isolated by the Islet Core at UCSF using standard islet isolation protocols.¹⁴⁷

Glucose stimulated insulin secretion

Insulin secretion was analyzed using a glucose stimulated insulin secretion assay. Cells were rested for 30 minutes in medium-containing 5 mM glucose and then stimulated using medium-containing 15 mM glucose. Culture supernatant was collected at 30 and 60 minutes after addition of high glucose. Insulin protein content in the culture supernatant was measured using an enzyme linked immunosorbant assay (Mercodia). The ratio of insulin secreted at high to low glucose conditions was used to calculate the glucose stimulation index.

Cytokine assay

To determine the effect of cytokines on the viability of encapsulated beta-cells, 250,000 cells in micro- or nanoporous devices were cultured in a cytokine cocktail consisting of TNF α (300ng/mL; VWR), IL1 β (110 ng/mL; VWR) and IFN γ (200ng/mL; Fisher) in high glucose DME media, with 10% fetal bovine serum, 1% penicillin, and 1% streptomycin. The devices were imaged daily for the mCherry signal using a standard spectrophotometer. The signal intensity was measured for each respective device for 7 days, and normalized against the initial signal.

Bioluminescent imaging

Thin-film devices with luciferase-expressing MIN6 (MIN6.LUC) cells were implanted, in either the subcutaneous space on the dorsal aspect, the abdominal cavity between the muscle wall and the liver of MOD.Cg-*Prkdc*^{scid} *Il2rg*^{tm1Wjl}/SxJ

(NSG) or BALB/C mice. Persistence of the encapsulated cells *in vivo* was assessed by monitoring luciferase activity using a Xenogene IVIS 200 imaging system (Perkin Elmer). The animals transplanted with MIN6.LUC cells, were injected IP with D-luciferin solution (Goldbio, St. Louis, MO) at the dose of 150mg/kg 8 minutes before imaging in order to capture the peak in bioluminescent intensity, as previously described¹⁴⁸. The mice were anesthetized with an isoflurane mixture (2% in 98% O₂) and imaged by using a Xenogen IVIS 200 imaging system. Bioluminescent images were acquired for 1 minute and then analyzed using the Living Image analysis software (Xenogen Corp., Alameda, CA). Regions of interests (ROI) were centered over the bioluminescent regions. Photons were counted within the ROI over the acquisition time. Adherence to the same imaging protocol ensured consistent signal detection and allowed us to compare data acquired over a period of at least three months.

Histology

Mouse tissue samples were collected and fixed in 4% paraformaldehyde for 24 hours, washed with phosphate buffered saline at 4 °C for 48 hours, then 30% sucrose for 24 hours. Samples were then taken to the Mouse Pathology Core at UCSF and Optimal Cutting Temperature (OCT) embedded, sliced, and Hematoxylin and Eosin stained or Masson Trichrome stained by either the Mouse Pathology Core or the Histology and Imaging Core at UCSF.

Vasculature

At 7, 14, 30, and 90 days after transplantation, PCL device-bearing mice were anesthetized with an intraperitoneal injection of Avertin solution 2.5% (Sigma) and subjected to optical imaging using a Leica MZ16F microscope (Leica Biosystems, Wetzlar, Germany). The animals were euthanized by cervical dislocation and the encapsulated devices were collected for further analysis. The images of the encapsulated grafts were analyzed using ImageJ software (NIH; <http://rsb.info.nih.gov/ij/>). Vessel density was measured by automated counting of red pixels divided by the area of the ROI within the device; a threshold was previously set for the red channel to subtract background.

Acknowledgements

The authors would like to thank Juvenile Diabetes Research Foundation, NIH P30DK063720 for UCSF Diabetes and Endocrinology Research Center, and Larry L. Hillblom Foundation fellowship (GF) for funding. The authors would like to thank Jessica L. Allen, Erica B. Schlesinger, Laura A. Walsh and Miquella G. Chavez for critiquing the manuscript, and members of the Desai laboratories for insightful discussion and conversations. The authors would also like to thank Erica B. Schlesinger additionally for her insight and expertise in material properties. The authors would also like to thank the Nikon Center at UCSF for Imaging, and the Center for Advanced Technologies at UCSF.

Disclosure

This chapter is a variation of the material as it appears in Nyitray et. Al. ACS Nano. It appears here with the permission from the authors.

Chapter 3: Nano Particle Diagnostics – Porphyrin-based Nanoparticles for Luminescent Oxygen Detection

Keywords: Nanoparticles, oxygen detection, heme-based dyes, diagnostics

Abstract:

Oxygen exchange is necessary for a variety of biological functions. One obvious requirement for cellular viability is adequate nutrient exchange, such as oxygen. Here we describe the development of a porphyrin-based nanoparticle system that can be used as tool to monitor oxygen availability by measuring changes in luminescence. The oxygen sensing nanoparticles are formed from the inter-polymerization of a porphyrin dye MAPB, maximizing sensing dye load per particle, and are covalently attached to a hydrogel. Here we demonstrate that the formation of the particles from the dye improves oxygen sensitivity, and furthermore that the integration of the particles into a hydrogel further improve oxygen sensitivity of the system. The design of this oxygen sensing system, uses standard acrylate chemistry to attach the nanoparticles to the hydrogel, and thus we believe these particles can be readily incorporated into a variety of alternative materials. Having an oxygen detecting nanoparticle that can be readily attached to a variety of materials, affords an elegant tool to easily add oxygen sensing functionality to a variety of materials.

Introduction:

Oxygen is a necessary molecule for all biological systems. Monitoring oxygen tension can help prevent cellular hypoxia from limited oxygen diffusion, transport and availability - a leading cause of cell death and tissue damage^{138,149-151}. Accordingly, accurate oxygen monitoring is important for a number of treatments requiring tissue transplantation and implantation where proper oxygen diffusion and exchange are required for tissue survival. Current oxygen probes are invasive and limited by tissue location and depth, restricting effective oxygen monitoring.

To overcome this challenge, porphyrin-based dyes, derived from hemoproteins, have been developed to bind oxygen and photo-actively respond to changes in oxygen availability (PROFUSA Ref). These dyes provide a great tool for detecting changes in oxygen, however, are unable to be used as hypoxia monitors or detectors. This highlights an inherent need to develop novel oxygen sensing platforms that harness the various advantages of porphyrin-based dyes.

Nanoparticles are useful tools because they bridge the gap between the properties of bulk materials and molecular interactions, by forming bulk materials on the nano scale¹⁵²⁻¹⁵⁷. Nano-sized materials have both functional and structural uses that can be applied in a variety of biological settings where chemistry alone is inadequate¹⁵⁸⁻¹⁶¹. To develop nanoparticles in a variety of sizes and shapes, an assortment of constantly evolving technologies and techniques have been developed^{157,162-164}.

In the biomedical field, nanoparticles are of great interest for their diverse applications in drug delivery and diagnostics^{152-156,165-172}. Creating nanoparticles of

oxygen sensing dye can enhance the stability and function of the dye¹⁷³. More recently, nanoparticles are being used to add multiple layers of functionality to a bulk material^{156,164,174,175}. By incorporating multiple functional nanoparticles to a bulk material, the function of a composite material can be enhanced, creating additional complex materials. With nanoparticles providing multiple functions to a bulk material, the physical and functional properties of the material can be decoupled. This allows the mechanical properties of the material and the functional properties of the material to be individually tuned, simplifying the chemistry and formulation necessary to have complex, interesting multifunctional materials.

Here we present a nanoparticle system that could be used to overcome the challenges of limited oxygen detection with improved stability. By cross-linking nanoparticles into a biocompatible hydrogel, we have demonstrated a significant improvement over traditional oxygen sensing dyes alone. Combining nanoparticles that photo-actively respond to changes in oxygen in biocompatible materials provides a noninvasive way to monitor cellular oxygen tension *in vitro* and *in vivo*. Further developments would allow this sensor to be implanted in tissue and monitor oxygen levels with an external detector, providing non-invasive, continuous hypoxia monitoring.

Results and Discussion

Detecting oxygen levels of biological systems is crucial for monitoring cellular oxygen tension and preventing hypoxia in low oxygen conditions. Porphyrin-based dyes, derived from hemoproteins in red blood cells, are known to

transport diatomic gases such as oxygen. Here we use a porphyrin-based dye, MAPB, to make nanoparticles (MAPB-nanoparticles), hydrogels with cross-linked dye (MAPB-hydrogel) and composite hydrogels with MAPB-nanoparticles (MAPB-composite). MAPB was designed to have a near-infrared (NIR) emission wavelength of 805 nm, which travels further through the skin than higher-energy wavelengths^{3,176} (PROFUSA REFERNECE) to allow improved oxygen detection. Additionally, MAPB's four methacrylate handles that branch off the porphyrin ring allow inter-molecular reactions, which result in creation of nanoparticles composed of dye alone. Figure 20, outlines the method for synthesizing these particles and embedding these particles within a hydrogel to form the sensing composite (MAPB-composite)

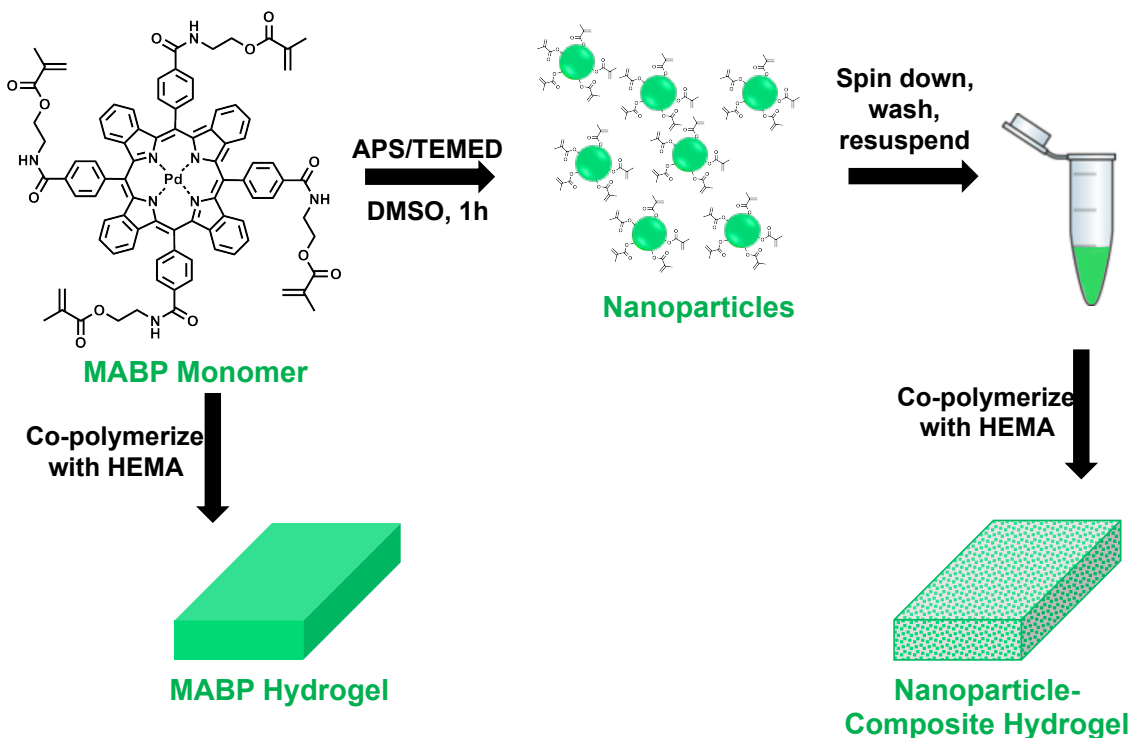


Figure 20 Nano particle synthesis.

A) MAPB an oxygen sensing dye was polymerized into B) MAPB-nanoparticles using radical chemistry. C) The MAPB-nanoparticles were then isolated and polymerized into a hydrogel creating the D) MAPB-composite.

After formation of the MAPB-nanoparticles through APS/TMED initiated polymerization of the free dye in solution, methacrylate groups remain available on the particles and can be reacted to other acrylated materials. The ability to covalently attach the MAPB-nanoparticles to the desired material eliminates the possibility of dye or particle leaching over time. Since the formation of the hydrogel and the particles are isolated, the concentration of the particles can be tuned, the hydrogel can be exchanged, and the overall shape of the composite can be adjusted individually, giving more control over the system.

To confirm the spectral properties of the MAPB-free dye were conserved during the synthesis of the MAPB-nanoparticles, absorbance spectra of the MAPB-free dye, MAPB-nanoparticles, MAPB-hydrogel and MAPB-composite gel were measured (Figure 2 A). No significant wavelength shifts or spectral differences were evident suggesting that the porphyrin dye structure remains intact after nanoparticle formation. Furthermore, when the MAPB-hydrogel and MAPB-composite hydrogel are excited at 440 nm, both have a more intense fluorescence emission than both the MAPB-free dye and MAPB-nanoparticles in solution (Figure 21 B). This is most likely due to decreased aggregation of the dye in a hydrogel matrix relative to that which occurs in solution. The physical compartmentalization of MAPB-nanoparticles in the MAPB-composite limits energy transfer between

MAPB molecules and MAPB-nanoparticles in the hydrogel promoting an improved response.

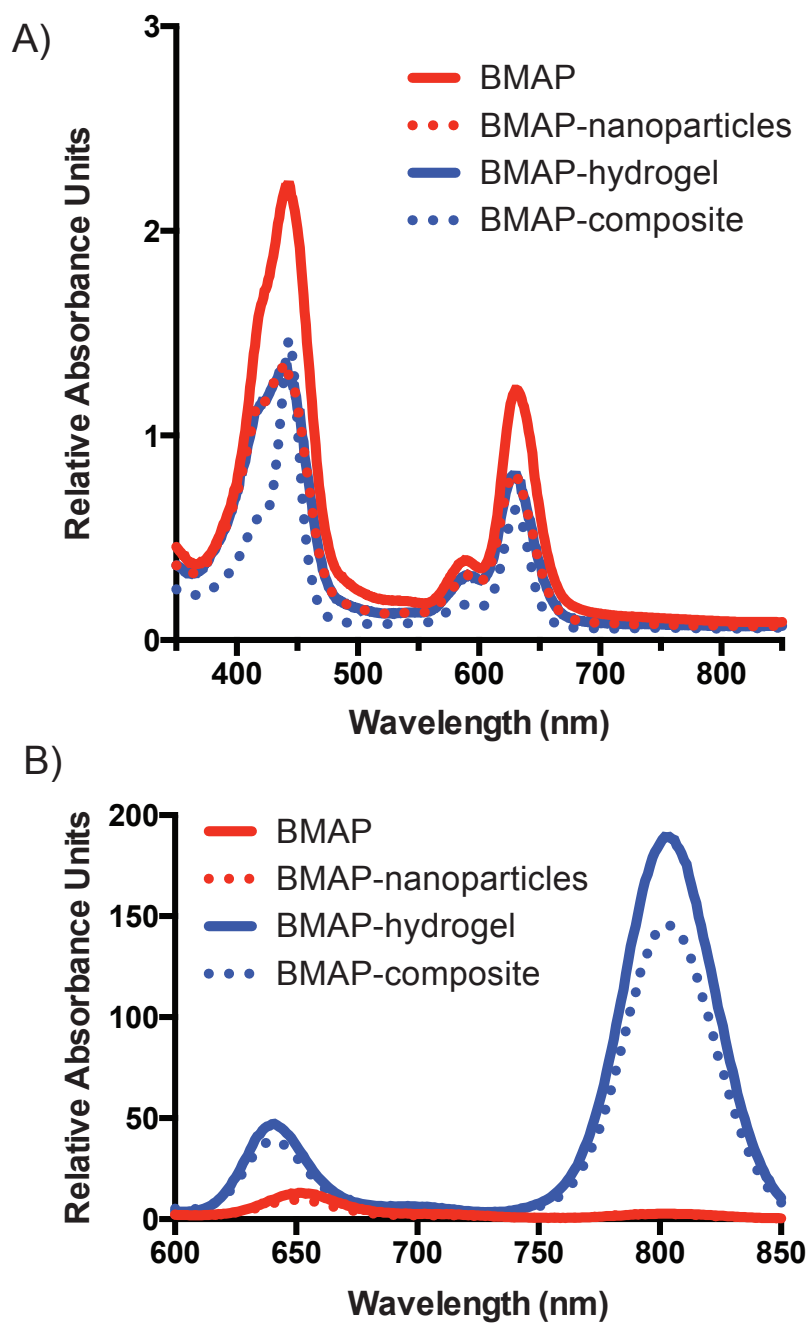


Figure 21 Spectroscopy of MAPB-free dye, MAPB-nanoparticles, MAPB-hydrogel and MAPB-composite.

A) Absorbance profile of MAPB-free dye, MAPB-nanoparticles, MAPB-hydrogel and MAPB-composite in solution from 350nm to 850nm. B) Emission spectra of MAPB-free dye, MAPB-nanoparticles, MAPB-hydrogel and MAPB composite in solution when excited at 440 nm and read from 700nm to 850 nm.

To measure MAPB-nanoparticle size, a scanning electron microscopy (SEM) image of the particles was taken (Figure 22 A). These particles are spherical in shape and measure approximately 100 nm in diameter(Figure 22 B). The size and property of the particles allows easy dispersion into various polymer materials. Moreover the addition of nanoparticles into the hydrogel composite has an unnoticeable effect on the mechanical properties of the bulk material. By maintaining a small particle size, the surface area-to-volume ratio of the sites available for sensing is maximized, which could enhance the function of these particles.

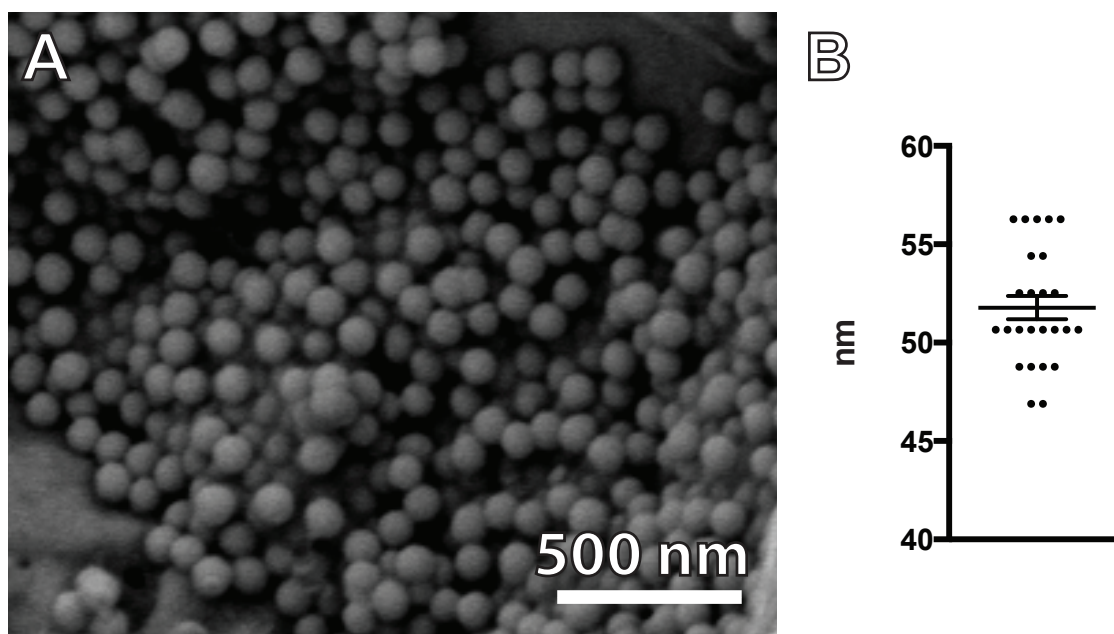


Figure 22 Size characterization.

A) Scanning electron microscopy of MAPB-nanoparticles. B) Average radius of nanoparticles measured from the SEM.

Palladium porphyrins are known for their oxygen-dependent luminescence^{177–181}. Both the MAPB-hydrogel and the MAPB-composite respond to the changes in atmospheric oxygen. In Figure 23, MAPB-hydrogel and MAPB-composite samples were cycled between normoxic and hypoxic conditions and their fluorescence response to oxygen was measured. The relative fluorescence is normalized to the initial normoxic condition, where the 2.5 to 3 fold increase in relative fluorescence highlights the ability of the MAPB-hydrogel and MAPB-composite materials to detect changes in atmospheric oxygen. This further demonstrates the MAPB-composite’s potential utility as a tool to monitor hypoxia.

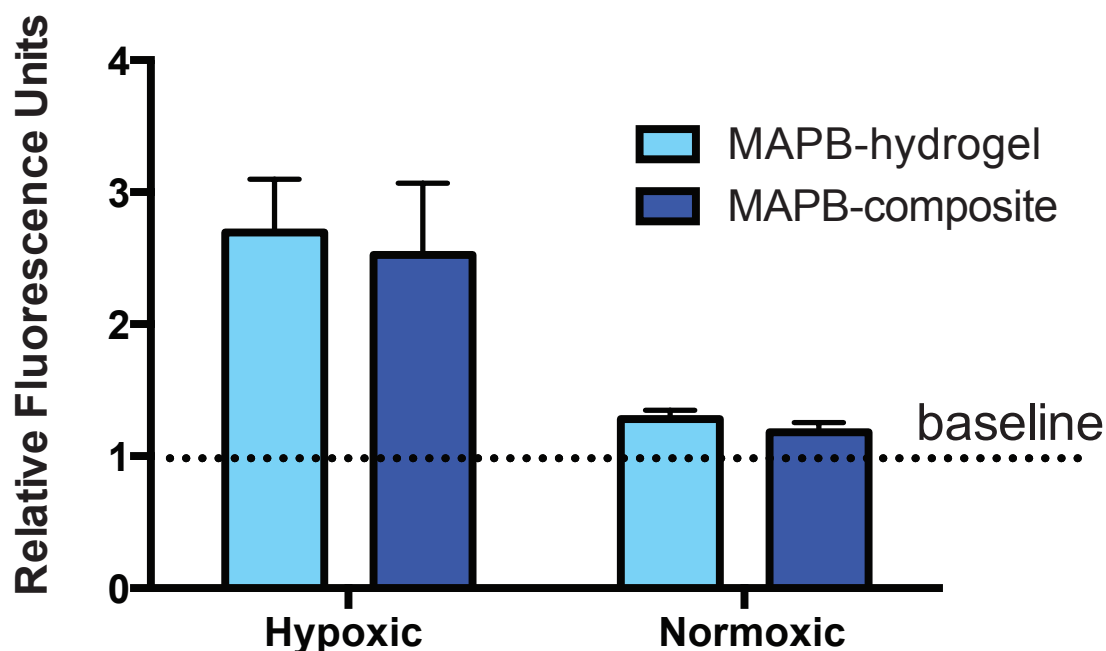


Figure 23 MAPB-hydrogel and MAPB-composite hypoxia detection.

MAPB-hydrogel and MAPB-composite demonstrate increased relative absorbance units, with decreased oxygen concentration.

Importantly, the MAPB-composite significantly outperforms the MAPB-hydrogel, and both MAPB-composite and MAPB-hydrogel outperform MAPB-free dye and MAPB-nanoparticles. In Figure 24, the relative fluorescence of MAPB-nanoparticles is greater than that of the MAPB-free dye, and the MAPB-composite is greater than that of the MAPB-hydrogel. In both solution and hydrogel conditions the nanoparticles in either solution or hydrogel outperform the free dye.

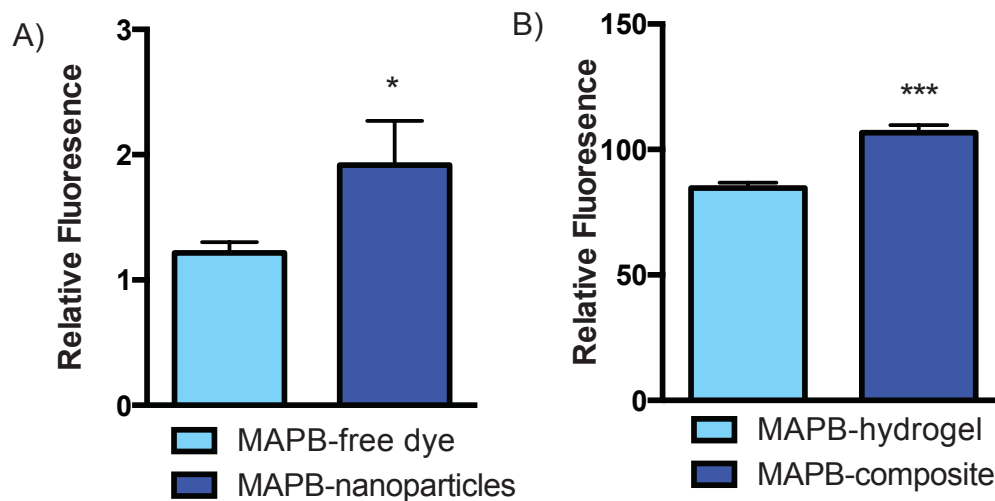


Figure 24 MABP detection.

A) MAPB and MAPB-nanoparticles relative fluorescence. B) MAPB-hydrogel and MAPB-composite relative fluorescence.

Furthermore the MAPB-composite has more than 100 times greater sensitivity than MAPB-free dye in solution. In addition to increased sensitivity, the MAPB-nanoparticles display enhanced photo-stability relative to MAPB-free dye in both solution and hydrogel formulation (Figure 25).

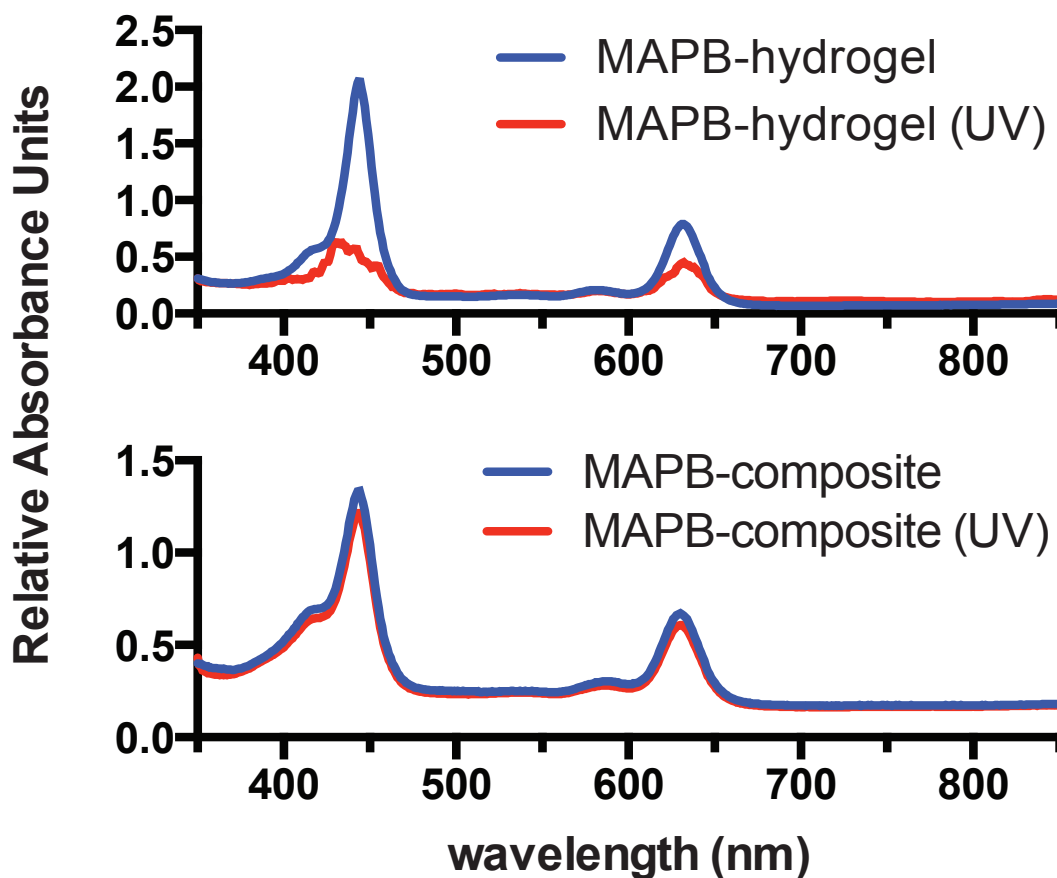


Figure 25. Hydrogel and composite degradation profile.

MAPB-hydrogel (top) and MAPB-composite (bottom) relative absorbance units before (blue) and after (red) UV treatment.

Conclusion

In conclusion, the MAPB-nanoparticles provide a simple way to make a variety of oxygen sensing materials. The acrylate handles can easily be reacted with many polymers, affording a simple way to increase complexity and function. The ability to incorporate predesigned functionalities in nanoparticles allows a material

to be designed without affecting the formulation or mechanical properties. Further development of these composite materials could provide a simple, non-invasive method to track oxygen tension, especially in tissue engineering fields where monitoring vascularization, and oxygen availability is necessary. With the growing advancements in sensor and wearable biometric readers, this technology could easily be incorporated and expanded to provide a more accurate health profile.

Materials and Methods:

All chemicals were purchased from Sigma Aldrich unless noted. All experiments were done with at least 3 replicates, and analyzed with an Anova.

Synthesis of MABP Nanoparticle

Oxygen sensing nanoparticles were formed using free radical chemistry. Briefly, 1mg of MAPB (Pd-Tetramethacrylate benzoporphyrin) dye, generously provided by by PROFUSA Inc. CA, was dissolved in 900uL of dimethyl sulfoxide (DMSO). Next, 0.5mg of ammonium persulfate (APS) dissolved in 90ul of DMSO, followed by 10 uL of tetramethylethylenediamine (TMED) (Biorad) were added. The reaction was covered from light and stirred for 1 hour at room temperature, resulting in nanoparticle formation from the inter-crosslinking reaction of the dye. To isolate the particles, the solution was spun at 15000 RPM using a Centrifuge 5424 (Eppendorf) for 30 minutes to pellet the particles. The clear supernatant was removed and the green pellet was washed with DI water and sonicated for 10 minutes to separate the aggregated particles. This solution was repelleted at 1500

RPM, the supernatant was removed and the pelleted particles were dissolved in 1mL of DMSO creating a stock solution of 0.001mg/uL.

Dye-hydrogel composite formation

To make the hydrogel composite, 2mg of 2,2'-Azobis[2-(2-imidazolin-2-yl)propane]dihydrochloride (VA-044, Waco) was dissolved in 40uL of ethylene glycol. Next, a 100 uL solution of (HEMA/TEGDMA, 98/2 molar ratio) was added. Next, 40uL of the free-dye or particle-dye DMSO solution at 0.001 mg/uL was added, followed by 20 uL of DI water. The solution was cast in a glass mold and flushed with nitrogen for 2 minutes. The reaction was thermally polymerized at 45C for 4 hours. The polymerized hydrogel was removed from the mold, and excess, unreacted monomers were removed by immersing the gels in pH 7.4 phosphate buffered saline (PBS) for 12 hours.

UV Dye Stability Study

Nanoparticles and free dye in a HEMA/TEGDMA hydrogels were illumined in a UV box at 30 joules, for 30 minutes to initiate photo-degradation. The absorbance profile of the samples was read from 350 nm to 850 nm.

Oxygen sensing study

MAPB-hydrogel and MAPB-composite slabs were synthesized and disks were cut using a 5mm punch. These discs were submerged in 200ul of PBS and nitrogen bubbled with nitrogen for 30 minutes, to create a low oxygen environment. Samples were then excited at 440 nm and read at 805 nm as oxygen returned to the sample over a period of 30 minutes.

Plate reading setup

Samples were read using a SpectraMax M5 (Molecular Devices) plate reader. The absorbance profile was used to determine the excitation wavelength. The free dyes, nanoparticles and composites had a 440 nm excitation and 805 nm emission wavelength.

Size analysis:

Nanoparticles were characterized with a Carl Zeiss Ultra 55 Field Emission Scanning Electron Microscope using an in-lens SE detector. Nanoparticle size was measured with ImageJ (<http://imagej.nih.gov/ij/>). The circumference and area was used to calculate the radius.

Acknowledgements

The authors would like to thank the NIH and NSF for funding.

Disclosure

This chapter was taken from the manuscript prepared for publication with PROFUSA Corps USA. It appears here with the permission from the authors.

Chapter 4: Conclusion and Future Directions

Concluding thoughts on cell based therapeutics

The struggle for a less invasive more patient friendly treatment for Type 1 Diabetes is real. Although insulin injection therapy is very effective, its' burdensome patient compliance limits the success of the regimen. As we advance technologically society has looked to electronics, such as pumps and closed-loop devices, to address the challenges associated with heavily invasive treatment therapies such as insulin injection therapy. The sheer number of patients using pumps more than hints at the deep rooted interest in a less invasive, freedom enabling therapy regime. What is even more surprising when understanding this therapeutic area is the current ability to effectively cure diabetes in smaller mammalian models, such as mice and rats, has yet to translate to humans. We believe that there are a number of key issues that have yet to be addressed that could aid in this therapy development. Specifically, by understanding the biological cues necessary for improved islet function in combination with a cell encapsulation device we could create a viable diabetic therapeutic.

The field of tissue engineering is seeing growing interest in adapting the ways in which scientist culture tissues. Beyond the interest to reconstruct tissues and organs, tissue engineering is being reinvigorated with the increasing interest in having stem-cell-derived cells, tissues and organs. Research are starting to question what do cells need beyond soluble factors to improve stem cell function and

differentiation, and more interestingly which factors are more important, soluble or functional.

In chapter 1, the topics and challenges associated with Type 1 Diabetes are introduced. Type 1 diabetes is growing at an alarming rate of 4-6% annually. Interestingly, the rate is elevated in well developed countries, such as the United States. This understanding highlights the need for a curative Type 1 Diabetes strategy.

This dissertation demonstrates how addressing beta cell architecture in both 2D and 3D can help improve insulin response. Some under explored areas of research that can be used to help develop an effective cell based therapeutics are tissue engineering and cellular encapsulation. Furthermore, we demonstrate that by tuning the mechanical cues exposed to the beta-cells we can further improve insulin response. Together, both mechanical cues and 3D architecture have now been shown to be important factors for improving beta cell response, possibly more important than supplementary soluble factors alone.

Launching from this finding, we show the development of a compliant thin-film cell encapsulation technology that promotes beta cell function while protecting the encapsulated cells from the native immune response. Even more exciting we show that these devices can protect encapsulated cells from infiltration of immune cells, and from soluble cytotoxic cytokines when in an excess of 10-fold the known cytotoxic concentration. Additionally, the devices alone promote neovascularization, which is essential for the success of any tissue transplant. And finally in chapter 4,

we introduce an additional nano technology that can be used to further monitor oxygen availability, and help monitor nutrient exchange.

Future Directions

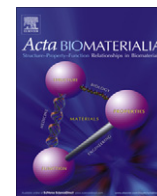
From this dissertation we have the tools to further develop a cell based Type 1 Diabetes therapeutic that could be used to restore patient freedom from constant injection. Together with the latest beta cell stem cell advancements this could provide an artificial-like pancreas that could be implanted without the need of immune suppression therapy. We have seen significant interest specifically in induced pluripotent insulin producing cell technologies that have resulted in multiple high impact publications, company formation, partnerships with big pharmaceutical companies, and even phase 2 clinical trials.

To determine the effectiveness of this therapy in humans two studies must be done. A human derived insulin-produce induced pluripotent stem cell study needs to be done to reaffirm the effectiveness of this technology with a number of stem cell sources. Once done, we can be confident this technology is a stand-alone device that can be readily adapted to suit the available cell types. Secondly a large mammalian study must be done to demonstrate the effectiveness of this therapy at the human scale. Upon success of both of these studies, one could gain more confidence to push this technology further towards patients.

This information can advance biological understanding of pancreatic islets and will also improve current techniques for evaluating beta-cell cluster

phenotypes. Additionally, these findings may improve current beta-cell therapy for type 1 diabetes, maybe even cure Type 1 Diabetes.

Appendix A



Size-controlled insulin-secreting cell clusters

Adam D. Mendelsohn^a, Crystal Nyitray^b, Mark Sena^a, Tejal A. Desai^{a,c,*}

^aJoint Graduate Group in Bioengineering, University of California at San Francisco and University of California at Berkeley, San Francisco, CA 94158, USA

^bDepartment of Chemistry and Chemical Biology, University of California at San Francisco, San Francisco, CA 94158, USA

^cDepartment of Bioengineering and Therapeutic Sciences, University of California at San Francisco, San Francisco, CA 94158, USA

ARTICLE INFO

Article history:

Received 3 April 2012

Received in revised form 3 August 2012

Accepted 8 August 2012

Available online 14 August 2012

Keywords:

Transplantation

Islet

Patterning

Pancreatic β -cell

Insulinoma

ABSTRACT

The search for an effective cure for type I diabetes from the transplantation of encapsulated pancreatic β -cell clusters has so far produced sub-optimal clinical outcomes. Previous efforts have not controlled the size of transplanted clusters, a parameter implicated in affecting long-term viability and the secretion of therapeutically sufficient insulin. Here we demonstrate a method based on covalent attachment of patterned laminin for fabricating uniformly size-controlled insulin-secreting cell clusters. We show that cluster size within the range 40–120 μm in diameter affects a variety of therapeutically relevant cellular responses including insulin expression, content and secretion. Our studies elucidate two size-dependent phenomena: (1) as the cluster size increases from 40 μm to 60 μm , glucose stimulation results in a greater amount of insulin produced per cell; and (2) as the cluster size increases beyond 60 μm , sustained glucose stimulation results in a greater amount of insulin secreted per cell. Our study describes a method for producing uniformly sized insulin-secreting cell clusters, and since larger cluster sizes risk nutrient availability limitations, our data suggest that 100–120 μm clusters may provide optimal viability and efficacy for encapsulated β -cell transplants as a treatment for type I diabetes and that further in vivo evaluation is warranted.

© 2012 Acta Materialia Inc. Published by Elsevier Ltd. All rights reserved.

1. Introduction

The development of a bio artificial pancreas began in 1933 when tissue containing insulin-secreting cells was first transplanted as a potential diabetes treatment [1]. Nearly 80 years later, human trials currently underway in New Zealand evaluating encapsulated islet transplants without immunosuppression report significant reductions in hypoglycemic events, but have yet to achieve reliable insulin independence. Transplantations of unencapsulated human cadaveric β -cells containing islets are currently available and provide at least one year of insulin independence for 80% of recipients [2]. While these pancreatic β -cells are able to sense glucose and secrete insulin at the appropriate level needed for glucose homeostasis, debilitating immunosuppression is required [3] and the availability of cadaveric islets is extremely limited [4]. Significant advances in encapsulation technologies over the past several decades promise to obviate the need for immunosuppression [5,6]. Additionally, animal sources [7,8] and human stem cell sources [9,10] are being cultivated to overcome supply limitations. While these developments promise to overcome some

of the limitations preventing wide-scale adoption of this therapeutic approach, efforts to control the size of transplanted clusters have been lacking.

Two independent size requirements must be satisfied in order to achieve viable islet transplants with sufficient insulin secretion. First, very small clusters do not exhibit therapeutically appropriate insulin secretion because of its dependence on sufficient cell–cell contact. For example, pancreatic β -cell pairs and monolayers secrete greater insulin per cell after glucose stimulation than isolated β -cells [11,12]. Furthermore, glucose-dependent calcium oscillations, a characteristic of appropriately functioning islets, occur more frequently in cell clusters compared with isolated cells [13]. Second, excessively large clusters suffer from nutrient availability limitations. Relying solely on passive diffusion, oxygen and nutrient requirements are attained only when cells are within 100–200 μm from a capillary [14–16]. In fact, necrosis has been observed on the inside of large isolated islets [17,18]. As expected from these results, islets smaller than 150 μm exhibit improved insulin secretion and viability in clinical studies than larger islets [19]. While cell encapsulation in a material with pore sizes small enough to inhibit the passage of antibodies protects transplants from the immune response [20], the same material also inhibits the growth of new blood vessels and prevents access to perfusion that is essential for nutrient availability throughout large islets in the native pancreas [21]. Despite significant evidence supporting

* Corresponding author at: Department of Bioengineering and Therapeutic Sciences, University of California at San Francisco, San Francisco, CA 94158, USA. Tel./fax: +1 415 514 4503.

E-mail address: Tejal.desai@ucsf.edu (T.A. Desai).

the impact that cluster size may have on insulin secretion and viability of encapsulated transplants, to date there appears no study that either explicitly explores the insulin response to varying cluster sizes or presents a method for fabricating uniformly sized clusters.

Here, we used the covalent microcontact printing of laminin, as described previously [22], to fabricate size-controlled patterned insulin-secreting cell clusters. The rat insulinoma cell line INS-1 (832/13) was selected for evaluation due to its dose-dependent glucose-stimulated insulin secretion within physiologically relevant glucose conditions [23,24]. We anticipate the use of stem cells to overcome supply limitations to clinical translation, as stem cells may be grown indefinitely prior to differentiation. Separately, we have demonstrated successful differentiation of size-controlled human embryonic stem cell clusters along the pancreatic lineage, as well as detachment of these clusters which may be necessary prior to transplantation [25]. Our data suggest the possibility of an optimal cluster size after evaluating its impact on insulin expression, content and secretion from uniformly sized 40–120 μm insulin-secreting cell clusters. The successful production of size-controlled insulin-secreting clusters that appropriately balance the need for cell-cell contact and nutrient availability is a necessary step towards achieving long-term insulin independence for the millions that suffer from type I diabetes.

2. Experimental section

2.1. Preparation of laminin patterns on aldehyde-terminated glass cover slips

Clean, dry plasma-treated glass cover slips were aldehyde-functionalized according to a procedure previously described [22], with the modification of – prior to and after glutaraldehyde incubation – sonicating with a 70:30 ethanol:Milli-Q water mixture instead of only Milli-Q, which improved patterned consistency compared with the previous method. We speculate that the improved patterning was the result of better removal of loosely attached glutaraldehyde. Laminin was covalently attached through microcontact printing from polydimethylsiloxane (PDMS) stamps using previously described techniques [22], with design modifications to the lithography mask to create 40–120 μm circular patterns evaluated in this study. The images of fluorescein isothiocyanate-conjugated bovine serum albumin (FITC-BSA) surrounding laminin patterns were taken with a wide-field fluorescent microscope (Olympus BX60).

2.2. Covalent attachment of PEG

After PDMS stamping of laminin on aldehyde-terminated glass cover slips, the cover slips were incubated with 25 μl of 3 mM methoxypolyethylene glycol-amine in methanol for >12 h to quench unreacted aldehyde groups, followed by reduction in sodium cyanoborohydride in methanol (>8 mM).

2.3. Cell culturing and glucose-stimulated insulin secretion (GSIS)

INS-1 (832/13) cells were cultured using previously described methods [22] on patterned cover slips in 12-well plates. Cells were seeded in the same media, except that RPMI 1640 w/HEPES (Invitrogen) was replaced with RPMI 1640 w/o glucose (Invitrogen) and HEPES (Cell Culture Facility, San Francisco) and glucose (Cell Culture Facility, San Francisco) were added separately, at 8.33×10^4 cells cm^{-2} on 40 μm patterned cover slips, 2.5×10^5 cells cm^{-2} on 60 μm patterned cover slips, and 5×10^5 cells cm^{-2} on 120 μm patterned cover slips. After 18–20 h, pattern confluency was

achieved and the cells were rinsed with 1 ml of a HEPES balanced salt solution described elsewhere [23], and then incubated in 1 ml of the same solution for 2 h.

2.4. Insulin mRNA expression

Insulin messenger ribonucleic acid (mRNA) expression was evaluated using an Applied Biosystems Step One Plus real-time polymerase chain reaction (PCR) system. Cells were lysed with TRIzol (Invitrogen) and total RNA was extracted with chloroform (Sigma ACS grade >99.8%). cDNA was synthesized with iScript cDNA Synthesis Kit (Biorad). Reverse transcriptase-PCR (RT-PCR) was performed using SYBR green FAST mix (Applied Biosystems). The expression level of insulin 2 was normalized against β -actin using a standard curve method (See Table 1 for primers) and the results were analyzed with the Version 2.0 software.

2.5. Insulin secretion

Insulin secretion was evaluated using an ultrasensitive rat insulin enzyme-linked immunosorbent assay (ELISA) kit (Mercodia). 40 μm , 60 μm and 120 μm patterned cover slips, after 2 h in the above glucose-free solution, were then exposed either to 1 ml of the same glucose-free solution or 1 ml of a 15 mM glucose created by adding the appropriate amount of D-glucose to the glucose-free solution at 37 °C. After 1 h, samples from each well were spun at 1500g, supernatants were removed and the concentrations of insulin, correlated to a standard curve using human insulin (Sigma), were determined by measuring the absorbance at 450 nm at the completion of the ELISA.

2.6. Characterization of cell patterning

Cover slips with patterned confluent clusters were rinsed with phosphate-buffered saline (PBS), fixed in 3.7% formaldehyde in PBS solution for 15 min, permeabilized with 0.5% Triton X-100 solution for 15 min, and exposed to Alexa Fluor 488 Phalloidin (165 nM in PBS) to stain the F-actin, and DAPI (4',6-diamidino-2-phenylindole, 300 nM in PBS) to stain the nuclei. Cover slips were imaged using wide-field fluorescent microscopy (Nikon Eclipse Ti-E motorized inverted microscope) with a 4 \times objective, and an 8 \times 8 large image was obtained using NIS-elements 3.1 to visualize the entire patterned area. Image analysis was performed with NIS-elements 3.1.

2.7. Evaluation of c-peptide content

832/13 insulinoma cells were seeded using the same 5 mM glucose media described above onto patterned cover slips with a combination of 40 μm , 60 μm , 80 μm , 100 μm and 120 μm circular laminin patterns at 2×10^5 cells cm^{-2} , or on 60 μm circular laminin patterns at 4×10^5 cells cm^{-2} . 18–20 h later, pattern confluency was achieved on the combined patterned cover slips, and both confluent monolayers as well as multilayered clusters were present on the 60 μm patterned cover slips. Cover slips were then rinsed with 1 ml of a HEPES balanced salt solution described elsewhere [23] with 0.2% essentially fatty acid free bovine serum albumin (BSA) and 0 mM glucose, and subsequently exposed to

Table 1
RT-PCR primers.

Insulin 2	Forward: 5'-GAA GTG GAG GAC CCA CAA GT-3' Reverse: 5'-AGT GCC AAG GTC TGA AGG TC-3'
β -actin	Forward: 5'-CAA CCG TGA AAA GAT GAC CCA GA-3' Reverse: 5'-ACG ACC AGA GGC ATA CAG GGA C-3'

incubation in 1 ml of the same solution for 2 h. Immediately prior to, 15 min after and 1 h after subsequent exposure to a 15 mM glucose solution, the cells were fixed with a solution of 3.7% formaldehyde in PBS solution for 15 min, permeabilized with 0.5% Triton X-100 solution for 15 min, immunostained with 1 $\mu\text{g ml}^{-1}$ of rabbit anti-c-peptide (Cell Signaling) and/or 2 $\mu\text{g ml}^{-1}$ mouse monoclonal anti-insulin (Santa Cruz Biotech) overnight at 4 °C with 5% goat serum in buffer (13 mM dipotassium phosphate, 150 mM sodium chloride and 0.2% Tween 20, pH 7.5; the same buffer was used as follows unless otherwise specified). The cover slips were then rinsed thoroughly with buffer prior to incubation with 10 $\mu\text{g ml}^{-1}$ donkey anti-mouse IgG Alexa Fluor 488 (Invitrogen) and/or goat anti-rabbit IgG Alexa Fluor 633 (Invitrogen) for 1 h at room temperature. The cells were rinsed with buffer thoroughly before staining the actin cytoskeleton with 165 nM Alexa Fluor 568 Phalloidin in PBS (Invitrogen) for 30 min. The nuclei were stained by sandwiching 3 μl of SlowFade Gold antifade reagent with DAPI (Invitrogen) between a microscope slide and a patterned cover slip, followed by nail polish to adhere the cover slip to the microscope slide.

Spinning disk confocal microscopy (Nikon Eclipse Ti-E motorized inverted microscope with Yokogawa CS22 Spinning Disk Confocal from Solamere Technology Group, Acquisition with Micro-Manager) was used to visualize the clusters. The cell borders of 0.25 μm thick z-stacks were defined by the phalloidin, and image intensity data within the confines of this volume were used for analysis using NIS-Elements. Lack of significant photobleaching was confirmed by evaluating five subsequent identical images for intensity differences at the laser power settings used.

3. Results

3.1. Consistent fabrication of uniform-size insulin-secreting cell clusters

Insulin-secreting cells selectively adhered to patterned laminin, resulting in uniformly size-controlled clusters on glass cover slips using a modified version of a previously described technique [22]. The extracellular matrix protein laminin was first microcontact printed from a lithographically created polydimethylsiloxane stamp onto an aldehyde-functionalized glass cover slip. Subsequent incubation with a fluorescent protein enabled visualization of the areas surrounding the laminin pattern (Fig. 1A). Laminin stamping was followed by the covalent attachment of polyethylene glycol, a polymer that resists cell attachment. Seeding density and incubation time were optimized to enable cells to neatly conform to varying laminin patterns (Fig. 1B). Pattern uniformity across the entire cover slip was made possible for the first time by modifying the procedure for attaching polyethylene glycol from a one-step to a two-step reaction as visualized by 40 μm (Fig. 1C), 60 μm (Fig. 1D) and 120 μm (Fig. 1E) circular cell patterns that are fixed and stained for nuclei and F-actin. We observed that the intensity of the nuclear stain correlates linearly with the number of nuclei within a given cluster (Supplementary Fig. S1A). As expected, the distribution of the number of cells in a cluster is Gaussian, and the average number of cells in a cluster, measured over multiple cover slips, increases with the size of the laminin pattern (Supplementary Figs. S1B and S1C).

3.2. Effect of cluster size on insulin mRNA expression and secretion

After achieving confluency on patterned glass cover slips, insulin-secreting cells were pre-treated in low glucose to achieve basal insulin production, which also reduced levels of insulin mRNA (Supplementary Fig. S2) before exposure to high glucose. Insulin

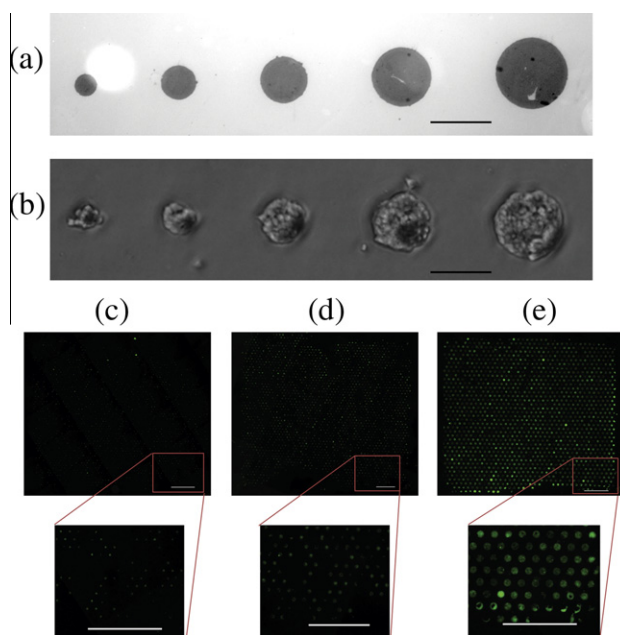


Fig. 1. Cells seeded on patterned laminin become uniform size-controlled clusters. (a) 40, 60, 80, 100 and 120 μm laminin-patterned glass cover slips were visualized after incubation with fluorescein isothiocyanate-conjugated bovine serum albumin (FITC-BSA) before polyethylene glycol (PEG) deposition; scale bar = 100 μm . (b) Bright-field microscopy verified conformation of 832/13 rat insulinoma cells to patterned laminin after PEG deposition; scale bar = 100 μm . Fluorescent staining of nuclei (DAPI, blue) and F-actin (Alexa Fluor 488 Phalloidin, green) illustrates the uniformity of (c) 40 μm , (d) 60 μm and (e) 120 μm patterns after seeded cells achieved confluency; scale bars = 1 mm.

2 mRNA expression, normalized to β -actin mRNA expression, was evaluated for 40, 60 and 120 μm clusters before, 15 min after and 1 h after high glucose stimulation. While no difference was observed prior to glucose stimulation, normalized insulin 2 mRNA expression was almost 2-fold smaller ($P < 0.021$) after 15 min of stimulation for the 40 μm clusters compared with the 60 and 120 μm clusters (Fig. 2A). After 1 h of stimulation, expression levels were the same for all measured cluster sizes.

Additionally, the effect of cluster size on insulin secretion was evaluated after GSIS. Samples were taken from wells containing patterned 40, 60 and 120 μm insulin-secreting cell clusters subjected to glucose starvation and then either continued glucose starvation or high glucose stimulation for 1 h. Whereas insulin secretion from 40 μm clusters remained unchanged when incubated with high glucose, it was 2.5-fold and nearly 3.5-fold higher for 60 and 120 μm clusters, respectively (Fig. 2B). Insulin secretion 15 min after stimulation was undetectable for all cluster sizes.

3.3. Effect of cluster size and cell number on insulin and C-peptide content

C-peptide content from patterned 832/13 insulinoma cells was evaluated as a surrogate for insulin content by first establishing colocalization of insulin and c-peptide immunofluorescence. Proinsulin is processed into insulin and c-peptide in an equimolar ratio; both products reside in the same secretory vesicles and are released simultaneously [26,27]. Positive c-peptide staining is therefore used to verify the presence of de novo insulin synthesis as opposed to exogenously introduced insulin [28]. Immunofluorescence reveals colocalization of insulin (green) and c-peptide (red) (Supplementary Fig. S3).

Since gap junction proteins modulate insulin secretion [29], multiple cell layers, as opposed to monolayers, could positively

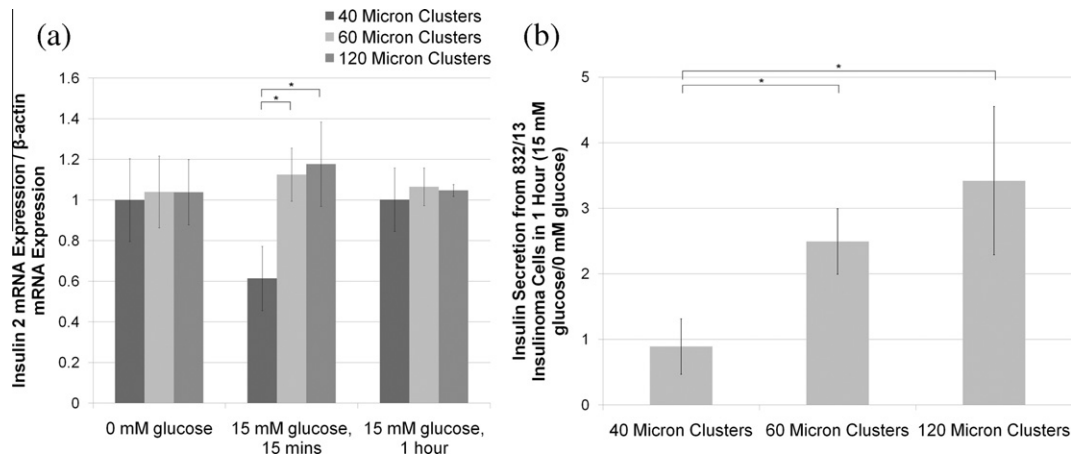


Fig. 2. Normalized insulin 2 mRNA expression and normalized insulin secretion increases with larger cluster sizes. (a) RT-PCR was used to determine normalized insulin 2 mRNA expression for 40, 60 and 120 μ m patterned confluent clusters 15 min after and 1 h after 832/13 insulinoma cells were exposed to GSIS (data normalized to the average of the 40 μ m clusters for each glucose condition). Additionally, (b) the impact of glucose stimulation on insulin secretion from 40 μ m, 60 μ m and 120 μ m clusters was determined by normalizing measured insulin secretion over 1 h from clusters stimulated with 15 mM glucose ($n = 3$) to clusters stimulated with 0 mM glucose that mimics basal secretion levels ($n = 3$) for each cluster size. Data are presented as an average \pm standard deviation. Statistical significance for the comparison of multiple groups was confirmed for each group indicated with an * using a Holm–Sidak test with $\alpha = 0.05$ after performing an analysis of variances (ANOVA).

impact the insulin response to glucose stimulation. Multilayer formation occurs when initially formed clusters contain too many cells to fit in one layer on the printed laminin and pile up as they retreat from the cell-repulsive PEG [22]. While no c-peptide content differences were observed using quantitative imaging prior to glucose stimulation, c-peptide content in multilayered 60 μ m clusters exceeded that of monolayered 60 μ m clusters after 15 min of glucose stimulation (Fig. 3a). Visualization of the c-peptide channel from representative images qualitatively confirms this effect, and zoomed-in section views of the cell clusters verify the presence of a monolayer or multilayered cluster (Fig. 4). This difference disappeared after stimulation was sustained for 1 h (Fig. 3a).

Additionally, normalized c-peptide staining intensity for 40, 60, 80, 100 and 120 μ m circular monolayered cell clusters over the three glucose conditions under evaluation revealed the impact of size on the extent to which insulin is stored after production. 15 min after glucose stimulation, a 2-fold increase in insulin content over unstimulated clusters was seen for all but the 40 μ m clusters (Fig. 3b). This 2-fold change was not exceeded with increasing cluster size. Furthermore, 1 h after glucose stimulation, smaller sized (40 and 60 μ m) clusters contained greater c-peptide than larger sized (100 and 120 μ m) clusters (Fig. 3b). Representative images qualitatively confirm these effects (Fig. 5). C-peptide localization analysis further reveals more uniformly distributed staining 15 min after stimulation, whereas the c-peptide in 40, 60 and 80 μ m clusters appears localized to only a portion of the cells in each cluster.

4. Discussion

This study suggests that as insulin-secreting cell cluster size increases from 40 μ m to 120 μ m, the insulin response to glucose stimulation is affected at two separate threshold sizes: the first results in greater insulin expression and translation shortly after glucose stimulation, and the second results in more efficient insulin secretion after sustained glucose stimulation. After expression and subsequent translation, a number of post-translational steps occur, resulting in the storage of mature insulin and c-peptide awaiting secretion [30]. One previous simulation of β -cell behavior speculated that a minimum of four β -cell– β -cell contacts are required for insulin bursting coordination, and that this coordination

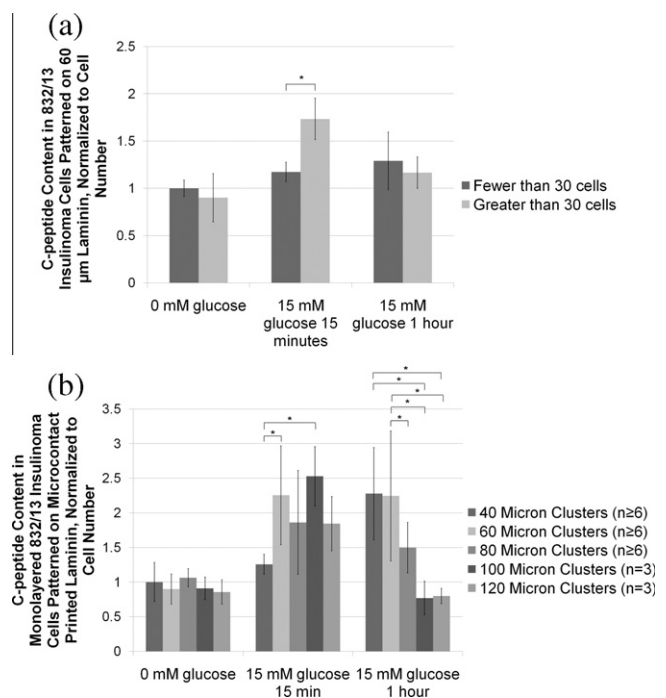


Fig. 3. Semi-quantitative immunocytochemistry reveals effects of cluster size on normalized c-peptide content under different glucose conditions. 832/13 insulinoma cell clusters are fixed, permeabilized and stained for c-peptide, F-actin and nuclei before, 15 min after and 1 h after glucose stimulation. Confocal images are acquired and total intensity of c-peptide staining is normalized to the nuclear stain intensity which correlates linearly with the number of nuclei (Supplementary Fig. S4). (a) Quantified normalized c-peptide intensity was then determined between monolayered and multilayered clusters for each glucose condition (data are normalized to the average of monolayered clusters before glucose stimulation). (b) Normalized c-peptide intensity is also evaluated between monolayered clusters on a single cover slip containing 40, 60, 80, 100 and 120 μ m are compared to each other for each glucose condition (data are normalized to the average of the 40 μ m clusters before glucose stimulation). Data are presented as an average \pm standard deviation. Statistical significance is indicated with an * and was established using the Student–Newman–Keuls test with $\alpha = 0.05$ after performing an ANOVA.

improves upon the addition of several more β -cells before reaching a plateau [31]. Characterization of our cell patterns revealed that 9040 μ m patterns contained on average between six and seven cells

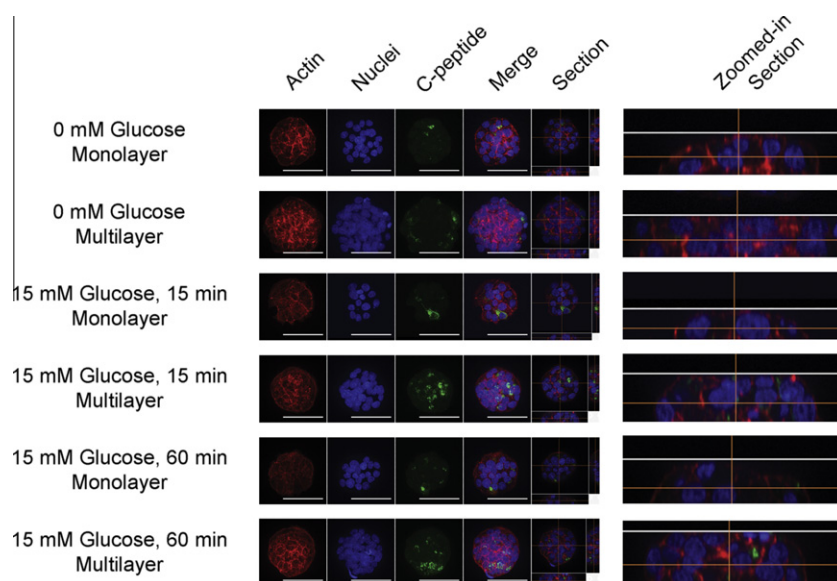


Fig. 4. Confocal imaging reveals the effect of multiple cell layers on c-peptide content under different glucose conditions. 832/13 insulinoma cells were grown to confluency on glass cover slips that only have 60 μm patterns. Cell clusters were fixed, permeabilized and stained for F-actin, nuclei and c-peptide. Representative confocal sectioned z-stacked images revealed both monolayered (<30 cells) and multilayered (>30 cells) clusters. A maximum intensity projection enabled visualization of staining throughout the z-stacks (actin, nuclei, c-pep and merge). One representative slice of the z-stack is displayed to the right of the maximum intensity projections (section), and the zoomed-in section view verifies that the cell clusters are either in a monolayer or in multiple layers. Scale bar = 50 μm .

per cluster, and 60 μm patterns contained on average between 15 and 16 cells per cluster (Supplementary Fig. S1C). Our data support this study's suggestion that insulin production behavior is affected by the number of β -cells in contact with each other, as well as the approximate number of cells required to effect such changes.

The existence of a second threshold cluster size enabling more efficient insulin secretion was less expected, and further exploration will be required prior to speculation of a responsible mechanism. Nonetheless, as the cluster size increased from 60 to 100 μm , c-peptide content after 1 h of glucose stimulation decreased in a size-dependent fashion, with no additional decrease between 100 and 120 μm clusters. Instead of a concurrent reduction in insulin secretion over this time period, cells in 120 μm clusters on average responded with significantly greater insulin secretion (~ 3.5 -fold) compared with cells in 60 μm clusters (~ 2.5 -fold), although this result was not significant (Fig. 2B). These two observations, when taken together, suggest that the larger cluster sizes secrete insulin more quickly, with less storage, after sustained glucose stimulation.

We realize that evaluation of insulin secretion included a portion of clusters with more cells than those used in content analyses, some of which were multilayered in nature (Supplementary Fig. S1B). We have also demonstrated that multilayered 60 μm clusters contain more c-peptide 15 min after glucose stimulation than monolayered 60 μm clusters (Fig. 3). However, multilayered clusters did not contain reduced c-peptide compared with monolayered clusters after 1 h of sustained glucose stimulation (Fig. 4), supporting the proposal that a second size-dependent threshold enabling more efficient insulin secretion exists, and that multilayered 60 μm clusters do not exceed this threshold. After considering all of these factors, our data suggest that 120 μm cell clusters secrete insulin more rapidly during sustained exposure to glucose after expression and translation than 60 μm cell clusters. Furthermore, since 100 μm clusters exhibited similarly low c-peptide content after sustained glucose stimulation, the threshold size for achieving more rapid insulin secretion is likely between 80 and 100 μm .

The oxygen levels associated with the in vivo environment surrounding a transplant will be significantly less than the incubator

oxygen levels under which the experiments reported here were performed. The superiority of islets smaller than 150 μm in a human study provides some confidence that the 100–120 μm cluster size recommended by this in vitro study may be sufficiently small to achieve sufficient in vivo nutrient availability [19]. However, any encapsulation material that prevents the need for immunosuppression will contribute to nutrient availability limitations, the effects of which will need to be considered in the design of the encapsulation material and evaluated in vivo before an optimal cluster size within a given encapsulation material can be definitively identified.

Multiple methods exist that would enable subsequent transplantation of these patterned clusters. First, the clusters could be transplanted in a patterned sheet, similar to a concept described previously and still in development [32]. This approach would require cell patterning to occur on a biocompatible substrate, or the transfer of patterned clusters to a biocompatible material. Second, microcapsules can encapsulate size-controlled clusters that are dislodged either naturally over time [25] or with exposure to collagenase-dispase (Supplementary Fig. S5). Both of these approaches will require further optimization for parameters affecting nutrient availability that have been extensively reviewed elsewhere [6]. Alternatively, immunosuppressed transplantation of size-controlled clusters via the portal vein may improve clinical outcomes without requiring cluster organization optimization. The insulinoma cells used in this study are not ideal candidates for transplantation, in part due to the immortalized nature of the cell line. We considered the use of primary β -cells from MIP-GFP mice, but the number of cells necessary for these studies would require the use of hundreds of animals. Instead, we are separately investigating the differentiation of human embryonic stem cells, which can be proliferated indefinitely prior to differentiation, into 120 μm size-controlled clusters along the pancreatic lineage, which become 100 μm spherical clusters when released [25]. Regardless of the encapsulation approach, incorporation of size-controlled clusters into encapsulated transplantation therapy promises to overcome one of the few remaining challenges impeding this therapy from achieving successful outcomes.

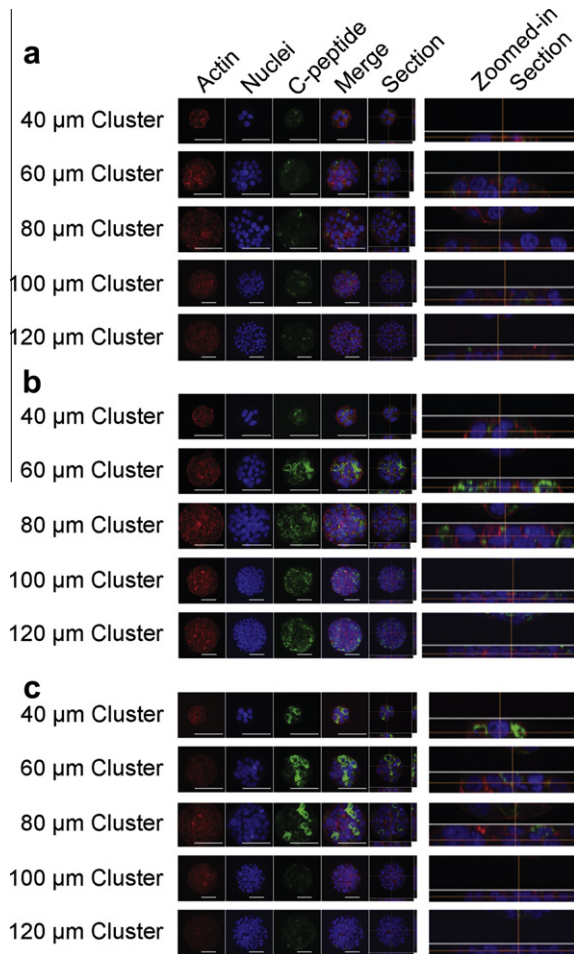


Fig. 5. Confocal imaging reveals the effect of monolayered cluster size on c-peptide content under different glucose conditions. 832/13 insulinoma cells were grown to confluency on glass cover slips that have a combination of 40, 60, 80, 100 and 120 μm patterns. Cell clusters were fixed (a) just prior, (b) 15 min after and (c) 1 h after glucose stimulation, permeabilized and stained for F-actin, nuclei and c-peptide. Confocal z-stack images were taken throughout each cluster. A maximum intensity projection enabled visualization of staining throughout the z-stacks (actin, nuclei, c-pep and merge). One representative slice of the z-stack is displayed to the right of the maximum intensity projections (section), and the zoomed-in section view verifies that the cell clusters are in a monolayer. Scale bar = 50 μm .

5. Conclusions

In conclusion, we described a method for fabricating uniformly size-controlled insulin-secreting cell clusters through covalent microcontact printing of laminin on aldehyde-functionalized cover slips. We demonstrate that cluster size affects the insulin response to glucose stimulation in a therapeutically relevant manner. Finally, the results of our studies suggest that, among the sizes evaluated here, 100–120 μm clusters demonstrate the greatest promise for encapsulated transplantation therapy for treating type I diabetes.

Disclosure of potential conflicts of interest

The authors declare no potential conflicts of interest.

Acknowledgements

This work was supported by the Juvenile Diabetes Research Foundation (JDRF grant awards 1-2010-152), the Sandler Family

Foundation and NIH Training Grant T32 DK07418. Images were taken at the Nikon Center at UCSF with the assistance of Kurt Thorn, Sebastien Peck and Alice Thwin. The authors would also like to thank Dr. Christopher Newgard for providing the 832/13 insulinoma cell line.

Appendix A. Figures with essential colour discrimination

Certain figures in this article, particularly Figs. 1, 4 and 5, is difficult to interpret in black and white. The full colour images can be found in the on-line version, at <http://dx.doi.org/10.1016/j.actbio.2012.08.010>.

Appendix B. Supplementary data

Supplementary data associated with this article can be found, in the online version, at <http://dx.doi.org/10.1016/j.actbio.2012.08.010>.

References

- [1] Bisceglie V. Über die antineoplastische Immunität. *E Krebsforsch* 1933;40:141–58.
- [2] Shapiro AM, Ricordi C, Hering B. Edmonton's islet success has indeed been replicated elsewhere. *Lancet* 2003;362(9391):1242.
- [3] Penn I. Post-transplant malignancy: the role of immunosuppression. *Drug Saf* 2000;23(2):101–13.
- [4] Matsumoto S et al. Estimation of donor usability for islet isolation with the modified Ricordi method. *Transplant Proc* 2008;40(2):362–3.
- [5] Mendelsohn A, Desai T. Inorganic nanoporous membranes for immunisolated cell-based drug delivery. *Adv Exp Med Biol* 2010;670:104–25.
- [6] Wilson JT, Chaikof EL. Challenges and emerging technologies in the immunoisolation of cells and tissues. *Adv Drug Deliv Rev* 2008;60(2):124–45.
- [7] Elliott RB et al. Live encapsulated porcine islets from a type 1 diabetic patient 9.5 yr after xenotransplantation. *Xenotransplantation* 2007;14(2):157–61.
- [8] Thanos CG, Elliott RB. Encapsulated porcine islet transplantation: an evolving therapy for the treatment of type 1 diabetes. *Expert Opin Biol Ther* 2009;9(1):29–44.
- [9] Kroon E et al. Pancreatic endoderm derived from human embryonic stem cells generates glucose-responsive insulin-secreting cells in vivo. *Nat Biotechnol* 2008;26(4):443–52.
- [10] Van Hoof D, D'Amour KA, German MS. Derivation of insulin-producing cells from human embryonic stem cells. *Stem Cell Res* 2009;3(2–3):73–87.
- [11] Meda P et al. Rapid and reversible secretion changes during uncoupling of rat insulin-producing cells. *J Clin Invest* 1990;86(3):759–68.
- [12] Brereton HC et al. Homotypic cell contact enhances insulin but not glucagon secretion. *Biochem Biophys Res Commun* 2006;344(3):995–1000.
- [13] Jonkers FC et al. Influence of cell number on the characteristics and synchrony of Ca^{2+} oscillations in clusters of mouse pancreatic islet cells. *J Physiol* 1999;520(Pt 3):839–49.
- [14] Orive G et al. Biocompatibility of alginate-poly-L-lysine microcapsules for cell therapy. *Biomaterials* 2006;27(20):3691–700.
- [15] Martin Y, Vermette P. Bioreactors for tissue mass culture: design, characterization, and recent advances. *Biomaterials* 2005;26(35):7481–503.
- [16] Muschler GF, Nakamoto C, Griffith LG. Engineering principles of clinical cell-based tissue engineering. *J Bone Joint Surg Am* 2004;86-A(7):1541–58.
- [17] De Vos P et al. Why do microencapsulated islet grafts fail in the absence of fibrotic overgrowth? *Diabetes* 1999;48(7):1381–8.
- [18] O'Sullivan ES et al. Rat islet cell aggregates are superior to islets for transplantation in microcapsules. *Diabetologia* 2010;53(5):937–45.
- [19] Lehmann R et al. Superiority of small islets in human islet transplantation. *Diabetes* 2007;56(3):594–603.
- [20] Desai TA et al. Microfabricated biocapsules provide short-term immunoisolation of insulinoma xenografts. *Biomed Microdevices* 1999;1(2):131–8.
- [21] Ballian N, Brunnicardi FC. Islet vasculature as a regulator of endocrine pancreas function. *World J Surg* 2007;31(4):705–14.
- [22] Mendelsohn AD et al. Patterning of mono- and multilayered pancreatic beta-cell clusters. *Langmuir* 2010;26(12):9943–9.
- [23] Hohmeier HE et al. Isolation of INS-1-derived cell lines with robust ATP-sensitive K^+ channel-dependent and -independent glucose-stimulated insulin secretion. *Diabetes* 2000;49(3):424–30.
- [24] Kuehn C et al. Culturing INS-1 cells on CDPGYIGSR-, RGD- and fibronectin surfaces improves insulin secretion and cell proliferation. *Acta Biomater* 2012;8(2):619–26.
- [25] Van Hoof D et al. Differentiation of human embryonic stem cells into pancreatic endoderm in patterned size-controlled clusters. *Stem Cell Res* 2011;6(3):276–85.

- [26] Block MB et al. Sequential changes in beta-cell function in insulin-treated diabetic patients assessed by C-peptide immunoreactivity. *N Engl J Med* 1973;288(22):1144–8.
- [27] Steiner DF et al. Insulin biosynthesis: evidence for a precursor. *Science* 1967;157(789):697–700.
- [28] Rajagopal J et al. Insulin staining of ES cell progeny from insulin uptake. *Science* 2003;299(5605):363.
- [29] Meda P. Cx36 involvement in insulin secretion: characteristics and mechanism. *Cell Commun Adhes* 2003;10(4–6):431–5.
- [30] Gold G et al. Heterogeneity and compartmental properties of insulin storage and secretion in rat islets. *J Clin Invest* 1982;69(3):554–63.
- [31] Nittala A, Ghosh S, Wang X. Investigating the role of islet cytoarchitecture in its oscillation using a new beta-cell cluster model. *PLoS One* 2007;2(10):e983.
- [32] Storrs R et al. Preclinical development of the Islet Sheet. *Ann NY Acad Sci* 2001;944:252–66.

Appendix B

Published in final edited form as:

Front Biosci (Landmark Ed). ; 19: 49–76.

Membranes to achieve immunoprotection of transplanted islets

Julien Schweicher¹, Crystal Nyitray¹, and Tejal A. Desai¹

¹Therapeutic Micro and Nanotechnology Laboratory, Department of Bioengineering and Therapeutic Sciences, University of California, San Francisco (UCSF), 1700 4th Street, Box 2520, San Francisco, CA, 94158, USA

Abstract

Transplantation of islet or beta cells is seen as the cure for type 1 diabetes since it allows physiological regulation of blood glucose levels without requiring any compliance from the patients. In order to circumvent the use of immunosuppressive drugs (and their side effects), semipermeable membranes have been developed to encapsulate and immunoprotect transplanted cells. This review presents the historical developments of immunoisolation and provides an update on the current research in this field. A particular emphasis is laid on the fabrication, characterization and performance of membranes developed for immunoisolation applications.

Keywords

Cell Immunoisolation; Cell Transplantation; Inorganic Membranes; Macrocapsules; Microcapsules; Organic Membranes; Type 1 Diabetes; Review

2. INTRODUCTION

As of today, it is estimated that diabetes affects 346 million people worldwide(1). This chronic disease is characterized by high levels of blood glucose (hyperglycemia) that, if untreated, lead to devastating complications such as heart disease, stroke, loss of vision, retinopathy, kidney failure, nervous system damage and even death(2). Type 1 diabetes (T1D), also known as “juvenile diabetes” or “insulin dependent diabetes mellitus”, represents about 10% of all cases. It is the most severe form of diabetes: the pancreatic beta cells (located in the islets of Langerhans) are progressively destroyed by the patient's immune system (autoimmune attack). These cells are essential since they normally produce the hormone insulin in amounts that regulate the blood glucose concentration. Their destruction reduces and then permanently stops the insulin production which translates in high blood glucose levels. The current treatment consists of several subcutaneous injections of insulin every day (based on a careful monitoring of blood glucose levels via finger pricking). This treatment is obviously inconvenient for patients and the bolus-type administration of insulin is not physiological. This has lead to the development of portable insulin pumps(3) and the hope to develop an artificial pancreas that would combine an implantable insulin pump, a continuous glucose monitoring system and a control

Send correspondence to: Tejal A. Desai, University of California, San Francisco (UCSF), 1700 4th Street, Box 2520, San Francisco, CA, 94158, USA, Tel: 415-514-9695, Fax: 415-514-9656, tejal.desai@ucsf.edu.

algorithm(4, 5). However, before the development of a clinical application, a closed-loop insulin delivery approach must still surmount obstacles related to the delay of insulin action when infused subcutaneously and to the blood glucose estimation made by subcutaneous interstitial measurement(5). More complex algorithms are thus needed to compensate for the time lags impairing the system reactivity.

An alternate approach that would be a real cure for type 1 diabetes patients is to replace their pancreas(6) or alternatively to transplant functional islets of Langerhans or beta cells alone(7-11). This constitutes the best solution in terms of physiological regulation of blood glucose and patient compliance. However, two major problems have hindered the successful development of transplantations up to now: 1) the supply of pancreas/islet cells available for transplantation is very limited; 2) the transplanted organs/cells are subject to the host's immune attack and destruction (resulting in brief viability and efficacy of the graft in the best case scenario). A lot of progress has been made to tackle both of these problems over the last few years but more effort will be needed to bring a safe transplantation approach to the whole community of type 1 diabetic patients.

2.1. Immunosuppressed pancreas/islet transplantation

Approximately 30,000 pancreases have been transplanted worldwide since 1966 with the annual numbers of transplants reaching a steady state since the late 1990s(6). The procedure is usually performed in conjunction with a kidney transplant for patients with type 1 diabetes and chronic renal failure (the patients receive both a pancreas and a kidney from a single deceased organ donor). With this method, the overall 1-year pancreas graft survival rate that achieves insulin independence is 85% and decreases to about 50% 10 years after transplantation(6, 12, 13). However, recipients of these transplants must adhere to a strict lifelong immunosuppressive therapy in order to avoid rejection of the grafts(6, 12). The currently used anti-rejection medications present side effects that are not acceptable for patients with type 1 diabetes only (insulin injections still constitute a better treatment for those). The complications associated with immunosuppressive drugs include increased incidence of infection and malignancy, decreased wound healing, renal dysfunction...(14-16) Only patients who require a kidney transplant are then incentivized in a whole pancreas graft.

An alternative therapy is to transplant isolated islet cells instead of a whole pancreas (here again, graft recipients have to take immunosuppressive drugs for the rest of their lives, with the associated complications)(11, 16-18). Only the endocrine component of the pancreas is transplanted in this case (~2-3% of the pancreas mass), considerably reducing the risks of the surgical procedure(17). Islets are usually injected in the portal vein and transported via the bloodstream into the liver where they take up residence(16). Over 1400 islet transplantation procedures have been performed worldwide since 1974(17). These transplantations lacked success before 2000: only 8% of recipients maintained insulin independence one year after transplantation from 1990 to 1998(19). However, in 2000, Shapiro *et al.* reported 7 consecutive recipients who were all insulin independent one year after transplantation, which is commonly referred to as the Edmonton Protocol(7). Success rates decreased after 5 years, with only 10% of patients still achieving insulin

independence(8). Nevertheless, clinical benefits are observed after islet transplantation even in the absence of insulin independence since the incidence of life-threatening hypoglycemia decreases dramatically(20).

2.2. Cell sources for islet transplantation

A normal human pancreas contains roughly 1 million islets(11); however islets purified from donor pancreases require several steps to be ready for transplantation, and all these steps can be detrimental to the harvested islets(17). Consequently, 2-4 donor pancreases are required to perform a successful islet transplantation procedure(17). The significant mismatch between the number of islets needed for transplantation and the islet availability highlights the urgent need to find additional islet sources. Various cell sources are currently envisaged to overcome this obstacle(17, 18, 21-24): expansion/replication of existing human beta cells(25-28), differentiation of human embryonic stem cells (hESC) to beta cells(29-35), conversion of either pancreatic or nonpancreatic adult stem/progenitor cells to beta cells(36-48) and animal islet cells. Among xenogeneic sources, porcine islets are particularly interesting due to the close homology between porcine and human insulin and the similarity of islets between both species(49).

Despite great promises from these diversified islet sources, several issues must be overcome before large-scale utilization will be made possible. Cells derived from stem cells are not yet fully functional beta cells and animal cells induce a more aggressive immune rejection than human cells. Moreover, the risk of transmittable diseases between animal and human will have to be carefully investigated(50).

2.3. Immunoisolated islet/cell transplantation

In order to circumvent the use of immunosuppressive drugs and their side effects following transplantation of islet or beta cells, the idea of encapsulating the cells in a protective semipermeable membrane has been developed. Such a membrane has to be immunoisolating (i.e. impede contact with immune cells, antibodies, complement...) yet at the same time this membrane must allow rapid transport of glucose, insulin, nutrients (oxygen (O₂)...) and waste products. Conceptually immunoisolation membranes are possible given the relatively smaller size of glucose (180 Da; Stokes radius: 0.4 nm)(51) and insulin (monomer/hexamer: 5.8/34.2 kDa; 1.35-2.75 nm)(52) compared to inflammatory cells (size of ~10 μm) and molecules responsible for immune rejection such as immunoglobulin G (IgG: 150 kDa; Stokes radius: 5.9 nm)(53, 54), complement C1q (410 kDa)(55), immunoglobulin M (IgM: 910 kDa)(55). Figure 1 presents the concept of immunoisolation on a molecular weight scale.

Cell encapsulation is sometimes referred to as cell-based drug delivery: in the case of islet or beta cells, they secrete insulin (a therapeutic protein) in quantities related to external glucose stimulation.

Two distinct approaches have been developed to immunoisolate cells using semipermeable membranes (see Figure 2): macrocapsules (macroencapsulation) confine a large number of transplanted cells in an implantable device (a macrocapsule can be transplanted extravascularly or intravascularly) and microcapsules (microencapsulation) only contain

from 1 to 3 islet cells in each device (typically 400-800 μm in diameter)(56, 57) (a very large number of these microbeads need to be transplanted in this case). New microencapsulation techniques with thinner or even nanoscaled coatings have recently been developed, introducing the terms conformal coatings and nanoencapsulation in the community(57). Nanoencapsulated islets could also be used in conjunction with macrocapsules to enhance the immune protection.

Possible transplantation sites are different for each type of device(58). Extravascular macrocapsules are generally transplanted intraperitoneally or subcutaneously whereas intravascular macrocapsules are connected as a shunt to systemic blood circulation. With macrocapsules, it is possible to encapsulate islet cells at a high tissue-like density or dispersed in a chosen extracellular gel matrix (alginate, chitosan, agarose...)(55). Extravascular microcapsules are usually transplanted in the peritoneal cavity.

All of these immunoisolation approaches present advantages and disadvantages that will be detailed in section 3. Other reviews of interest may be found elsewhere as well(49, 56-65).

Despite many promising encapsulation studies and the development of numerous devices, cell encapsulation has yet to make an impact in the clinical setting. Some of the factors limiting widespread application of encapsulated islets include incomplete isolation of islets from the immune system and inadequate physiological nutrient accessibility for cells within the devices.

In fact, transplanting immunoisolated islet cells is challenging since both the innate and the adaptive immune responses have to be overcome. Membranes presenting pores smaller than 1 μm easily block the passage of immune cells but blockage of antibodies (the smallest being IgG) or cytokines is much more challenging(55). These problems are even more important for xenogeneic transplants. Avgoustiniatos *et al.* estimated that both IgM and C1q should be completely blocked by a membrane with a maximum pore diameter of 30 nm(55). However, IgG will require smaller pores to be fully blocked and this will significantly hinder the diffusion of glucose and insulin. Thus, a compromise has to be found. It is also interesting to note that a tiny permeability of IgG may not be so detrimental to encapsulated cells: Iwata *et al.* showed that complement components are rapidly inactivated, and therefore it should be sufficient to hinder IgG diffusion in the first days after transplantation rather than totally block it(66).

As mentioned before, the other issue with encapsulated cells is poor access to oxygen and nutrients caused by the membrane barrier. In a healthy pancreas, islets are perfused by blood and supplied with O_2 at arterial levels(55, 56). When encapsulated, islets can easily be located more than 150-200 μm away from the nearest blood vessel, which can induce hypoxic conditions leading to cell necrosis(55, 56, 67, 68). Furthermore, biocompatibility of the device material is extremely important(56): if the foreign body response induces the formation of an avascular layer on the membrane (typically on the order of 100 μm), there is little chance that the cells will be able to survive. On the other hand, biocompatible materials can induce neovascularization (growth and proliferation of new blood vessels near the membrane interface) that will drastically improve diffusion of O_2 and nutrients. However,

the development of such vasculature takes 2-3 weeks, meaning that grafted cells will experience the most severe nutrient limitations immediately after transplantation since they will only depend on peripheral diffusion from the surrounding tissue(55). Some solutions are currently investigated to tackle this problem: prevascularization of the macrocapsule before adding cells(69), faster vascularization with growth factors(70), incorporation of oxygen carriers or oxygen-generating biomaterials(71-78).

Another interesting idea to improve islet transplant success would be to use controlled size beta cell clusters(79, 80) within the capsules. It has been shown that clusters of cells secrete insulin more efficiently than single cells(80-84), indicating that communication between cells should be preserved in transplantation situations to improve cell function. Moreover, cluster size could be optimized to avoid insufficient O₂ or nutrient supply to the cells.

3. IMMUNOISOLATION OF TRANSPLANTED ISLETS: DIFFERENT APPROACHES

3.1. Extravascular macrocapsules

3.1.1. Advantages and disadvantages—Extravascular macrocapsules present several advantages for cell encapsulation: they can be made from a variety of different materials, they are easily retrievable and/or reloadable (clear advantage if an issue arises after implantation), they can be implanted with minimally invasive surgeries and the extracellular matrix can be chosen independently (important to ensure a suitable environment for encapsulated cells). Pancreatic beta cell behavior is known to depend on the surrounding matrix environment(85). Moreover, a very tight pore size distribution is now achievable for inorganic nanoporous membranes(61), which is of utmost importance for immunoisolation properties. Finally, the fact that cells can exist as clusters (as in a healthy pancreas) within the macrocapsules is beneficial regarding the communication between cells and the synchronization of insulin secretion pulses(86).

The main drawback of these macrocapsules is their lack of direct vascular access. This results in increased diffusion times for O₂ and glucose. As a consequence, the production of insulin and its release are also delayed. Moreover, if large concentrations of insulin build up inside the chamber, the enclosed islets may be subject to insulin inhibition from their own products(87). Another problem of macroencapsulation is the potential lack of oxygenation for the islets located far away from the membranes, creating risks of central necrosis and cellular death. It is well known that cells have to be close to blood vessels, typically at a distance less than 150-200 μ m to allow diffusion of O₂ and nutrients and to perform metabolic processes appropriately(55, 56, 67, 68). Thus, membranes have to be thin (to address the possible hypoxic conditions for the inner part of the graft) and at the same time mechanically and chemically robust.

3.1.2. Historical aspects and developments—The first study that used encapsulated biological material for diabetes treatment was reported in 1933 by Bisceglie who placed human insulinoma tissue in membranous bags transplanted into rats(88). However, the concept of immunoisolated transplantation was really developed in the early 1950's by

Algire *et al.*(89-93). These researchers were interested in immune rejection mechanisms and wanted to know if cellular or humoral factors were responsible for the destruction of nonvascularized transplants. In order to answer that question, they designed a diffusion chamber by gluing together two thin membrane disks made of porous cellulose (supported by plastic rings) around the cells (see Figure 3). They used different pore sizes: some allowing free passage of host immune cells (leukocytes and macrophages) and others blocking those entities (pore diameters $< 0.45 \mu\text{m}$). Their results showed that allogenic tissue transplanted in mice was destroyed more rapidly with large pore membranes that permitted external cellular invasion. The lack of contact with immune cells prevented the direct antigen presentation pathway that leads to immune-mediated destruction.

Subsequently, many endocrine tissues were transplanted in similar extravascular diffusion chambers. However, only after the isolation of the islets of Langerhans in 1965 by Moskalewski(94) did immunoisolated islet cell research really begin.

The company *Millipore* produced a commercial extravascular transplantation chamber with $0.45 \mu\text{m}$ pores by modifying the design from Algire(64) (see Figure 3). Researchers used this chamber to confirm the improved survival of grafts within protective capsules(95, 96). Other types of membranes were developed and tested(64): nitrocellulose ester membranes, cuprophane (cellulose) bags, hydrogel membranes, hollow fibers... In 1991, Lacy *et al.* developed hollow fibers fabricated from an acrylic copolymer and used them to encapsulate rat islets immobilized in an alginate hydrogel. They transplanted these fibers either subcutaneously or intraperitoneally in diabetic mice(97) and these implants reverted diabetes for up to 60 days.

Transplant failure occurred sooner or later with these early extravascular macrocapsules due to fibroblastic overgrowth inside or/and outside the chamber(64). Inadequate oxygenation of the grafted cells was also advocated as a significant issue with macrocapsules(56).

Major advances have been made since the early developments of extravascular macrocapsules, which have been reviewed in details elsewhere(61, 64). Section 4 will also give a complete update about current designs for immunoprotective membranes for extravascular macroencapsulation of islet/beta cells.

3.1.3. Commercialization of extravascular macrocapsules—Several companies have produced extravascular chambers for islet encapsulation since the 1980s. *Baxter Healthcare Corp.* (Round Lake, Illinois) designed an encapsulation planar device called *TheraCyte* (see Figure 4) that is still in use today in several laboratories around the world(98, 99). The *TheraCyte* system is made of polytetrafluoroethylene (PTFE) and is composed of a cell impermeable membrane (400 nm pore diameter) laminated to another membrane ($5 \mu\text{m}$ pore diameter) that promotes neovascularization (angiogenesis). This double layer approach seeks to reduce diffusion time delays by development of a new vasculature within the large pores while the small pores immunoprotect the encapsulated cells. Angiogenesis can also be promoted by infusion of vascular endothelial growth factor (VEGF) transcutaneously into the device(70). Some success has been achieved in animal models using islets encapsulated in *TheraCyte* devices(100-102); however, there are no

reported studies of clinical success in human subjects and it is improbable that the 400 nm porous structure would lead to a full immunoisolation (IgG and cytokines will be able to cross the membrane of these devices).

Several other companies have also come and gone over the years: *Encelle* (A.-L. Usala) (pig islets macroencapsulated in a hydrogel matrix wrapped in a polyester net coated with a stealth polymer, device transplanted intramuscularly), *BetaGene* (C. Newgard) partnered with *Gore Hybrid Technologies* (cartridge of immortalized cells inserted in a prevascularized flexible tube transplanted subcutaneously) and *iMedd* (T. Desai and M. Ferrari) (macroencapsulation of islets with nanoporous silicon membranes)(103-107). The failure of these companies was mainly related to difficulties in achieving long-term viability of the encapsulated islets (fibroblastic growth over membranes, poor islet oxygenation and poor diffusion of nutrients) and lack of funding due to unmet objectives.

Two other companies are still in operation today: *Cerco Medical* and *ViaCyte*. *Cerco Medical* (formerly *Islet Sheet Medical*, Scott R. King, San Francisco) is developing the *Islet Sheet*, which consists of islets encapsulated in an alginate sheet(108, 109). This very thin (0.3 mm) device is the size of a business card (4 cm × 6 cm) and can sustain approximately 100,000 islets (see Figure 4). About 6 sheets will be necessary per transplanted human patient to achieve insulin independence. The envisioned implantation sites are the peritoneal cavity or a subcutaneous space. The *Islet Sheet* is intended to be fully retrievable and replaceable, ensuring safety. *Cerco Medical* is probably the most advanced company working with macroencapsulation today and is currently performing trials on pancreatectomized dogs (their pancreas has been totally removed to mimic type 1 diabetes) with encapsulated canine islets.

ViaCyte (formerly *Novocell*) (San Diego) is developing a macroencapsulation device called *Encaptra* (based on the *TheraCyte* device) that is designed to be transplanted subcutaneously. This retrievable and vascularizing capsule will contain pancreatic progenitor cells that are expected to differentiate into functioning islet cells(29-32, 110). Stem-cell derived pancreatic islets represent a promising alternative to the short supply of human islets available for transplantation. However, Matveyenko *et al.* are currently doubtful about the clinical application of such engineered cell types(33). They believe the extent of endocrine cell formation and secretory function is insufficient to be clinically relevant.

3.2. Intravascular macrocapsules

3.2.1. Intravascular diffusion chambers: advantages and disadvantages—

Intravascular diffusion chambers (see schematic representation in Figure 5) present a clear advantage over extravascular devices: they have a direct access to blood and thus more accurate tracking of blood glucose levels. This reduces delays for insulin secretion and the islets are also very well oxygenated due to the blood proximity. Extracellular matrix can also be chosen independently with intravascular macrocapsules to ensure the most suitable environment for cells.

However, these devices also present disadvantages, including a complicated and risky surgical procedure and blood coagulation issues after transplantation(64). Blood flow distortion at the interface between the blood vessel and the device can induce platelet deposition leading to thrombosis. Moreover, the tubing and membranes themselves can cause blood coagulation. Unfortunately, systemic anticoagulation medication is unadvisable for people suffering from type 1 diabetes.

3.2.2. Intravascular diffusion chambers: historical aspects and developments

—Development of intravascular macrocapsules began in 1972 when Knazek *et al.* fabricated an artificial capillary system for continuous perfusion culture systems(111). Three years later, Chick *et al.* reported the first culture of islets in such a device and referred to it as an “artificial endocrine pancreas”(112). In 1977, Chick managed to reverse diabetes in rats by transplanting this device in the aorta with heparin anticoagulation(113). The membrane was made of *Amicon* (polyacrylonitrilepolyvinyl chloride copolymer (PAN/PVC)). Tze(114), Sun(115) and Orsetti(116) published similar results with diabetic rats. These studies constituted a proof of concept for intravascular macrocapsules, although coagulation and hemorrhage complications occurred after several days(117-119). Scharp *et al.* obtained similar results with tubular polycarbonate membranes(64).

Development of intravascular capsules was subsequently slowed or even stopped because of clotting issues. However, a report from Prochorov *et al.* published in 2008 has renewed interest in this approach(86). They transplanted a nylon macrocapsule (pore diameter: 1-2 μm) into the arteria profunda femoris or into the forearm cubital vein of 19 diabetic human patients, 3 of them with diabetes resulting from pancreonecrosis (non-immune nature). They used islets from fetal rabbits and no immunosuppressive therapy was used, only standard antithrombotic therapy for 5 days after surgery. Positive results were still observed in 14 patients two years after transplantation. Exogenous insulin demand was reduced by 60-65% and hypo- and hyperglycemic comas disappeared completely. C-peptide and immunoreactive insulin levels increased significantly.

T-cell immunity to grafting was absent and neither vascular lumen narrowing nor thrombosis was observed. However, approximately 40% of the islets died in the first weeks because of poor vascularization in the chamber (neovascularization only developed in the macrocapsule after 2 weeks).

3.2.3. Intravascular ultrafiltration chambers—A slight design modification of intravascular diffusion chambers lead to ultrafiltration chambers (see schematic representation in Figure 6). This configuration eliminates any diffusion-based delay in the transport of nutrients and therapeutic products: blood is ultrafiltered by the membrane, crosses the islets and stimulates them with respect to its glucose concentration and finally delivers the secreted insulin via the venous connection. This approach permits the best oxygen and nutrient availability to encapsulated cells. However, these intravascular macrocapsules present the same blood coagulation problems as the diffusion chambers. Moreover, deposition of proteins can also occur on ultrafiltration membranes over time, ultimately leading to clogging and thrombosis(64).

Ultrafiltration chambers have been used in diabetic rats by Reach *et al.*(120) and Scharp *et al.*(64). However, the devices only worked for hours before being clotted. Their development has been on hold since then.

3.2.4. Commercialization of intravascular macrocapsules—In 1985, Hayes and Chick founded *BioHybrid Technologies* that developed a reseedable intravascular chamber with limited success transplanting allogenic islets into pancreatectomized dogs(121). Their device was connected to the vascular system as an arteriovenous shunt. 6 out of 10 dogs remained insulin-independent after 5 months but the glycemic control in response to a meal or an intravenous glucose tolerance test remained abnormal. They also implanted a device with bovine islets in a pancreatectomized dog that remained insulin-independent for 80 days. Developments of this company were halted because of the previously mentioned issues with intravascular approaches.

3.3. Microcapsules

3.3.1. Advantages and disadvantages—Microencapsulation presents several advantages: the microbeads (see Figure 7) are implanted via minimally invasive surgery (simple injections are even possible), and their high surface to volume ratio confers better diffusion characteristics than extravascular macrocapsules (at least in theory). Faster diffusion kinetics are beneficial for cell oxygenation and glucose-stimulated insulin production and release.

However, microcapsules also present several disadvantages. They are difficult if not impossible to retrieve after implantation (that may be very dangerous in case of a complication). They have indirect access to blood, which causes delays in diffusion of O₂, glucose and insulin. The thickness of microcapsules is also a barrier for diffusion, although recent strategies have permitted a reduction of it. Moreover, since the cells are encapsulated while forming the microcapsules, these lack the capacity to choose a different material for the extracellular matrix. Another problem arises from the broad pore size distributions of microcapsules associated with their polymeric nature (with the exception of recently developed self-folding microcontainers presented in section 4.2.4., microcapsules can only be made of polymers). This could be an issue for complete immunoisolation of cells. Indeed, even if only 1% of pores are larger than the cut-off goal, passage of antibodies, complement, and cytokines will be sufficient to initiate immunorejection pathways(56). Finally, microcapsules prevent formation of clusters of encapsulated cells, unlike a real pancreas.

3.3.2. Materials—The most popular materials for microencapsulation are alginates. Alginates (primarily extracted from seaweeds) are natural anionic polysaccharides composed of homopolymeric regions of beta-D-mannuronic acid (“M-blocks”) and alpha-L-guluronic acid (“G-blocks”) interspaced with regions of mixed sequence (“MG-blocks”). They have hydrogel-forming properties with di- or trivalent cations (Ca²⁺, Ba²⁺, Fe³⁺...) used as cross-linking agents(122). Alginates are a good material choice for cell encapsulation due to their good biocompatibility and the fact that the encapsulation procedure can be performed under mild conditions not detrimental to cells(123).

Alginate-based microencapsulation usually consists of extruding a suspension made of a solution of sodium alginate plus islets through a microdroplet generator that incorporates a peristaltic pump and an air flow source (electrostatic droplet generation)(62). The suspension is continuously cut (by air shearing forces) into small spherical droplets. These drop into a positively-charged cation bath (usually CaCl_2 or BaCl_2) and immediately turn into water-immiscible gel microbeads that contain one or a few islets. The beads are then coated with an aminoacidic cation solution, typically poly-L-lysine (PLL) or poly-L-ornithine (PLO). The amine groups bind to carboxylic alginate radicals, preventing access by unwanted cellular and humoral mediators of the host's immune system(62). Less frequently, non-spherical microcapsules have also been produced by using polymeric replica molds in polydimethylsiloxane (PDMS)(124) or polypropylene (PP)(125).

3.3.3. Historical aspects and developments—The term microencapsulation was first mentioned by Chang in 1964 to describe aqueous solutions of protein within polymer microcapsules of 1-100 μm in diameter(126). However, the first microencapsulation of pancreatic islets was performed by Lim and Sun in 1980(127). They showed that insulin was released from spherical microcapsules made of alginate-polylysine-polyethyleneimine. They also managed to revert diabetes in rats for 3 weeks using intraperitoneal implants. The graft failed after that period due to poor material biocompatibility. Biocompatibility was improved in 1984 by O'shea and Sun who used intraperitoneal implants of islets in alginate-polylysine-alginate microcapsules(128). Diabetes was reverted in rats for up to 1 year. Subsequent chemical purification of alginates further improved the biocompatibility of microcapsules(129-131). Polyethylene glycol (PEG) hydrogels have also been used as a coating on microcapsules to improve their biocompatibility(132). In 1997, Wang *et al.* evaluated over a thousand combinations of water-soluble polyanions and polycations to find the best polymer for encapsulation of living cells(133). Their most promising combination consisted of sodium alginate, cellulose sulfate, poly(methylene-co-guanidine) hydrochloride, calcium chloride and sodium chloride. This formulation allowed independent control of capsule size, wall thickness, mechanical strength and permeability. Reversal of diabetes was maintained for up to 6 months in mice with intraperitoneal implants.

Besides alginates, other materials have also been studied for microencapsulation, including sol-gel silica (SiO_2)(134, 135), polyacrylates(136), agarose(137, 138), chitosan(139)...

In order to improve nutrient availability for microencapsulated cells, several groups tried to decrease the thickness of the capsules. With this perspective, they developed techniques to directly deposit very thin (1.5 to 50 μm)(57) conformal coatings of protective biomaterial (usually alginate) on the surface of islets. The transplant volume in this case is determined only by the size of objects being coated and the coating thickness, reducing void volume and diffusion delays. In theory, immunoisolation could also be achieved by applying even thinner coatings down to submicron or nanoscale thickness. The terms nanoencapsulation and molecular camouflage have been introduced to refer to this subclass of microcapsules(57). Polyethylene glycol (PEG) chains are usually anchored to the cell or islet surface to create a barrier preventing molecular recognition between cell surface receptors and soluble ligands(140, 141). Attachment of PEG is generally performed by covalently coupling PEG to amines of cell surface proteins or carbohydrates, or by direct insertion of

PEG-lipid conjugates into the cell membrane(141). Despite promising results with PEG protected islets transplanted in rats, it is unclear how long PEG coatings will remain stable enough to provide protection for a graft(57). Besides PEGylation, it is also possible to construct nanothin films of controlled permeability and surface chemistry directly on the surface of cells via layer-by-layer (LbL) polymer self-assembly(57, 142, 143). Polyelectrolyte multilayer (PEM) films are created that way by using polycations and polyanions: poly(L-lysine)(PLL)/alginate, chitosan/hyaluronic acid, PLL/hyaluronic acid, poly(diallyldimethylammonium chloride)/poly(styrene sulfonate)(PSS)... However, the possible toxicity of polycations and the immunoisolation properties of these multilayers need to be further investigated.

Microcapsules have already been evaluated in clinical tests on humans. Soon-Shiong reported the first case of transplantation into a human in 1994(144). This team used human cadaveric islets microencapsulated in purified alginate with a high guluronic acid content. Insulin independence was demonstrated 9 months after the procedure, yet the patient was already on low-dose immunosuppression due to a kidney transplant.

More recently, in 2006, Calafiore led a clinical trial on non-immunosuppressed patients using alginate microcapsules (containing human islets) that were double-coated with poly-L-ornithine and sodium alginate(145). They first reported results from two patients showing amelioration of their mean daily blood glucose levels and reduction of daily exogenous insulin (although exogenous insulin independence was unsuccessful)(146). In 2011, they reported new results from a total of four non-immunosuppressed patients including the previous two patients(147). Patients were followed through 3 years after transplantation of the microcapsules and no sign of islet rejection was seen (absence of islet cell antibodies and anti-MHC class I-II antibodies). Amelioration of blood glucose levels was achieved for all patients as well as reduced need for exogenous insulin. However, these improvements dissipated over time and patients had reverted to their original exogenous insulin therapy regimen at the end of the trial.

Developments and current research in microencapsulation have also been extensively reviewed elsewhere(57, 62, 148-153). Rabanel specifically reviewed fabrication techniques for microcapsules(123). Among the different reviews, de Vos *et al.* provided recommendations for characterization of microcapsules for cellular encapsulation(151). They stressed the importance of standardizing characterization procedures to resolve current lab-to-lab variations and lack of reproducibility in organic microcapsules. They have identified five criteria that should be detailed in any research related to microencapsulation: polymer characterization (high-resolution NMR), permeability, surface properties (FT-IR, XPS, TOF-SIMS, Microscopies), biocompatibility and storage conditions.

3.3.4. Commercialization of microcapsules—The company *Living Cell Technologies (LCT)* (Auckland, New Zealand) has been using alginate microencapsulation over the last few years. *LCT* is investigating the use of encapsulated porcine islets following a study on a human recipient published in 2007(154). *LCT* is the first company to enter clinical trials using therapeutic porcine cell implants. They have completed a successful Phase I/IIa clinical trial in Russia and currently have Phase IIb clinical trials underway in New Zealand

and Argentina. *LCT* and *Otsuka Pharmaceutical Factory* created a new company in 2011, *Diatranz Otsuka Limited (DOL)*, to accelerate development and commercialization of their porcine cell product. *LCT* is poised to be the first company to launch a product on the market within the next few years.

MicroIslet (San Diego) also developed a strategy to microencapsulate porcine islets to treat type 1 diabetes in humans, but the company is no longer operating.

Microencapsulation is also currently envisaged by the company *ALTuCELL* (Dix Hills, New York) that plans to transplant microencapsulated porcine-derived Sertoli cells into humans to revert type 1 diabetes (Dr. Calafiore is also involved in this company)(155).

4. CURRENT IMMUNOPROTECTIVE MEMBRANE DESIGNS

This chapter will discuss the current membrane designs for cellular immunoprotection. It is divided in 2 parts: organic (polymeric) membranes and inorganic ones. Another recent review discusses broader medical and biological applications of nanoporous membranes(156).

4.1. Organic membranes

The first and most common materials used to fabricate immunoprotective membranes are polymers. Their main drawback is a relatively broad pore size distribution (variations as large as 30% for polymeric membranes formed by solvent-casting)(157). The use of ion-track etching to form polycarbonate filter membranes (e.g.: *Isopore* from *Millipore*) has permitted much tighter pore size distributions (~10%) but these membranes have low porosities (maximum 20%), limited pore sizes and randomly distributed pores across their surface(158). These limited properties have excluded commercial track etch filters from cell encapsulation applications.

The most studied polymeric materials for cell immunoisolation are not synthetic but natural polymers, the alginates (a hydrogel consisting of anionic polysaccharides extracted from seaweeds). They currently lead the field of microencapsulation and are also gaining a lot of attention in macroencapsulation as “islet sheets”, layers of islets sandwiched between thin layers of alginate (described in section 4.1.1.).

Besides alginates, other polymeric materials have also been studied for cell encapsulation. They can mainly be separated in two classes: hydrogels and thermoplastic polymers(63, 159). Hydrogels are water swollen 3D networks of hydrophilic homopolymers or copolymers(160). Their structural integrity relies on cross-links formed between polymer chains (chemical bonds and physical interactions). Due to their viscoelasticity and high H₂O content, they resemble natural biological tissues and often induce minimal inflammatory response. Their permeability is adjustable, which is promising for cell immunoisolation, but since they rely on crosslinks, these materials will always present a broad pore size distribution (which is broader than inorganic membranes). This can be an issue for complete immunoprotection of encapsulated cells. Indeed, even if only 1% of pores are larger than the size cut-off goal, the pores will allow sufficient passage of antibodies, complement, and

cytokines to initiate immunorejection(56). Besides alginates, hydrogels that have been studied for cell encapsulation include: polyethylene glycol (PEG)(161, 162), agarose (macrobeads)(163, 164), polyvinyl alcohol (PVA) (islet sheet)(165, 166), polyvinyl alcohol and polyacrylic acid copolymers (PVA/PAA) (membrane)(167).

The other category of encapsulating polymers is thermoplastics. They consist of long, linear and water insoluble chains that can be processed into multiple configurations by heat melting followed by cooling. Their chemical and mechanical stability properties are superior to those of hydrogels, which explains why thermoplastics have mainly been used for macrocapsules. However, hydrogels still remain the most popular choice for cell encapsulation due to their very good biocompatibility.

Thermoplastic materials that are currently used for cell immunoprotection are polyacrylonitrile and polyvinyl chloride copolymers (PAN/PVC or *Amicon*; hollow fibers) (97, 113, 168, 169), polyurethane (PU) and polyurethane and polyvinyl pyrrolidone copolymers (PU/PVP) (macrocapsules)(170, 171), PU (membranes)(172), polysulfone (hollow fibers)(173, 174), AN69 renal dialysis membranes (69% acrylonitrile and 31% sodium methallyl sulphonate) modified by electrical discharges(175), polytetrafluoroethylene (PTFE) membranes(98, 99, 176, 177), dual porosity nylon membrane(178)...

Among organic materials that have been tested for cell immunoisolation, alginates are certainly the most promising, both as microcapsules (see section 3.3.) and as the “islet sheets” (macrocapsules) described below.

Another interesting approach that is still in its infancy is the fabrication of SU-8 (an epoxy) microcapsules with very precise nanopores. The use of photolithographic techniques permits to obtain a very narrow pore size distribution which is normally never achieved with polymeric materials. Section 4.1.2. gives more detail about this technique.

4.1.1. Alginate islet sheets—While alginates have led the microencapsulation field, they have also been used for macroencapsulation by Dufrane *et al.* who recently developed an alginate device(179, 180). Briefly, their device consists of a collagen matrix on which islets are seeded to produce a cell monolayer, allowing faster diffusion kinetics as compared to clusters of islets. This monolayer is then covered by a gelled layer of alginate 3% wt./vol. rich in mannuronic acid (the other side of the collagen matrix is also covered by an alginate layer). This produces an islet sheet (“monolayer cellular device”, MCD) that is ready to be transplanted (see Figure 8).

Dufrane *et al.* have already reported very promising results with this type of devices in 2010(180). They transplanted (without any immunosuppression) encapsulated pig islets in streptozotocin-induced diabetic monkeys: 4 primates received alginate microcapsules transplanted under the kidney capsule and 5 primates received 3 to 5 alginate MCDs transplanted into abdominal subcutaneous tissue (same batch of alginate for micro and macrocapsules). Only two animals within the microcapsule group showed complete control of diabetes and for a very limited time (2 weeks). The animals that received the

Then, the mold is used to superficially imprint nanoslots in a SU-8 membrane. A metal is then deposited at an oblique angle to the membrane to protect the superficial imprint features. The nanoslots are finally etched chemically and anisotropically through the entire cross section of the membrane producing a semipermeable membrane that can be used for cell immunoisolation. The final pores present a width of 20 nm that is precisely controlled over the whole membrane surface and a length of about 1 μm . The reusable mold permits to achieve reproducibility and allows possible high-throughput fabrication.

The nanoslotted membranes are then integrated into the surfaces of SU-8 cuboid microcapsules fabricated by lithography. The microcapsules provide support to the thin (350–450 nm) nanoporous membranes and consist in a base with a female structure that hosts the insulin-secreting cells and a lid with a male structure (see Figure 9).

One difference of this approach as compared to other photolithographic techniques is that it aims to produce microcapsules, rather than macrocapsules like those presented in section 4.2.1. on Si nanoporous membranes. These SU-8 microcapsules are designed to house a single pancreatic islet, or an equivalent cluster of insulin-secreting cells, with an encapsulation space of $200 \times 200 \times 200 \mu\text{m}^3$. They thus present the advantages of microencapsulation but have better diffusion characteristics due to their very thin membranes (as compared to the thicker alginate microcapsules). Moreover, the pore width is very precise and uniform, comparing favorably with polymer conformal coatings.

A key feature of these nanoporous containers is their optical and MRI transparency, allowing multimodal imaging of encapsulated islets post-transplantation (two-photon confocal microscopy and MRI)(181). *In vitro* experiments showed that islet function is unimpaired after 48 h of encapsulation(181). Other experiments studied the diffusion of fluorescent probe molecules across the nanoporous membranes: IgG-FITC(182), lectin-FITC (140 kDa) and FM 4-64 (608 Da)(183). While FM 4-64 diffused without any problem, some diffusion of the larger molecules (that would ideally be blocked) was also observed. This may be attributed either to the slit shape of the nanopores, possibly enabling flexible proteins to cross the barrier, or to a gap between the lid and the base of the microcapsules (no experiment has been carried out yet to determine the degree of sealing of the assembly). In order to investigate cell oxygenation within these nanoporous containers, 9L rat glioma cells were engineered to bioluminesce under hypoxic conditions(182), which could potentially be used for future *in vivo* experiments. The preliminary results indicate that the nanoporous capsules may provide restricted oxygenation of the encapsulated cells.

It is also important to mention the robustness of these microcapsules(181), which do not fracture or rupture when manipulated during manufacture and encapsulation. This is another advantage over alginate-based microcapsules that are not so mechanically stable.

Although this research is still in its infancy, nanoporous SU-8 containers may prove useful to encapsulate islet cells in the future. Concerns about the lack of biocompatibility of this polymer may be solved by applying coatings of biofriendly molecules or bioinert materials, such as gold(181).

4.2. Inorganic membranes

Advances in inorganic materials research in the electronics, sensors and photovoltaics industries have enabled the development of inorganic nanoporous membranes with well controlled pore sizes and geometries. The produced nanoporous membranes have inspired researchers active in drug delivery and cell encapsulation. For instance, silicon microfabricated membranes were already proposed for biomedical applications in 1995(186, 187).

Three inorganic materials currently present very promising properties for the production of immunoisolating membranes(61): silicon (Si), aluminum/aluminum oxide (Al/Al₂O₃) and titanium/titanium oxide (Ti/TiO₂). The extravascular macrocapsules that use those membranes present several advantages over their polymeric counterparts: a tighter pore size distribution and faster diffusion kinetics due to decreased membrane thickness(105). For Si and Al/Al₂O₃ membranes, these advantages have to be balanced with decreased levels of biocompatibility. The three materials will be presented in the following sections. The fabrication techniques discussed here are not the only ones available, yet they present a major advantage over other techniques: they lead to materials with straight nanopores, ensuring the fastest diffusion possible for nutrients and therapeutic products. Indeed, powder sintering and sol-gel methods also produce nanoporous SiO₂, Al₂O₃ and TiO₂ - but the pores are always tortuous in these cases(156). Commercial porous Al₂O₃ filter membranes, *Anopore* from *Whatman*, could also be interesting to encapsulate cells. They present uniform pore sizes with high pore densities (>10¹⁰/cm²), but available pore size is quite limited.

Finally, a last section will present a different and very innovative approach to produce nanoporous microcontainers that assemble by self-folding. One interesting feature of this technique is that numerous materials can be used to form these microcapsules.

Since the science behind these inorganic nanoporous membranes is rather new, these materials have not been tested as much as the polymeric membranes for cell encapsulation. However, they have the potential to catch up with the currently popular alginate microcapsules and sheets by offering better stability and tighter control of porosity.

4.2.1. Silicon nanoporous membranes—Inspired by the fabrication techniques used for the production of silicon computer chips, silicon nanoporous membranes were initially developed and used to encapsulate pancreatic islets by Desai and Ferrari(103). The development of this silicon membrane technology has been extensively reviewed elsewhere(53, 105, 158, 188). The process scheme is presented in Figure 10.

Fabrication of Si nanoporous membranes starts with a Si wafer. A support ridge structure is first etched by photo-lithography to provide mechanical support to the final structure (not shown in Figure 10). A very thin silicon nitride (Si₃N₄) layer is then deposited on top of the wafer, serving as an etch-stop for future processes. A structural base layer of polysilicon is deposited on top of the Si₃N₄ (Figure 10a), and its thickness will determine the overall thickness of the final nanoporous membrane (0.5 μm to 5 μm). Holes are then etched through poly Si by a chlorine plasma (Figure 10b), and a sacrificial silicon oxide (SiO₂) layer is thermally grown over the Si base layer (Figure 10c). The sacrificial oxide thickness

determines the pore size in the final membrane, and pores ranging from 7 nm to 100 nm have been obtained with tight pore size distributions (<5% pore width variation)(105, 158). The next step consists in depositing plug poly Si in the holes of the base layer (Figure 10d). The surface is then planarized, leaving a smooth exposed surface of sacrificial oxide (Figure 10e). Subsequently, a Si₃N₄ protective layer is deposited uniformly across the wafer. Windows are etched through this layer on the bottom side of the wafer to expose the bulk Si in specified areas. The wafer is then placed in a KOH bath at 80°C where bulk Si is dissolved up to the Si₃N₄ etch stop layer (Figure 10f). Finally, the protective and etch-stop Si₃N₄ layers and the sacrificial SiO₂ layer are removed by etching in hydrofluoric acid (HF) (g). The finished product is a Si nanoporous membrane of controlled thickness presenting slit nanopores of controlled channel widths. These pores are organized in parallel arrays along the membrane major dimension. The length of the pores is fixed at 45 μm and there are 10,000 pores/mm² (105). Hence, the total pore area increases linearly with the pore size.

Figure 11 shows a picture of one Si nanoporous membrane as well as SEM micrographs illustrating the pore structure.

The very tight pore size distributions (<5%)(158) of these Si nanoporous membranes make them advantageous over their polymer counterparts for which pore size distributions of 30% are common(157).

Desai *et al.* used 18, 66 and 78 nm porous Si membranes to encapsulate rat islets. They performed a glucose stimulated insulin secretion test and showed that encapsulated islets presented a similar release profile as compared to unencapsulated islets(103, 189). Moreover, 18 nm pores significantly hindered the passage of IgG as compared to the larger pores, although with incomplete blockage(189). They also incubated islet-filled capsules in a serum complement/antibody solution during 2 weeks. At day 14, the insulin secretion following stimulation by glucose was approximately 5 times higher for the encapsulated islets (18 and 78 nm pores) as compared to free islets, proving the potential of this immunoisolation technology.

In vivo tests were also performed with encapsulated rat and mouse insulinoma cells implanted intraperitoneally in mice(190). After 8 days, biocapsules were removed for cell viability and functionality tests. The insulinoma cells encapsulated by 18 nm membranes exhibited higher insulin secretion upon glucose stimulation than the cells in 66 nm porous capsules, highlighting the correlation between smaller pores and immunoprotection. Membranes with pores below 18 nm have also been tested for diffusion of glucose, albumin (67 kDa) and IgG(53, 191). The diffusion of glucose was constrained with pores below 13 nm (non-Fickian diffusion) and albumin was unable to pass through 7 nm pores. Diffusion of IgG was greatly hindered, especially for 7 nm pores. However, total immunoisolation was not achieved, despite early estimations that pore sizes between 30 and 50 nm should be able to exclude IgG(192). This can be explained by the flexible characteristics of the Y-shaped IgG protein that can adopt different conformational changes(53), easing its diffusion through the slit pores (a few nm wide but 45 μm long). Unfolding of the 3D protein structure may also occur, easing the passage of IgG as well. Therefore, slow diffusion of IgG may be expected even for pore sizes below 20 nm. A strategy that could be applied to block IgG is

to decrease the length of the pores. However, a very tiny leak of IgG may not be so detrimental to the cells. Iwata and others showed that complement components are rapidly inactivated, and therefore it should be good enough to hinder IgG diffusion in the first days after implantation rather than completely block it(66, 193, 194).

Thus, a Si membrane with pores just below 20 nm should be able to immunoprotect cells while allowing sufficient diffusion of glucose and insulin (due to their very low thickness of a few micrometers).

Silicon membranes can also be modified in terms of surface chemistry. Strategies have been developed to decrease unwanted adsorption by coating Si with polyethylene glycol (PEG) (195, 196). The PEG chains can be covalently attached to Si and permit reduced adsorption of albumin, IgG and fibrinogen by 76, 82 and 64%, respectively, as compared to untreated Si.

The assembly of these Si nanoporous membranes into actual biocapsules has been performed differently over the years. The interested reader can find information on that matter elsewhere(53, 105-107, 189, 197).

4.2.2. Alumina nanoporous membranes—It is well known that surfaces of aluminum (Al) present a high affinity for oxygen, resulting in the formation of an aluminum oxide layer covering the metal. However, this natural oxide layer is uncontrolled, and this has led researchers to develop anodization techniques to grow controlled porous or non-porous layers of aluminum oxide (Al_2O_3) on Al substrates(198). An interesting feature of these porous layers is that they present ordered straight circular pores in a hexagonal arrangement. Provided the layers are separated from the underlying Al, they could be used as membranes for cell immunoisolation.

Following Itoh *et al.* in 1996(199, 200), Gong *et al.* reported in 2003 a sequential etching technique to produce an Al_2O_3 nanoporous membrane embedded in a cylindrical Al tube(201) (see Figure 12). They showed that such devices could control release of dextran conjugates of varying molecular weight by adapting the pore size, via the anodization voltage. The same fabrication process has also been used to produce flat membranes of Al_2O_3 (202).

Briefly, the external surface of an Al tube is coated with a thin layer of protective polymer, e.g. nail polish (Figure 12a). Then, an anodization step is performed from the inner side of the tube in 0.25 M oxalic acid, producing a layer of nanoporous Al_2O_3 . Voltage selection determines the pore size (diameter). This layer is then etched in a mixture of H_2CrO_4 and H_3PO_4 , leaving a uniform concave array of nucleation sites that are critical to obtaining narrow pore size distributions during the subsequent anodization step. A second anodization step is then performed at the same voltage, producing the final Al_2O_3 nanoporous membrane with circular pores (Figure 12b). The duration of this anodization determines the membrane thickness. In order to expose the nanoporous membrane, window-areas are created with acetone in the protective outer polymer film. Both ends of the Al tube are then protected with *Parafilm* and the tube is dipped in a 10 wt. % HCl and 0.1M CuCl_2 solution that

selectively etches unprotected Al areas, thereby revealing a transparent Al₂O₃ membrane (Figure 12c). Since the nanoporous membranes are incorporated in the Al tube, they are strong enough for easy handling and use. The final step is to etch the barrier layer present at the outer surface of the Al₂O₃ membranes in a mixture of H₂CrO₄ and H₃PO₄. The *Parafilm* and polymer protection layers are then removed (Figure 12d), resulting in an Al cylinder with Al₂O₃ nanoporous membrane windows (see Figure 13).

Superior control over the size and shape of the nanoporous Al₂O₃ windows within a flat Al frame can be achieved by using a photoresist polymer as the initial protective coating that can then be removed at selected locations by photolithography(203).

The general technique presented here produces nanoporous Al₂O₃ membranes in a variety of configurations that may be used for immunoisolated cell encapsulation(204). Anodization technology is really simple and inexpensive, especially if no photolithography step is involved. Diameters of circular vertical nanopores reported in the literature are comprised between 25 and 80 nm and the thicknesses of these membranes range from 55 to 100 μ m(201-204). Pore size distributions of Al₂O₃ membranes(204) are worse than those of microfabricated Si membranes but they are still better than those of their polymeric counterparts. The thicknesses of Al₂O₃ membranes are larger than those of Si. Thicker membranes obviously impede diffusion of oxygen, glucose and insulin but simultaneously render the whole device more robust and resistant. Moreover, the high density of pores ($\sim 10^{10}/\text{cm}^2$)(204) achievable for alumina membranes could compensate for their increased thickness from a diffusional point of view.

La Flamme *et al.* compared diffusion coefficients of glucose and IgG for an Al₂O₃ 75 nm membrane, for a Si 49 nm membrane, and for a poly(vinyl alcohol) 10-30 nm hydrogel(204). Transport of glucose was comparable for all 3 membranes, but diffusion of IgG was significantly reduced for Al₂O₃ vs. Si and the hydrogel, even though these two presented a smaller pore size. The circular shape of Al₂O₃ nanopores seems to be really advantageous over rectangular slit pores of Si or the hydrogel pores regarding blockage of the flexible IgG. *In vitro* encapsulation studies have also been performed by La Flamme with MIN6 insulinoma cells(204). They showed insulin secretion upon glucose stimulation although the secreted insulin amounts were lower with the 75 nm Al₂O₃ membranes than with unencapsulated cells due to the physical barrier of the membrane.

The main concern for the use of Al₂O₃ nanoporous membranes is the extent of biocompatibility for this material. However, *in vitro* tests have shown that these membranes are nontoxic to fibroblast cells and do not induce significant complement activation(205). It has also been shown that incorporation of a polyethylene glycol (PEG) coating(202, 206) reduces the interactions of serum albumin with the material(205). This reduction in protein adsorption will certainly help to prevent any clogging of the pores. Finally, *in vivo* tests of up to 4 weeks with empty Al/Al₂O₃ capsules have demonstrated that implantation of these capsules into the abdominal cavity of rats induces a transient inflammatory response (probably due to the surgery and not to the capsule), and that PEG coatings were useful in minimizing the host response(205). The membranes were fully intact and free from fibrous growth at the end of the 4 weeks.

Despite encouraging preliminary results, Al₂O₃ nanoporous membranes have not yet been tested *in vivo* with encapsulated cells.

4.2.3. Titania nanotubular membranes—As for aluminum, surfaces of titanium (Ti) present a high affinity for oxygen, resulting in the formation of an oxide layer covering the metal. Since this natural oxide layer is not controlled, anodization techniques have also been developed for this material. Less studied than Al anodization, Ti surface modification encountered a major breakthrough in 1999 when Zwilling *et al.* anodized a Ti sample in a solution of H₂CrO₄ and HF and observed the formation of a porous layer of TiO₂ nanotubes in a hexagonal arrangement(207). In 2001, Gong *et al.* obtained uniform arrays of well-aligned TiO₂ nanotubes after anodization of a Ti foil in an aqueous solution containing 0.5 to 3.5 wt. % HF(208).

Numerous studies of the formation and characterization of TiO₂ nanotubes have been published afterwards(209-220). The influence of anodization experimental parameters (electrolyte composition, temperature, voltage, current, anodization time...) on the resulting nanotubular TiO₂ arrays has been thoroughly investigated in these studies. Layers of vertically-oriented nanotubes with diameters from 15 to 150 nm (mainly controlled by anodization voltage) and lengths from a few nm to 1000 μ m (mainly controlled by anodization time) have been produced. Synthesis of TiO₂ nanotubes by anodization, properties of these tubes and their applications have been reviewed extensively elsewhere(221-224).

Arrays of TiO₂ nanotubes present several excellent characteristics for biofiltration applications such as cell-based drug delivery and immunoisolation: they have circular nanopores that are ideal for blocking flexible proteins like IgG and a very narrow pore size distribution coupled to a very high pore density(217), their thickness can be varied over a broad range, and their biocompatibility is excellent(225).

A variety of procedures are given in the literature to produce a uniform TiO₂ nanotubular layer. A simple recipe that is widely used currently is to anodize a Ti foil in an ethylene glycol solution containing 0.3 wt. % of NH₄F and 2 vol. % of H₂O (220). A nanotube length of about 200 μ m (pore diameter 125 nm, standard deviation 10 nm) is obtained after anodization of the Ti foil at 60V for 72 h. SEM micrographs of such a TiO₂ nanotubular layer are presented in Figure 14.

A common practice to improve the close-packed hexagonal arrangement of the nanotubes is to carry out 2 subsequent anodizations on the same Ti foil(217). A first anodization produces a layer of TiO₂ nanotubes that is not perfectly ordered, which is then removed. This leaves a dimpled pattern on the Ti surface. A second anodization conducted with this textured surface then produces a layer of TiO₂ nanotubes with improved ordering.

Despite promising properties for immunoisolation, TiO₂ nanotubes have not yet been applied to cell encapsulation. This is mainly due to the fact that this avenue of research is still in its infancy for Ti. Techniques to produce a free-standing membrane of TiO₂

nanotubes are not as mature as they are for nanoporous Al_2O_3 . TiO_2 nanotubes have to be detached as an array from the Ti foil and their bottom ends (barrier layer) need to be opened.

Different techniques have been reported so far(219, 220, 226-234) but these approaches remain difficult to realize in practice, especially for large area membranes.

Another very interesting approach to produce membranes was developed in 2010 by Albu *et al.* (see Figure 15)(235). They evaporated a 5 μm film of Al on a 6 μm Ti foil. After depositing a positive photoresist on Ti (Figure 15a), they defined a grid structure via photolithography (Figure 15b). They subsequently performed anodization in an ethylene glycol electrolyte containing NH_4F and DI H_2O , producing TiO_2 nanotubes connected to Al_2O_3 nanopores (no TiO_2 barrier layer in this case) (Figure 15c). The Al substrate and the Al_2O_3 porous area were then selectively etched in an acidic solution of $19(\text{H}_3\text{PO}_4):1(\text{HNO}_3):1(\text{CH}_3\text{COOH}):2(\text{H}_2\text{O})$ parts by volume (Figure 15d). The remaining Ti frame allows for a high mechanical flexibility. The nanopores present a diameter of 30 ± 10 nm. These membranes have been tested for diffusion of methylene blue and nanospheres of 20 and 200 nm, showing total blockage of the latter while 20 nm spheres diffused slower than methylene blue.

Other studies on TiO_2 nanotubular arrays for membrane applications have investigated diffusion of methylene blue(226), phenol red(219), phenol red, glucose, bovine serum albumin (BSA) and IgG(220). This last study used a 200 μm thick membrane with 125 ± 10 nm pores and showed that the diffusion coefficient of IgG was about 100 times smaller than that of BSA and 1000 times smaller than that of glucose, which are encouraging results for islet encapsulation applications.

TiO_2 nanotubular layers seem to be an excellent choice for incorporation into macrocapsules for cell immunoisolation. However, the research in this field is still in its infancy and a lot of work will need to be carried out to assess the potential of this material for biofiltration applications.

4.2.4. Self-folding microencapsulation devices—An innovative microencapsulation approach that was developed by Gracias *et al.* utilizes patterned self-folding devices to host and immunoprotect cells(236-238).

Current microfabrication and lithography techniques can produce very precise pores at the nanoscale on 2D surfaces, and resulting cell-containing capsules typically incorporate 1 or 2 of these membranes. This can result in hypoxic conditions for cells residing far away from these porous surfaces. In order to tackle this problem, Gracias *et al.* developed a technique derived from the ancient Japanese art of paper folding, origami. Using lithography techniques, they produce a patterned 2D precursor structure with hinges. The next step involves self-folding of the 2D structure along the hinges to produce a precise 3D hollow structure. Different polyhedra have been produced this way, and the main advantage resides in that nearly all faces of these objects can be porous. Precisely patterned hollow polyhedra with overall dimensions from 100 nm to 1 cm have been fabricated with a variety of materials, including metals, ceramics and polymers(236-242). Straight or curved pores as

narrow as 15 nm have been produced on the faces of these objects using electron beam lithography(240). These very small containers present all the advantages of microencapsulation but have better diffusion characteristics due to their very thin walls (as compared to thicker alginate microcapsules). Moreover, their pores are very uniform and present a narrow size distribution due to lithography. These microcontainers thus compare favorably with polymer conformal coatings. Very similar in size to SU-8 nanoporous microcapsules from Gimi *et al.*, self-folded capsules present the advantage of being porous on all of their faces, improving oxygenation of the encapsulated cells and enhancing diffusion of nutrients and therapeutic products. The variety of materials that are compatible with this approach is another advantage of this technique.

The self-folding phenomenon is usually driven by minimization of surface energy(238, 239, 243) or the release of thin film stress(244). The first technique is currently the most popular, and it is the only one described here. Briefly, a low melting point material is deposited between panels to generate folding hinges and at panel edges to generate locking hinges. After 2D microfabrication, the templates are released from the substrate and heated to liquefy the solid solder hinges. Upon heating, the hinges fold and lead to the final 3D structure, where liquefied locking hinges fuse and subsequently harden upon cooling. The use of locking hinges produces well-sealed, mechanically robust hollow polyhedra that can be manipulated without breaking. Figure 16A presents video snapshots of the self-folding phenomenon that is typically carried out in a high-boiling-point solvent (e.g. N-methylpyrrolidone)(238, 239). Figure 16B shows a gold (Au)-coated hollow cube with patterned pores on 5 faces (the bottom face is left open for subsequent cell loading) and Figure 16C shows a close-up of different pores. It is also possible to induce self-folding by exposing Ni/Sn objects to a CF₄/O₂ plasma (the angular orientation between panels can be controlled by altering the flow rate of O₂ gas)(240). However, gaps are present in between panels with this approach that is thus not directly applicable to cell immunoprotection.

As already mentioned, different materials have been successfully used to fabricate these patterned 3D microcapsules. The faces of the cubes can easily be made with copper (Cu) or nickel (Ni)(238, 239), using pure tin (Sn) or tin/lead (Sn/Pb) as the solder hinge material. Before any contact with biological molecules, gold (Au) is electrodeposited onto all surfaces of these microcontainers to improve their biocompatibility(245, 246). The Au electrodeposition time can also be varied to control the final pore size of the membranes with considerable precision down to the nanoscale(246).

In order to encapsulate cells, 3D cubes with one missing face (microwells) are produced by self-assembly(245). Cells can then be loaded by tumbling the microwells in a concentrated cell solution (~10⁴ cells/ml). Loaded microwells are then oriented with their open face upwards using a glass pipette. An adhesive tape (or polyurethane adhesive spin-coated on a glass slide) is then brought into contact with the open face of multiple microwells. The polymer cures typically within 30 minutes in cell media, thereby sealing the microwells. Arrays of microcontainers can then be formed on rigid or flexible (curved) geometries. It is also possible to create arrays of microcontainers by first positioning the microwells in an SU-8 holder patterned with recessed slots. The cells can also be loaded by simple settling after positioning the microwells in the holder.

Insulinoma cells (beta-TC-6) have been encapsulated for up to 1 month into such 500 μm -sized cube arrays with 1, 3 and 5 porous faces (6-7 μm pores)(245). These *in vitro* tests showed increased and faster glucose-stimulated insulin production for cubes with higher number of porous faces after 7 days of encapsulation. Moreover, the steady-state release of insulin following glucose stimulation (after 240 minutes) was compared between the 1, 3 and 5 porous-faced microwell arrays at different time points following encapsulation. The insulin steady-state release was similar after 1 day for the 3 categories but decreased over time for 1 and 3 porous faces. The 1 porous face group did not produce insulin any more after 28 days whereas the 5 porous faces group maintained its insulin concentration levels. Some microwells were also peeled from the substrates at different time points to study cell viability using a live/dead cytotoxicity assay. Higher numbers of live cells were consistently observed within the 5 porous faces cubes as compared to the 1 porous face cubes. These experiments clearly demonstrate the advantage of 3D porous microcontainers (cubes with 5 porous faces) as compared to 2D porous microcapsules (cubes with 1 porous face) for cell encapsulation. Cells encapsulated in the latter suffer from inadequate oxygenation and die after some weeks. It is interesting to note that these experimental results are in agreement with cell viability simulations solely based on O_2 diffusion(245).

Diffusion of insulin and IgG has also been studied with 500 μm -sized cubes presenting different precise pore sizes (from 78 nm to 2 μm) on 5 faces(246). It has been shown that 78 nm pores permitted diffusion of insulin over one week while blocking IgG diffusion, which is encouraging for cell immunoisolation applications. Insulinoma cells (beta-TC-6) have also been encapsulated within 78 nm porous microcontainers. After 2 days in the capsules, the cells produced insulin within 5 minutes in response to a glucose challenge and a continuous insulin production was measured for up to 2 hours.

These results show a proof-of-concept for this self-folding encapsulation technology, although this procedure is still in its infancy. Numerous *in vitro* and *in vivo* tests will have to be carried out to assess the stability and biocompatibility of these microcontainers over time. The hinges will have to be carefully studied for potential toxicity or leaking after several weeks in media.

The self-folding microcapsules have also recently been produced from all-polymer materials(242). The polyhedral objects, made of SU-8 faces and biodegradable polycaprolactone (PCL) hinges, spontaneously assemble upon heating at 58°C. This approach produces transparent microcontainers, enabling *in situ* imaging of encapsulated content using bright-field or fluorescence microscopy. Here again, all faces of the polyhedra can be porous which represents an improvement over Gimi's approach discussed previously. However, since PCL degrades over time in the body, this solder material is not suitable for islet/beta cell encapsulation (however, it is interesting for drug delivery applications). Indeed, the current SU-8/PCL containers release their content both through pores patterned on the faces of the capsules and by hinge degradation.

5. CONCLUSIONS

While encapsulation of islet or beta cells by semipermeable membranes has a history of more than 50 years, no definitive cure for type 1 diabetes has been seen so far. This situation is explained by the complexity of the compromise that must be reached: membrane pores have to be small enough to block the molecules and cells responsible for immune rejection but the very same pores need to be as large as possible to facilitate transport of O₂, glucose and insulin. While prevention of an immune attack on encapsulated cells seems to be nearly achieved today, the adequate supply of nutrients, especially O₂, is still a problem. This explains why capsule designs that minimize the distance between cells and the surrounding environment have gained a lot of interest in the past few years. For instance, alginate microcapsules and alginate islet sheets are the most advanced realizations in terms of clinical application. However, the broad pore size distribution of polymeric materials (such as alginates) may be a problem for immunoisolation over long periods. On the other hand, nanoporous inorganic membranes (Si, TiO₂, Al₂O₃...) possess well defined pore sizes that are expected to perform better in immunoprotection applications. The research in this field is still in its infancy but could lead to interesting results in the near future.

Besides membrane biocompatibility and design, several other approaches could help to produce a long-lasting implantable capsule with islet or beta cells: prevascularization of macrocapsules prior to cell transplantation, use of growth factors and oxygen generating materials, or arrangement of beta cells in controlled size clusters.

Apart from the materials science point-of-view, a cure for type 1 diabetes will require additional reliable sources of islet or beta cells since islet availability from donor pancreases is insignificant as compared to demand. Xenogeneic cells and cells derived from stem cells seem to be promising substitutes for human islets, but several remaining issues with these cell sources have yet to be overcome.

A lot of research and development is still required before encapsulated islets or beta cells will be able to cure type 1 diabetes, but such a treatment would represent a tremendous improvement over the multiple injections of insulin that patients currently have to undergo every day.

Acknowledgments

The authors would like to acknowledge Dr. Daniel Bernards for valuable review of this manuscript. This work was supported by the Juvenile Diabetes Research Foundation. J.S. is also grateful for a postdoctoral grant (2010-2011) from the King Baudouin Foundation (Belgium) and the Belgian American Educational Foundation.

REFERENCES

1. Scully T. Diabetes in numbers. *Nature*. 2012; 485(7398):S2–S3. [PubMed: 22616094]
2. Van Belle TL, Coppieters KT, von Herrath MG. Type 1 Diabetes: Etiology, Immunology, and Therapeutic Strategies. *Physiological Reviews*. 2011; 91(1):79–118. [PubMed: 21248163]
3. Didangelos T, Iliadis F. Insulin pump therapy in adults. *Diabetes Research and Clinical Practice*. 2011; 93(1):S109–S113. [PubMed: 21864741]
4. Renard E. Implantable closed-loop glucose-sensing and insulin delivery: the future for insulin pump therapy. *Current Opinion in Pharmacology*. 2002; 2(6):708–716. [PubMed: 12482735]

5. Renard E, Farret A, Place J, Wojtuszczyz A, Bringer J. Towards an artificial pancreas at home. *Diabetes and Metabolism*. 2011; 37(4):S94–S98. [PubMed: 22208718]
6. Vogel T, Friend P. *Pancreas transplantation*. Surgery (Oxford). 2011; 29(7):348–352.
7. Shapiro AMJ, Lakey JRT, Ryan EA, Korbitt GS, Toth E, Warnock GL, Kneteman NM, Rajotte RV. Islet Transplantation in Seven Patients with Type 1 Diabetes Mellitus Using a Glucocorticoid-Free Immunosuppressive Regimen. *New England Journal of Medicine*. 2000; 343(4):230–238. [PubMed: 10911004]
8. Ryan EA, Paty BW, Senior PA, Bigam D, Alfadhli E, Kneteman NM, Lakey JRT, Shapiro AMJ. Five-Year Follow-Up After Clinical Islet Transplantation. *Diabetes*. 2005; 54(7):2060–2069. [PubMed: 15983207]
9. Kessler L. La therapie cellulaire du diabete de type 1. Situation actuelle et perspective. *Medecine Nucleaire*. 2010; 34(10):589–596.
10. Shapiro, AMJ.; Shaw, JAM. *Islet Transplantation and Beta Cell Replacement Therapy*. Informa Healthcare; New York: 2007.
11. Robertson RP. Islet Transplantation as a Treatment for Diabetes - A Work in Progress. *New England Journal of Medicine*. 2004; 350(7):694–705. [PubMed: 14960745]
12. Andreoni KA, Brayman KL, Guidinger MK, Sommers CM, Sung RS. Kidney and Pancreas Transplantation in the United States, 1996-2005. *American Journal of Transplantation*. 2007; 7(9): 1359–1375. [PubMed: 17428285]
13. Stratta RJ. Immunosuppression in pancreas transplantation: progress, problems and perspective. *Transplant Immunology*. 1998; 6(2):69–77. [PubMed: 9777694]
14. Gummert JF, Ikonen T, Morris RE. Newer Immunosuppressive Drugs. *Journal of the American Society of Nephrology*. 1999; 10(6):1366–1380. [PubMed: 10361877]
15. Penn I. Post-Transplant Malignancy: The Role Of Immunosuppression. *Drug Safety*. 2000; 23(2): 101–113. [PubMed: 10945373]
16. Naftanel MA, Harlan DM. Pancreatic Islet Transplantation. *PLoS Medicine*. 2004; 1(3):198–201.
17. Johnson PRV, Jones KE. Pancreatic islet transplantation. *Seminars in Pediatric Surgery*. 2012; 21(3):272–280. [PubMed: 22800980]
18. Stock PG, Bluestone JA. Beta-Cell Replacement for Type I Diabetes. *Annual Review of Medicine*. 2004; 55(1):133–156.
19. Bretzel RG. Current status and perspectives in clinical islet transplantation. *Journal of Hepato-Biliary-Pancreatic Surgery*. 2000; 7(4):370–373. [PubMed: 11180857]
20. Leita CB, Tharavanij T, Cure P, Pileggi A, Baidal DA, Ricordi C, Alejandro R. Restoration of Hypoglycemia Awareness After Islet Transplantation. *Diabetes Care*. 2008; 31(11):2113–2115. [PubMed: 18697903]
21. Bonner-Weir S, Weir GC. New sources of pancreatic B-cells. *Nature Biotechnology*. 2005; 23(7): 857–861.
22. Sahu S, Tosh D, Hardikar AA. New sources of B-cells for treating diabetes. *Journal of Endocrinology*. 2009; 202(1):13–16. [PubMed: 19420008]
23. Miszta-Lane H, Mirbolooki M, James Shapiro AM, Lakey JRT. Stem cell sources for clinical islet transplantation in type 1 diabetes: Embryonic and adult stem cells. *Medical Hypotheses*. 2006; 67(4):909–913. [PubMed: 16762516]
24. Serup P, Madsen OD, Mandrup-Poulsen T. Islet and stem cell transplantation for treating diabetes. *BMJ*. 2001; 322(7277):29–32. [PubMed: 11141151]
25. Zulewski H, Abraham EJ, Gerlach MJ, Daniel PB, Moritz W, Muller B, Vallejo M, Thomas MK, Habener JF. Multipotential Nestin-Positive Stem Cells Isolated From Adult Pancreatic Islets Differentiate Ex Vivo Into Pancreatic Endocrine, Exocrine, and Hepatic Phenotypes. *Diabetes*. 2001; 50(3):521–533. [PubMed: 11246871]
26. Linning KD, Tai M-H, Madhukar BV, Chang CC, Reed DNJ, Ferber S, Trosko JE, Olson LK. Redox-Mediated Enrichment of Self-Renewing Adult Human Pancreatic Cells That Possess Endocrine Differentiation Potential. *Pancreas*. 2004; 29(3):e64–e76. [PubMed: 15367896]

27. Gershengorn MC, Hardikar AA, Wei C, Geras-Raaka E, Marcus-Samuels B, Raaka BM. Epithelial-to-Mesenchymal Transition Generates Proliferative Human Islet Precursor Cells. *Science*. 2004; 306(5705):2261–2264. [PubMed: 15564314]
28. Lechner A, Nolan AL, Blacken RA, Habener JF. Redifferentiation of insulin-secreting cells after in vitro expansion of adult human pancreatic islet tissue. *Biochemical and Biophysical Research Communications*. 2005; 327(2):581–588. [PubMed: 15629153]
29. D'Amour KA, Bang AG, Eliazar S, Kelly OG, Agulnick AD, Smart NG, Moorman MA, Kroon E, Carpenter MK, Baetge EE. Production of pancreatic hormone-expressing endocrine cells from human embryonic stem cells. *Nature Biotechnology*. 2006; 24(11):1392–1401.
30. Baetge EE. Production of B-cells from human embryonic stem cells. *Diabetes, Obesity and Metabolism*. 2008; 10(4):186–194.
31. Kelly OG, Chan MY, Martinson LA, Kadoya K, Ostertag TM, Ross KG, Richardson M, Carpenter MK, D'Amour KA, Kroon E, Moorman M, Baetge EE, Bang AG. Cell-surface markers for the isolation of pancreatic cell types derived from human embryonic stem cells. *Nature Biotechnology*. 2011; 29(8):750–756.
32. Schulz TC, Young HY, Agulnick AD, Babin MJ, Baetge EE, Bang AG, Bhoumik A, Cepa I, Cesario RM, Haakmeester C, Kadoya K, Kelly JR, Kerr J, Martinson LA, McLean AB, Moorman MA, Payne JK, Richardson M, Ross KG, Sherrer ES, Song X, Wilson AZ, Brandon EP, Green CE, Kroon EJ, Kelly OG, D'Amour KA, Robins AJ. A Scalable System for Production of Functional Pancreatic Progenitors from Human Embryonic Stem Cells. *PLoS ONE*. 2012; 7(5):1–17.
33. Matveyenko AV, Georgia S, Bhushan A, Butler PC. Inconsistent formation and nonfunction of insulin-positive cells from pancreatic endoderm derived from human embryonic stem cells in athymic nude rats. *American Journal of Physiology - Endocrinology And Metabolism*. 2010; 299(5):E713–E720. [PubMed: 20587750]
34. Chen S, Borowiak M, Fox JL, Maehr R, Osafune K, Davidow L, Lam K, Peng LF, Schreiber SL, Rubin LL, Melton D. A small molecule that directs differentiation of human ESCs into the pancreatic lineage. *Nature Chemical Biology*. 2009; 5(4):258–265.
35. Van Hoof D, Mendelsohn AD, Seerke R, Desai TA, German MS. Differentiation of human embryonic stem cells into pancreatic endoderm in patterned size-controlled clusters. *Stem Cell Research*. 2011; 6(3):276–285. [PubMed: 21513906]
36. Bonner-Weir S, Toschi E, Inada A, Reitz P, Fonseca SY, Aye T, Sharma A. The pancreatic ductal epithelium serves as a potential pool of progenitor cells. *Pediatric Diabetes*. 2004; 5(s2):16–22. [PubMed: 15601370]
37. Baeyens L, De Breuck S, Lardon J, Mfopou J, Rooman I, Bouwens L. In vitro generation of insulin-producing beta cells from adult exocrine pancreatic cells. *Diabetologia*. 2005; 48(1):49–57. [PubMed: 15616797]
38. Bonner-Weir S, Taneja M, Weir GC, Tatarkiewicz K, Song K-H, Sharma A, O'Neil JJ. In vitro cultivation of human islets from expanded ductal tissue. *Proceedings of the National Academy of Sciences*. 2000; 97(14):7999–8004.
39. Gao R, Ustinov J, Pulkkinen M-A, Lundin K, Korsgren O, Otonkoski T. Characterization of Endocrine Progenitor Cells and Critical Factors for Their Differentiation in Human Adult Pancreatic Cell Culture. *Diabetes*. 2003; 52(8):2007–2015. [PubMed: 12882917]
40. Suarez-Pinzon WL, Lakey JRT, Brand SJ, Rabinovitch A. Combination Therapy with Epidermal Growth Factor and Gastrin Induces Neogenesis of Human Islet B-Cells from Pancreatic Duct Cells and an Increase in Functional B-Cell Mass. *Journal of Clinical Endocrinology & Metabolism*. 2005; 90(6):3401–3409. [PubMed: 15769977]
41. Fujita Y, Cheung AT, Kieffer TJ. Harnessing the gut to treat diabetes. *Pediatric Diabetes*. 2004; 5(s2):57–69. [PubMed: 15601375]
42. Ber I, Shternhall K, Perl S, Ohanuna Z, Goldberg I, Barshack I, Benvenisti-Zarum L, Meivar-Levy I, Ferber S. Functional, Persistent, and Extended Liver to Pancreas Transdifferentiation. *Journal of Biological Chemistry*. 2003; 278(34):31950–31957. [PubMed: 12775714]
43. Zalzman M, Gupta S, Giri RK, Berkovich I, Sappal BS, Karnieli O, Zern MA, Fleischer N, Efrat S. Reversal of hyperglycemia in mice by using human expandable insulin-producing cells

- differentiated from fetal liver progenitor cells. *Proceedings of the National Academy of Sciences*. 2003; 100(12):7253–7258.
44. Yang L, Li S, Hatch H, Ahrens K, Cornelius JG, Petersen BE, Peck AB. In vitro trans-differentiation of adult hepatic stem cells into pancreatic endocrine hormone-producing cells. *Proceedings of the National Academy of Sciences*. 2002; 99(12):8078–8083.
 45. Cao L-Z, Tang D-Q, Horb ME, Li S-W, Yang L-J. High Glucose Is Necessary for Complete Maturation of Pdx1-VP16 - Expressing Hepatic Cells into Functional Insulin-Producing Cells. *Diabetes*. 2004; 53(12):3168–3178. [PubMed: 15561947]
 46. Aviv V, Meivar-Levy I, Rachmut IH, Rubinek T, Mor E, Ferber S. Exendin-4 Promotes Liver Cell Proliferation and Enhances the PDX-1-induced Liver to Pancreas Transdifferentiation Process. *Journal of Biological Chemistry*. 2009; 284(48):33509–33520. [PubMed: 19755420]
 47. Nagaya M, Katsuta H, Kaneto H, Bonner-Weir S, Weir GC. Adult mouse intrahepatic biliary epithelial cells induced in vitro to become insulin-producing cells. *Journal of Endocrinology*. 2009; 201(1):37–47. [PubMed: 19168505]
 48. Zhou Q, Brown J, Kanarek A, Rajagopal J, Melton DA. In vivo reprogramming of adult pancreatic exocrine cells to B-cells. *Nature*. 2008; 455(7213):627–632. [PubMed: 18754011]
 49. O'Sullivan ES, Vegas A, Anderson DG, Weir GC. Islets Transplanted in Immunoisolation Devices: A Review of the Progress and the Challenges that Remain. *Endocrine Reviews*. 2011; 32(6):827–844. [PubMed: 21951347]
 50. Abrahante JE, Martins K, Papas KK, Hering BJ, Schuurman H-J, Murtaugh MP. Microbiological safety of porcine islets: comparison with source pig. *Xenotransplantation*. 2011; 18(2):88–93. [PubMed: 21496116]
 51. Pappenheimer JR, Renkin EM, Borrero LM. Filtration, Diffusion and Molecular Sieving Through Peripheral Capillary Membranes: A Contribution to the Pore Theory of Capillary Permeability. *American Journal of Physiology*. 1951; 167(1):13–46. [PubMed: 14885465]
 52. Oliva A, Fariña J, Llabrés M. Development of two high-performance liquid chromatographic methods for the analysis and characterization of insulin and its degradation products in pharmaceutical preparations. *Journal of Chromatography B: Biomedical Sciences and Applications*. 2000; 749(1):25–34.
 53. Leoni L, Desai TA. Micromachined biocapsules for cell-based sensing and delivery. *Advanced Drug Delivery Reviews*. 2004; 56(2):211–229. [PubMed: 14741117]
 54. Kang J, Erdodi G, Kennedy JP. Third-generation amphiphilic conetworks. III. Permeabilities and mechanical properties. *J. Polym. Sci. A Polym. Chem*. 2007; 45(18):4276–4283.
 55. Avgoustiniatos, ES.; Wu, H.; Colton, CK. *Principles of Tissue Engineering*. Lanza, RP.; Langer, R.; Vacanti, J., editors. Academic Press; San Diego: 2000. p. 331–350.
 56. Colton CK. Implantable biohybrid artificial organs. *Cell Transplantation*. 1995; 4(4):415–436. [PubMed: 7582573]
 57. Wilson JT, Chaikof EL. Challenges and emerging technologies in the immunoisolation of cells and tissues. *Advanced Drug Delivery Reviews*. 2008; 60(2):124–145. [PubMed: 18022728]
 58. de Vos P, Marchetti P. Encapsulation of pancreatic islets for transplantation in diabetes: the untouchable islets. *Trends in Molecular Medicine*. 2002; 8(8):363–366. [PubMed: 12127717]
 59. Lysaght MJ, Frydel B, Gentile F, Emerich D, Winn S. Recent progress in immunoisolated cell therapy. *J. Cell. Biochem*. 1994; 56(2):196–203. [PubMed: 7829581]
 60. Lanza RP, Kuhtreiber WM, Chick WL. Encapsulation Technologies. *Tissue Engineering*. 1995; 1(2):181–196. [PubMed: 19877926]
 61. Mendelsohn, A.; Desai, T. *Therapeutic Applications of Cell Microencapsulation*. Pedraz, JL.; Orive, G., editors. Vol. 670. Springer; New York: 2010. p. 104–125.
 62. Basta G, Calafiore R. Immunoisolation of Pancreatic Islet Grafts with No Recipient's Immunosuppression: Actual and Future Perspectives. *Current Diabetes Reports*. 2011; 11(5):384–391. [PubMed: 21826429]
 63. Nafea EH, L.A. P-W, Marson A, Martens PJ. Immunoisolating semi-permeable membranes for cell encapsulation: Focus on hydrogels. *Journal of Controlled Release*. 2011; 154(2):110–122. [PubMed: 21575662]

64. Scharp DW, Mason NS, Sparks RE. Islet immuno-isolation: The use of hybrid artificial organs to prevent islet tissue rejection. *World Journal of Surgery*. 1984; 8(2):221–229. [PubMed: 6375147]
65. Beck J, Angus R, Madsen B, Britt D, Vernon B, Nguyen KT. Islet Encapsulation: Strategies to Enhance Islet Cell Functions. *Tissue Engineering*. 2007; 13(3):589–599. [PubMed: 17518605]
66. Iwata H, Morikawa N, Fujii T, Takagi T, Samejima T, Ikada Y. Does immunoisolation need to prevent the passage of antibodies and complement? *Transplantation Proceedings*. 1995; 27(6): 3224–3226.
67. Thomlinson RH, Gray LH. The histological structure of some human lung cancers and the possible implications for radiotherapy. *British Journal of Cancer*. 1955; 9(4):539–549. [PubMed: 13304213]
68. Avgoustiniatos ES, Colton CK. Effect of External Oxygen Mass Transfer Resistances on Viability of Immunoisolated Tissue. *Annals of the New York Academy of Sciences*. 1997; 831(1):145–166. [PubMed: 9616709]
69. Pileggi A, Molano RD, Ricordi C, Zahr E, Collins J, Valdes R, Inverardi L. Reversal of Diabetes by Pancreatic Islet Transplantation into a Subcutaneous, Neovascularized Device. *Transplantation*. 2006; 81(9):1318–1324. [PubMed: 16699461]
70. Trivedi N, Steil GM, Colton CK, Bonner-Weir S, Weir GC. Improved vascularization of planar membrane diffusion devices following continuous infusion of vascular endothelial growth factor. *Cell Transplantation*. 2000; 9(1):115–124. [PubMed: 10784073]
71. Adlercreutz P, Mattiasson B. Oxygen Supply to Immobilized Cells: Oxygen Supply by Hemoglobin or Emulsions of Perfluorochemicals. *European Journal of Applied Microbiology and Biotechnology*. 1982; 16(4):165–170.
72. Fraker CA, Alejandro R, Ricordi C. Use of Oxygenated Perfluorocarbon Toward Making Every Pancreas Count. *Transplantation*. 2002; 74(12):1811–1812. [PubMed: 12499906]
73. Wu H, Avgoustiniatos ES, Swette L, Bonner-Weir S, Weir GC, Colton CK. In Situ Electrochemical Oxygen Generation with an Immunoisolation Device. *Annals of the New York Academy of Sciences*. 1999; 875(1):105–125. [PubMed: 10415561]
74. Bloch K, Papismedov E, Yavriyants K, Vorobeychik M, Beer S, Vardi P. Photosynthetic Oxygen Generator for Bioartificial Pancreas. *Tissue Engineering*. 2006; 12(2):337–344. [PubMed: 16548692]
75. Harrison BS, Eberli D, Lee SJ, Atala A, Yoo JJ. Oxygen producing biomaterials for tissue regeneration. *Biomaterials*. 2007; 28(31):4628–4634. [PubMed: 17681597]
76. Oh SH, Ward CL, Atala A, Yoo JJ, Harrison BS. Oxygen generating scaffolds for enhancing engineered tissue survival. *Biomaterials*. 2009; 30(5):757–762. [PubMed: 19019425]
77. Ludwig B, Zimmerman B, Steffen A, Yavriants K, Azarov D, Reichel A, Vardi P, German T, Shabtay N, Rotem A, Evron Y, Neufeld T, Mimon S, Ludwig S, Brendel M,D, Bornstein S,R, Barkai U. A Novel Device for Islet Transplantation Providing Immune Protection and Oxygen Supply. *Horm Metab Res*. 2010; 42(13):918–922. [PubMed: 21031332]
78. Pedraza E, Coronel MM, Fraker CA, Ricordi C, Stabler CL. Preventing hypoxia-induced cell death in beta cells and islets via hydrolytically activated, oxygen-generating biomaterials. *Proceedings of the National Academy of Sciences*. 2012; 109(11):4245–4250.
79. Mendelsohn AD, Bernards DA, Lowe RD, Desai TA. Patterning of Mono- and Multilayered Pancreatic Beta-Cell Clusters. *Langmuir*. 2010; 26(12):9943–9949. [PubMed: 20218546]
80. Bernard AB, Lin C-C, Anseth KS. A Microwell Cell Culture Platform for the Aggregation of Pancreatic B-Cells. *Tissue Engineering Part C: Methods*. 2012; 18(8):583–592. [PubMed: 22320435]
81. Meda P, Bosco D, Chanson M, Giordano E, Vallar L, Wollheim C, Orci L. Rapid and reversible secretion changes during uncoupling of rat insulin-producing cells. *J Clin Invest*. 1990; 86(3):759–768. [PubMed: 1697604]
82. Jaques F, Jousset H.L.n. Tomas A, Prost A-L, Wollheim CB, Irminger J-C, Demaurex N, Halban PA. Dual Effect of Cell-Cell Contact Disruption on Cytosolic Calcium and Insulin Secretion. *Endocrinology*. 2008; 149(5):2494–2505. [PubMed: 18218692]

83. Brereton HC, Carvell MJ, Asare-Anane H, Roberts G, Christie MR, Persaud SJ, Jones PM. Homotypic cell contact enhances insulin but not glucagon secretion. *Biochemical and Biophysical Research Communications*. 2006; 344(3):995–1000. [PubMed: 16643853]
84. Mendelsohn AD, Nyitray C, Sena M, Desai TA. Size-controlled Insulin Secreting Cell Clusters. *Acta Biomaterialia*. 2012; 8(12):4278–4284. [PubMed: 22902301]
85. Wang R, Rosenberg L. Maintenance of beta-cell function and survival following islet isolation requires re-establishment of the islet-matrix relationship. *Journal of Endocrinology*. 1999; 163(2): 181–190. [PubMed: 10556766]
86. Prochorov A, Tretjak S, Goranov V, Glinnik A, Goltsev M. Treatment of insulin dependent diabetes mellitus with intravascular transplantation of pancreatic islet cells without immunosuppressive therapy. *Advances in Medical Sciences*. 2008; 53(2):240–244. [PubMed: 19230310]
87. Bergen JF, Mason NS, Scharp DW, Sparks RE. Insulin Feedback Inhibition as a Factor in the Reduction of Insulin Release from Islet Transplantation Diffusion Chambers. *Artificial Organs*. 1981; 5(A):67–67. [PubMed: 6264901]
88. Bisceglie V. Über die antineoplastische Immunität. *Zeitschrift für Krebsforschung*. 1933; 40(1): 122–140.
89. Algire GH, Legallais FY. Recent Developments in the Transparent-Chamber Technique as Adapted to the Mouse. *Journal of the National Cancer Institute*. 1949; 10(2):225–253. [PubMed: 15393709]
90. Algire GH, Weaver JM, Prehn RT. Growth of Cells In Vivo in Diffusion Chambers. I. Survival of Homografts in Immunized Mice. *Journal of the National Cancer Institute*. 1954; 15(3):493–507. [PubMed: 13233904]
91. Prehn RT, Weaver JM, Algire GH. The Diffusion-Chamber Technique Applied to a Study of the Nature of Homograft Resistance. *Journal of the National Cancer Institute*. 1954; 15(3):509–517. [PubMed: 13233905]
92. Weaver JM, Algire GH, Prehn RT. The Growth of Cells in Vivo in Diffusion Chambers. II. The Role of Cells in the Destruction of Homografts in Mice. *Journal of the National Cancer Institute*. 1955; 15(6):1737–1767. [PubMed: 14381895]
93. Algire GH. Diffusion-Chamber Techniques for Studies of Cellular Immunity. *Annals of the New York Academy of Sciences*. 1957; 69(4):663–667. [PubMed: 13488321]
94. Moskalewski S. Isolation and culture of the islets of Langerhans of the guinea pig. *General and Comparative Endocrinology*. 1965; 5(3):342–353. [PubMed: 14338040]
95. Strautz R. Studies of hereditary-obese mice (obob) after implantation of pancreatic islets in Millipore filter capsules. *Diabetologia*. 1970; 6(3):306–312. [PubMed: 4914667]
96. Gates R, Smith R, Hunt MI, Lazarus N. Return to Normal of Blood-Glucose, Plasma-Insulin, and Weight Gain in New Zealand Obese Mice after Implantation of Islets of Langerhans. *The Lancet*. 1972; 300(7777):567–570.
97. Lacy PE, Hegre OD, Gerasimidi-Vazeou A, Gentile FT, Dionne KE. Maintenance of normoglycemia in diabetic mice by subcutaneous xenografts of encapsulated islets. *Science*. 1991; 254(5039):1782–1784. [PubMed: 1763328]
98. Brauker JH, Carr-Brendel VE, Martinson LA, Crudele J, Johnston WD, Johnson RC. Neovascularization of synthetic membranes directed by membrane microarchitecture. *Journal of Biomedical Materials Research*. 1995; 29(12):1517–1524. [PubMed: 8600142]
99. Loudovaris T, Jacobs S, Young S, Maryanov D, Brauker J, Johnson RC. Correction of diabetic nod mice with insulinomas implanted within Baxter immunoisolation devices. *Journal of Molecular Medicine*. 1999; 77(1):219–222. [PubMed: 9930967]
100. Binette TM, Seeberger KL, Lyon JG, Rajotte RV, Korbitt GS. Porcine Endogenous Retroviral Nucleic Acid in Peripheral Tissues Is Associated with Migration of Porcine Cells Post Islet Transplant. *American Journal of Transplantation*. 2004; 4(7):1051–1060. [PubMed: 15196061]
101. Sorenby AK, Kumagai-Braesch M, Sharma A, Hultenby KR, Wernerson AM, Tibell AB. Preimplantation of an Immunoprotective Device Can Lower the Curative Dose of Islets to That of Free Islet Transplantation-Studies in a Rodent Model. *Transplantation*. 2008; 86(2):364–366. [PubMed: 18645504]

102. Sweet IR, Yanay O, Waldron L, Gilbert M, Fuller JM, Tupling T, Lernmark A, Osborne WRA. Treatment of diabetic rats with encapsulated islets. *Journal of Cellular and Molecular Medicine*. 2008; 12(6b):2644–2650. [PubMed: 18373735]
103. Desai TA, Chu WH, Tu JK, Beattie GM, Hayek A, Ferrari M. Microfabricated immunoisolating biocapsules. *Biotechnol. Bioeng.* 1998; 57(1):118–120. [PubMed: 10099185]
104. Desai TA, Hansford DJ, Kulinsky L, Nashat AH, Rasi G, Tu J, Wang Y, Zhang M, Ferrari M. Nanopore Technology for Biomedical Applications. *Biomedical Microdevices*. 1999; 2(1):11–40.
105. Desai TA, West T, Cohen M, Boiarski T, Rumpersaud A. Nanoporous microsystems for islet cell replacement. *Advanced Drug Delivery Reviews*. 2004; 56(11):1661–1673. [PubMed: 15350295]
106. Smith C, Kirk R, West T, Bratzel M, Cohen M, Martin F, Boiarski A, Rumpersaud AA. Diffusion Characteristics of Microfabricated Silicon Nanopore Membranes as Immunoisolation Membranes for Use in Cellular Therapeutics. *Diabetes Technology & Therapeutics*. 2005; 7(1):151–162. [PubMed: 15738713]
107. Martin F, Walczak R, Boiarski A, Cohen M, West T, Cosentino C, Ferrari M. Tailoring width of microfabricated nanochannels to solute size can be used to control diffusion kinetics. *Journal of Controlled Release*. 2005; 102(1):123–133. [PubMed: 15653139]
108. King SR, Dorian R, Storrs RW. Requirements for Encapsulation Technology and the Challenges for Transplantation of Islets of Langerhans. *Graft*. 2001; 4(7):491–499.
109. Storrs R, Dorian R, King SR, Lakey J, Rilo H. Preclinical Development of the Islet Sheet. *Annals of the New York Academy of Sciences*. 2001; 944(1):252–266. [PubMed: 11797674]
110. Kroon E, Martinson LA, Kadota K, Bang AG, Kelly OG, Eliazar S, Young H, Richardson M, Smart NG, Cunningham J, Agulnick AD, D'Amour KA, Carpenter MK, Baetge EE. Pancreatic endoderm derived from human embryonic stem cells generates glucose-responsive insulin-secreting cells in vivo. *Nature Biotechnology*. 2008; 26(4):443–452.
111. Knazek RA, Gullino PM, Kohler PO, Dedrick RL. Cell Culture on Artificial Capillaries: An Approach to Tissue Growth in vitro. *Science*. 1972; 178(4056):65–67. [PubMed: 4560879]
112. Chick W, Like A, Lauris V. Beta cell culture on synthetic capillaries: an artificial endocrine pancreas. *Science*. 1975; 187(4179):847–849. [PubMed: 1114330]
113. Chick W, Perna J, Lauris V, Low D, Galletti P, Panol G, Whittemore A, Like A, Colton C, Lysaght M. Artificial pancreas using living beta cells: effects on glucose homeostasis in diabetic rats. *Science*. 1977; 197(4305):780–782. [PubMed: 407649]
114. Tze WJ, Wong FC, Chen LM, O'Young S. Implantable artificial endocrine pancreas unit used to restore normoglycaemia in the diabetic rat. *Nature*. 1976; 264(5585):466–467. [PubMed: 826831]
115. Sun AM, Parisius W, Healy GM, Vacek I, Macmorine HG. The Use, in Diabetic Rats and Monkeys, of Artificial Capillary Units Containing Cultured Islets of Langerhans (Artificial Endocrine Pancreas). *Diabetes*. 1977; 26(12):1136–1139. [PubMed: 412720]
116. Orsetti A, Guy C, Zouai N, Deffay R. Implantation du distributeur bio-artificiel d'insuline chez le chien utilisant des ilots de Langerhans d'especes animales differentes. *Comptes-Rendus des Seances de la Societe de Biologie (Paris)*. 1978; 172(1):144–150.
117. Tze W, Wong F, Chen L. Implantable artificial capillary unit for pancreatic islet allograft and xenograft. *Diabetologia*. 1979; 16(4):247–252. [PubMed: 107055]
118. Tze W, Tai J, Wong F, Davis H. Studies with implantable artificial capillary units containing rat islets on diabetic dogs. *Diabetologia*. 1980; 19(6):541–545. [PubMed: 6780399]
119. Sun A, Parisius W, Macmorine H, Sefton M, Stone R. An Artificial Endocrine Pancreas Containing Cultured Islets of Langerhans. *Artificial Organs*. 1980; 4(4):275–278.
120. Reach G, Poussier P, Sausse A, Assas R, Itoh M, Gerich JE. Functional evaluation of a bioartificial pancreas using isolated islets perfused with blood ultrafiltrate. *Diabetes*. 1981; 30(4):296–301. [PubMed: 7009277]
121. Sullivan S, Maki T, Borland K, Mahoney M, Solomon B, Muller T, Monaco A, Chick W. Biohybrid artificial pancreas: long-term implantation studies in diabetic, pancreatectomized dogs. *Science*. 1991; 252(5006):718–721. [PubMed: 2024124]

122. Goh CH, Heng PWS, Chan LW. Alginates as a useful natural polymer for microencapsulation and therapeutic applications. *Carbohydrate Polymers*. 2012; 88(1):1–12.
123. Rabanel J-M, Banquy X, Zouaoui H, Mokhtar M, Hildgen P. Progress technology in microencapsulation methods for cell therapy. *Biotechnol Progress*. 2009; 25(4):946–963.
124. McGuigan AP, Bruzewicz DA, Glavan A, Butte M, Whitesides GM. Cell Encapsulation in Sub-mm Sized Gel Modules Using Replica Molding. *PLoS ONE*. 2008; 3(5):e2258. [PubMed: 18493609]
125. Dang TT, Xu Q, Bratlie KM, O'Sullivan ES, Chen XY, Langer R, Anderson DG. Microfabrication of homogenous, asymmetric cell-laden hydrogel capsules. *Biomaterials*. 2009; 30(36):6896–6902. [PubMed: 19800116]
126. Chang TMS. Semipermeable Microcapsules. *Science*. 1964; 146(3643):524–525. [PubMed: 14190240]
127. Lim F, Sun AM. Microencapsulated islets as bioartificial endocrine pancreas. *Science*. 1980; 210(4472):908–910. [PubMed: 6776628]
128. O'Shea GM, Goosen MFA, Sun AM. Prolonged survival of transplanted islets of Langerhans encapsulated in a biocompatible membrane. *Biochimica et Biophysica Acta (BBA) - Molecular Cell Research*. 1984; 804(1):133–136.
129. Zimmermann U, Klock G, Federlin K, Hannig K, Kowalski M, Bretzel RG, Horcher A, Entenmann H, Sieber U, Zekorn T. Production of mitogen-contamination free alginates with variable ratios of mannuronic acid to guluronic acid by free flow electrophoresis. *ELECTROPHORESIS*. 1992; 13(1):269–274. [PubMed: 1396520]
130. Klock G, Frank H, Houben R, Zekorn T, Horcher A, Siebers U, Wohrle M, Federlin K, Zimmermann U. Production of purified alginates suitable for use in immunoisolated transplantation. *Applied Microbiology and Biotechnology*. 1994; 40(5):638–643. [PubMed: 7764423]
131. de Vos P, Haan BJD, Wolters GHJ, Strubbe JH, Schilfgaarde RV. Improved biocompatibility but limited graft survival after purification of alginate for microencapsulation of pancreatic islets. *Diabetologia*. 1997; 40(3):262–270. [PubMed: 9084963]
132. Sawhney AS, Pathak CP, Hubbell JA. Interfacial photopolymerization of poly(ethylene glycol)-based hydrogels upon alginate-poly(L-lysine) microcapsules for enhanced biocompatibility. *Biomaterials*. 1993; 14(13):1008–1016. [PubMed: 8286667]
133. Wang T, Lacik I, Brissova M, Anilkumar AV, Prokop A, Hunkeler D, Green R, Shahrokhi K, Powers AC. An encapsulation system for the immunoisolation of pancreatic islets. *Nature Biotechnology*. 1997; 15(4):358–362.
134. Peterson KP, Peterson CM, Pope EJA. Silica Sol-Gel Encapsulation of Pancreatic Islets. *Proceedings of the Society for Experimental Biology & Medicine*. 1998; 218(4):365–369. [PubMed: 9714081]
135. Boninsegna S, Bosetti P, Carturan G, Dellagiocoma G, Dal Monte R, Rossi M. Encapsulation of individual pancreatic islets by sol-gel SiO₂: A novel procedure for perspective cellular grafts. *Journal of Biotechnology*. 2003; 100(3):277–286. [PubMed: 12443859]
136. Sefton M, Stevenson W. Microencapsulation of live animal cells using polyacrylates. *Advances in Polymer Science*. 1993; 107(1):143–197.
137. Iwata H, Amemiya H, Matsuda T, Takano H, Akutsu T. Microencapsulation of Langerhans Islets in Agarose Microbeads and Their Application for a Bioartificial Pancreas. *Journal of Bioactive and Compatible Polymers*. 1988; 3(4):356–369.
138. Iwata H, Takagi T, Amemiya H, Shimizu H, Yamashita K, Kobayashi K, Akutsu T. Agarose for a bioartificial pancreas. *Journal of Biomedical Materials Research*. 1992; 26(7):967–977. [PubMed: 1607377]
139. Yang K-C, Qi Z, Wu C-C, Shirouza Y, Lin F-H, Yanai G, Sumi S. The cytoprotection of chitosan based hydrogels in xenogeneic islet transplantation: An in vivo study in streptozotocin-induced diabetic mouse. *Biochemical and Biophysical Research Communications*. 2010; 393(4):818–823. [PubMed: 20171166]

122. Goh CH, Heng PWS, Chan LW. Alginates as a useful natural polymer for microencapsulation and therapeutic applications. *Carbohydrate Polymers*. 2012; 88(1):1–12.
123. Rabanel J-M, Banquy X, Zouaoui H, Mokhtar M, Hildgen P. Progress technology in microencapsulation methods for cell therapy. *Biotechnol Progress*. 2009; 25(4):946–963.
124. McGuigan AP, Bruzewicz DA, Glavan A, Butte M, Whitesides GM. Cell Encapsulation in Sub-mm Sized Gel Modules Using Replica Molding. *PLoS ONE*. 2008; 3(5):e2258. [PubMed: 18493609]
125. Dang TT, Xu Q, Bratlie KM, O'Sullivan ES, Chen XY, Langer R, Anderson DG. Microfabrication of homogenous, asymmetric cell-laden hydrogel capsules. *Biomaterials*. 2009; 30(36):6896–6902. [PubMed: 19800116]
126. Chang TMS. Semipermeable Microcapsules. *Science*. 1964; 146(3643):524–525. [PubMed: 14190240]
127. Lim F, Sun AM. Microencapsulated islets as bioartificial endocrine pancreas. *Science*. 1980; 210(4472):908–910. [PubMed: 6776628]
128. O'Shea GM, Goosen MFA, Sun AM. Prolonged survival of transplanted islets of Langerhans encapsulated in a biocompatible membrane. *Biochimica et Biophysica Acta (BBA) - Molecular Cell Research*. 1984; 804(1):133–136.
129. Zimmermann U, Klock G, Federlin K, Hannig K, Kowalski M, Bretzel RG, Horcher A, Entenmann H, Sieber U, Zekorn T. Production of mitogen-contamination free alginates with variable ratios of mannuronic acid to guluronic acid by free flow electrophoresis. *ELECTROPHORESIS*. 1992; 13(1):269–274. [PubMed: 1396520]
130. Klock G, Frank H, Houben R, Zekorn T, Horcher A, Siebers U, Wohrle M, Federlin K, Zimmermann U. Production of purified alginates suitable for use in immunoisolated transplantation. *Applied Microbiology and Biotechnology*. 1994; 40(5):638–643. [PubMed: 7764423]
131. de Vos P, Haan BJD, Wolters GHJ, Strubbe JH, Schilfgaarde RV. Improved biocompatibility but limited graft survival after purification of alginate for microencapsulation of pancreatic islets. *Diabetologia*. 1997; 40(3):262–270. [PubMed: 9084963]
132. Sawhney AS, Pathak CP, Hubbell JA. Interfacial photopolymerization of poly(ethylene glycol)-based hydrogels upon alginate-poly(L-lysine) microcapsules for enhanced biocompatibility. *Biomaterials*. 1993; 14(13):1008–1016. [PubMed: 8286667]
133. Wang T, Lacik I, Brissova M, Anilkumar AV, Prokop A, Hunkeler D, Green R, Shahrokhi K, Powers AC. An encapsulation system for the immunoisolation of pancreatic islets. *Nature Biotechnology*. 1997; 15(4):358–362.
134. Peterson KP, Peterson CM, Pope EJA. Silica Sol-Gel Encapsulation of Pancreatic Islets. *Proceedings of the Society for Experimental Biology & Medicine*. 1998; 218(4):365–369. [PubMed: 9714081]
135. Boninsegna S, Bosetti P, Carturan G, Dellagiocoma G, Dal Monte R, Rossi M. Encapsulation of individual pancreatic islets by sol-gel SiO₂: A novel procedure for perspective cellular grafts. *Journal of Biotechnology*. 2003; 100(3):277–286. [PubMed: 12443859]
136. Sefton M, Stevenson W. Microencapsulation of live animal cells using polyacrylates. *Advances in Polymer Science*. 1993; 107(1):143–197.
137. Iwata H, Amemiya H, Matsuda T, Takano H, Akutsu T. Microencapsulation of Langerhans Islets in Agarose Microbeads and Their Application for a Bioartificial Pancreas. *Journal of Bioactive and Compatible Polymers*. 1988; 3(4):356–369.
138. Iwata H, Takagi T, Amemiya H, Shimizu H, Yamashita K, Kobayashi K, Akutsu T. Agarose for a bioartificial pancreas. *Journal of Biomedical Materials Research*. 1992; 26(7):967–977. [PubMed: 1607377]
139. Yang K-C, Qi Z, Wu C-C, Shirouza Y, Lin F-H, Yanai G, Sumi S. The cytoprotection of chitosan based hydrogels in xenogeneic islet transplantation: An in vivo study in streptozotocin-induced diabetic mouse. *Biochemical and Biophysical Research Communications*. 2010; 393(4):818–823. [PubMed: 20171166]

140. Panza JL, Wagner R, W. Rilo HLR, Harsha Rao R, Beckman EJ, Russell AJ. Treatment of rat pancreatic islets with reactive PEG. *Biomaterials*. 2000; 21(11):1155–1164. [PubMed: 10817268]
141. Kellam B, De Bank PA, Shakesheff KM. Chemical modification of mammalian cell surfaces. *Chemical Society Reviews*. 2003; 32(6):327–337. [PubMed: 14671788]
142. Decher G. Fuzzy Nanoassemblies: Toward Layered Polymeric Multicomposites. *Science*. 1997; 277(5330):1232–1237.
143. Wilson JT, Cui W, Kozlovskaya V, Kharlampieva E, Pan D, Qu Z, Krishnamurthy VR, Mets J, Kumar V, Wen J, Song Y, Tsukruk VV, Chaikof EL. Cell Surface Engineering with Polyelectrolyte Multilayer Thin Films. *Journal of the American Chemical Society*. 2011; 133(18):7054–7064. [PubMed: 21491937]
144. Soon-Shiong P, Heintz RE, Merideth N, Yao QX, Yao Z, Zheng T, Murphy M, Moloney MK, Schmehl M, Harris M, Mendez R, Mendez R, Sandford PA. Insulin independence in a type 1 diabetic patient after encapsulated islet transplantation. *The Lancet*. 1994; 343(8903):950–951.
145. Thanos CG, Calafiore R, Basta G, Bintz BE, Bell WJ, Hudak J, Vasconcellos A, Schneider P, Skinner SJM, Geaney M, Tan P, Elliot RB, Tatnell M, Escobar L, Qian H, Mathiowitz E, Emerich DF. Formulating the alginate-polyornithine biocapsule for prolonged stability: Evaluation of composition and manufacturing technique. *J. Biomed. Mater. Res*. 2007; 83A(1): 216–224.
146. Calafiore R, Basta G, Luca G, Lemmi A, Montanucci MP, Calabrese G, Racanicchi L, Mancuso F, Brunetti P. Microencapsulated Pancreatic Islet Allografts Into Nonimmunosuppressed Patients With Type 1 Diabetes. *Diabetes Care*. 2006; 29(1):137–138. [PubMed: 16373911]
147. Basta G, Montanucci P, Luca G, Boselli C, Noya G, Barbaro B, Qi M, Kinzer KP, Oberholzer J, Calafiore R. Long-Term Metabolic and Immunological Follow-Up of Nonimmunosuppressed Patients With Type 1 Diabetes Treated With Microencapsulated Islet Allografts. *Diabetes Care*. 2011; 34(11):2406–2409. [PubMed: 21926290]
148. Orive G, Maria Hernandez R, Rodriguez Gascon A, Calafiore R, Swi Chang TM, Vos P.d. Hortelano G, Hunkeler D, Lacik I, Luis Pedraz J. History, challenges and perspectives of cell microencapsulation. *Trends in Biotechnology*. 2004; 22(2):87–92. [PubMed: 14757043]
149. de Vos P, Faas MM, Strand B, Calafiore R. Alginate-based microcapsules for immunoisolation of pancreatic islets. *Biomaterials*. 2006; 27(32):5603–5617. [PubMed: 16879864]
150. Calafiore, R.; Basta, G. *Methods in Molecular Medicine*. Hauser, H.; Fussenegger, M., editors. Vol. 140. Humana Press; Totowa: 2007. p. 197–236.
151. de Vos P, Bucko M, Gemeiner P, Navrátil M, Svitel J, Faas M, Strand BL, Skjak-Braek G, Morch YA, Vikartovská A, Lacík I, Kolláriková G, Orive G, Poncelet D, Pedraz JL, Ansorge-Schumacher MB. Multiscale requirements for bioencapsulation in medicine and biotechnology. *Biomaterials*. 2009; 30(13):2559–2570. [PubMed: 19201460]
152. Pedraz, JL.; Orive, G. *Therapeutic Applications of Cell Microencapsulation*. Springer; New York: 2010.
153. Calafiore, R.; Basta, G. *Stem Cell Therapy for Diabetes*. Efrat, S., editor. Vol. 3. Humana Press; New York: 2010. p. 241–262.
154. Elliott RB, Escobar L, Tan PLJ, Muzina M, Zwain S, Buchanan C. Live encapsulated porcine islets from a type 1 diabetic patient 9.5yr after xenotransplantation. *Xenotransplantation*. 2007; 14(2):157–161. [PubMed: 17381690]
155. Fallarino F, Luca G, Calvitti M, Mancuso F, Nastruzzi C, Fioretti MC, Grohmann U, Becchetti E, Burgevin A, Kratzer R, Endert P.v. Boon L, Puccetti P, Calafiore R. Therapy of experimental type 1 diabetes by isolated Sertoli cell xenografts alone. *Journal of Experimental Medicine*. 2009; 206(11):2511–2526. [PubMed: 19822646]
156. Adiga SP, Jin C, Curtiss LA, Monteiro-Riviere NA, Narayan RJ. Nanoporous membranes for medical and biological applications. *WIREs: Nanomed Nanobiotech*. 2009; 1(5):568–581.
157. Dunleavy M. Polymeric membranes. A review of applications. *Medical Device Technology*. 1996; 7(4):18–21. [PubMed: 10163670]

158. Desai TA, Hansford DJ, Leoni L, Essenpreis M, Ferrari M. Nanoporous anti-fouling silicon membranes for biosensor applications. *Biosensors and Bioelectronics*. 2000; 15(9-10):453–462. [PubMed: 11419640]
159. Li RH. Materials for immunoisolated cell transplantation. *Advanced Drug Delivery Reviews*. 1998; 33(1-2):87–109. [PubMed: 10837655]
160. Peppas NA, Huang Y, Torres-Lugo M, Ward JH, Zhang J. Physicochemical Foundations and Structural Design of Hydrogels in Medicine and Biology. *Annual Review of Biomedical Engineering*. 2000; 2(1):9–29.
161. Weber LM, He J, Bradley B, Haskins K, Anseth KS. PEG-based hydrogels as an in vitro encapsulation platform for testing controlled B-cell microenvironments. *Acta Biomaterialia*. 2006; 2(1):1–8. [PubMed: 16701853]
162. Weber LM, Cheung CY, Anseth KS. Multifunctional Pancreatic Islet Encapsulation Barriers Achieved Via Multilayer PEG Hydrogels. *Cell Transplantation*. 2008; 16(10):1049–1057. [PubMed: 18351021]
163. Magarinos AM, Jain K, Blount ED, Reagan L, Smith BH, McEwen BS. Peritoneal implantation of macroencapsulated porcine pancreatic islets in diabetic rats ameliorates severe hyperglycemia and prevents retraction and simplification of hippocampal dendrites. *Brain Research*. 2001; 902(2):282–287. [PubMed: 11384623]
164. Gazda LS, Vinerean HV, Laramore MA, Diehl CH, Hall RD, Rubin AL, Smith BH. Encapsulation of Porcine Islets Permits Extended Culture Time and Insulin Independence in Spontaneously Diabetic BB Rats. *Cell Transplantation*. 2007; 16(6):609–620. [PubMed: 17912952]
165. Qi M, Gu Y, Sakata N, Kim D, Shirouzu Y, Yamamoto C, Hiura A, Sumi S, Inoue K. PVA hydrogel sheet macroencapsulation for the bioartificial pancreas. *Biomaterials*. 2004; 25(27):5885–5892. [PubMed: 15172501]
166. Qi Z, Shen Y, Yanai G, Yang K, Shirouzu Y, Hiura A, Sumi S. The in vivo performance of polyvinyl alcohol macro-encapsulated islets. *Biomaterials*. 2010; 31(14):4026–4031. [PubMed: 20149430]
167. Lelli L, Barbani N, Bonaretti A, Giusti P, Marchetti P, Giannarelli R, Navalesi R, Viacava P. Preparation and characterization of permselective, biocompatible membranes for the macroencapsulation of pancreatic islets. *Journal of Materials Science: Materials in Medicine*. 1994; 5(12):887–890.
168. Scharp D, Swanson C, Olack B, Latta P, Hegre O, Doherty E, Gentile F, Flavin K, Ansara M, Lacy P. Protection of encapsulated human islets implanted without immunosuppression in patients with Type I or Type II diabetes and in nondiabetic control subjects. *Diabetes*. 1994; 43(9):1167–1170. [PubMed: 8070618]
169. Bridge MJ, Broadhead KW, Hlady V, Tresco PA. Ethanol treatment alters the ultrastructure and permeability of PAN-PVC hollow fiber cell encapsulation membranes. *Journal of Membrane Science*. 2002; 195(1):51–64.
170. George S, Nair PD, Risbud MV, Bhonde RR. Nonporous Polyurethane Membranes as Islet Immunoisolation Matrices - Biocompatibility Studies. *Journal of Biomaterials Applications*. 2002; 16(4):327–340. [PubMed: 12099511]
171. Kadam SS, Sudhakar M, Nair PD, Bhonde RR. Reversal of experimental diabetes in mice by transplantation of neo-islets generated from human amnion-derived mesenchymal stromal cells using immuno-isolatory macrocapsules. *Cytotherapy*. 2010; 12(8):982–991. [PubMed: 20807019]
172. Zondervan GJ, Hoppen HJ, Pennings AJ, Fritschy W, Wolters G, van Schilfgaard R. Design of a polyurethane membrane for the encapsulation of islets of Langerhans. *Biomaterials*. 1992; 13(3):136–144. [PubMed: 1567937]
173. Cheung SSC, Tai J, Tze WJ. Effect of molecular weight exclusion of polysulfone fibers on macroencapsulated pig islet xenograft function in diabetic mice. *Transplantation Proceedings*. 1997; 29(4):2144–2145. [PubMed: 9193562]

174. Silva AI, Mateus M. Development of a polysulfone hollow fiber vascular bio-artificial pancreas device for in vitro studies. *Journal of Biotechnology*. 2009; 139(3):236–249. [PubMed: 19121345]
175. Kessler L, Legeay G, Jesser C, Damge C, Pinget M. Influence of corona surface treatment on the properties of an artificial membrane used for Langerhans islets encapsulation: permeability and biocompatibility studies. *Biomaterials*. 1995; 16(3):185–191. [PubMed: 7748994]
176. Suzuki K, Bonner-Weir S, Hollister J, Weir GC. A method for estimating number and mass of islets transplanted within a membrane device. *Cell Transplantation*. 1996; 5(6):613–625. [PubMed: 8951219]
177. Suzuki K, Bonner-Weir S, Hollister-Lock J, Colton CK, Weir GC. Number and Volume of Islets Transplanted in Immunobarrier Devices. *Cell Transplantation*. 1998; 7(1):47–52. [PubMed: 9489762]
178. Krishnan L, Clayton LR, Boland ED, Reed RM, Hoying JB, Williams SK. Cellular Immunoisolation for Islet Transplantation by a Novel Dual Porosity Electrospun Membrane. *Transplantation Proceedings*. 2011; 43(9):3256–3261. [PubMed: 22099770]
179. Dufrane, D.; Gianello, P.; Melvik, JE. Alginate coated, collagen matrix cellular device, preparative methods, and uses thereof.. Jun 13. 2007 Patent WO/2007/144389
180. Dufrane D, Goebbels R-M, Gianello P. Alginate Macroencapsulation of Pig Islets Allows Correction of Streptozotocin-Induced Diabetes in Primates up to 6 Months Without Immunosuppression. *Transplantation*. 2010; 90(10):1054–1062. [PubMed: 20975626]
181. Gimi B, Kwon J, Kuznetsov A, Vachha B, Magin RL, Philipson LH, Lee J-B. A Nanoporous, Transparent Microcontainer for Encapsulated Islet Therapy. *Journal of Diabetes Science and Technology*. 2009; 3(2):297–303. [PubMed: 19746206]
182. Gimi B, Kwon J, Liu L, Su Y, Nemani K, Trivedi K, Cui Y, Vachha B, Mason R, Hu W, Lee J-B. Cell encapsulation and oxygenation in nanoporous microcontainers. *Biomedical Microdevices*. 2009; 11(6):1205–1212. [PubMed: 19629700]
183. Kwon J, Trivedi K, Krishnamurthy NV, Hu W, Lee J-B, Gimi B. SU-8-based immunoisolation microcontainer with nanoslots defined by nanoimprint lithography. *Journal of Vacuum Science and Technology B*. 2009; 27(6):2795–2800.
184. Gimi B. Making a Case: Nanofabrication Techniques in Encapsulated Cell Therapy for People with Diabetes. *Journal of Diabetes Science and Technology*. 2010; 4(4):1016–1021. [PubMed: 20663470]
185. Voskerician G, Shive MS, Shawgo RS, Recum H.v. Anderson JM, Cima MJ, Langer R. Biocompatibility and biofouling of MEMS drug delivery devices. *Biomaterials*. 2003; 24(11):1959–1967. [PubMed: 12615486]
186. van Rijn CJM, Elwenspoek MC. Microfiltration membrane sieve with silicon micromachining for industrial and biomedical applications. *Micro Electro Mechanical Systems, 1995, MEMS '95, Proceedings*. 1995:83–87. IEEE DO - 10.1109/MEMSYS.1995.472549.
187. Ferrari M, Chu IW, Desai IT, Hansford D, Mazzoni G, Huen T, Zhang M. Silicon Nanotechnology for Biofiltration and Immunoisolated Cell Xenografts. *MRS Proceedings*. 1995; 414(1):101–106.
188. Desai TA, Hansford DJ, Ferrari M. Micromachined interfaces: new approaches in cell immunoisolation and biomolecular separation. *Biomolecular Engineering*. 2000; 17(1):23–36. [PubMed: 11042474]
189. Desai TA, Hansford D, Ferrari M. Characterization of micromachined silicon membranes for immunoisolation and bioseparation applications. *Journal of Membrane Science*. 1999; 159(1-2):221–231.
190. Desai T, Chu W, Rasi G, Sinibaldi-Vallebona P, Guarino E, Ferrari M. Microfabricated Biocapsules Provide Short-Term Immunoisolation of Insulinoma Xenografts. *Biomedical Microdevices*. 1999; 1(2):131–138. [PubMed: 16281113]
191. Leoni L, Boiarski A, Desai TA. Characterization of Nanoporous Membranes for Immunoisolation: Diffusion Properties and Tissue Effects. *Biomedical Microdevices*. 2002; 4(2):131–139.

192. Colton CK, Avgoustiniatos ES. Bioengineering in Development of the Hybrid Artificial Pancreas. *J. Biomech. Eng.* 1991; 113(2):152–170. [PubMed: 1875688]
193. Iwata H, Kobayashi K, Takagi T, Oka T, Yang H, Amemiya H, Tsuji T, Ito F. Feasibility of agarose microbeads with xenogeneic islets as a bioartificial pancreas. *Journal of Biomedical Materials Research.* 1994; 28(9):1003–1011. [PubMed: 7814428]
194. Lanza RP, Hayes JL, Chick WL. Encapsulated cell technology. *Nature Biotechnology.* 1996; 14(9):1107–1111.
195. Zhang M, Desai T, Ferrari M. Proteins and cells on PEG immobilized silicon surfaces. *Biomaterials.* 1998; 19(10):953–960. [PubMed: 9690837]
196. Sharma S, Johnson RW, Desai TA. Ultrathin poly(ethylene glycol) films for silicon-based microdevices. *Applied Surface Science.* 2003; 206(1-4):218–229.
197. Leoni L, Desai TA. Nanoporous biocapsules for the encapsulation of insulinoma cells: biotransport and biocompatibility considerations. *Biomedical Engineering, IEEE Transactions.* 2001; 48(11):1335–1341.
198. Diggle JW, Downie TC, Goulding CW. Anodic oxide films on aluminum. *Chemical Reviews.* 1969; 69(3):365–405.
199. Itoh N, Kato K, Tsuji T, Hongo M. Preparation of a tubular anodic aluminum oxide membrane. *Journal of Membrane Science.* 1996; 117(1-2):189–196.
200. Itoh N, Tomura N, Tsuji T, Hongo M. Strengthened porous alumina membrane tube prepared by means of internal anodic oxidation. *Microporous and Mesoporous Materials.* 1998; 20(4-6):333–337.
201. Gong D, Yadavalli V, Paulose M, Pishko M, Grimes CA. Controlled Molecular Release Using Nanoporous Alumina Capsules. *Biomedical Microdevices.* 2003; 5(1):75–80.
202. Popat KC, Mor G, Grimes CA, Desai TA. Surface Modification of Nanoporous Alumina Surfaces with Poly(ethylene glycol). *Langmuir.* 2004; 20(19):8035–8041. [PubMed: 15350069]
203. Swan EEL, Popat KC, Grimes CA, Desai TA. Fabrication and evaluation of nanoporous alumina membranes for osteoblast culture. *J. Biomed. Mater. Res.* 2005; 72A(3):288–295.
204. La Flamme KE, Mor G, Gong D, La Tempa T, Fusaro VA, Grimes CA, Desai TA. Nanoporous Alumina Capsules for Cellular Macroencapsulation: Transport and Biocompatibility. *Diabetes Technology & Therapeutics.* 2005; 7(5):684–694. [PubMed: 16241869]
205. La Flamme KE, Popat KC, Leoni L, Markiewicz E, La Tempa TJ, Roman BB, Grimes CA, Desai TA. Biocompatibility of nanoporous alumina membranes for immunoisolation. *Biomaterials.* 2007; 28(16):2638–2645. [PubMed: 17335895]
206. Popat KC, Mor G, Grimes C, Desai TA. Poly (ethylene glycol) grafted nanoporous alumina membranes. *Journal of Membrane Science.* 2004; 243(1-2):97–106.
207. Zwilling V, Darque-Ceretti E, Boutry-Forveille A, David D, Perrin MY, Aucouturier M. Structure and physicochemistry of anodic oxide films on titanium and TA6V alloy. *Surf. Interface Anal.* 1999; 27(7):629–637.
208. Gong D, Grimes CA, Varghese OK, Hu W, Singh RS, Chen Z, Dickey EC. Titanium oxide nanotube arrays prepared by anodic oxidation. *Journal of Materials Research.* 2001; 16(12):3331–3334.
209. Beranek R, Hildebrand H, Schmuki P. Self-Organized Porous Titanium Oxide Prepared in H₂SO₄/HF Electrolytes. *Electrochem. Solid-State Lett.* 2003; 6(3):B12–B14.
210. Macak JM, Sirotna K, Schmuki P. Self-organized porous titanium oxide prepared in Na₂SO₄/NaF electrolytes. *Electrochimica Acta.* 2005; 50(18):3679–3684.
211. Macak JM, Tsuchiya H, Schmuki P. High-Aspect-Ratio TiO₂ Nanotubes by Anodization of Titanium. *Angew. Chem. Int. Ed.* 2005; 44(14):2100–2102.
212. Macak JM, Tsuchiya H, Taveira L, Aldabergerova S, Schmuki P. Smooth Anodic TiO₂ Nanotubes. *Angew. Chem. Int. Ed.* 2005; 44(45):7463–7465.
213. Cai Q, Paulose M, Varghese OK, Grimes CA. The effect of electrolyte composition on the fabrication of self-organized titanium oxide nanotube arrays by anodic oxidation. *Journal of Materials Research.* 2005; 20(1):230–236.

214. Ruan C, Paulose M, Varghese OK, Mor GK, Grimes CA. Fabrication of Highly Ordered TiO₂ Nanotube Arrays Using an Organic Electrolyte. *The Journal of Physical Chemistry B*. 2005; 109(33):15754–15759. [PubMed: 16852999]
215. Macak JM, Schmuki P. Anodic growth of self-organized anodic TiO₂ nanotubes in viscous electrolytes. *Electrochimica Acta*. 2006; 52(3):1258–1264.
216. Paulose M, Shankar K, Yoriya S, Prakasam HE, Varghese OK, Mor GK, Latempa TA, Fitzgerald A, Grimes CA. Anodic Growth of Highly Ordered TiO₂ Nanotube Arrays to 134 μ m in Length. *The Journal of Physical Chemistry B*. 2006; 110(33):16179–16184. [PubMed: 16913737]
217. Macak JM, Albu SP, Schmuki P. Towards ideal hexagonal self-ordering of TiO₂ nanotubes. *Phys. Status Solidi RRL*. 2007; 1(5):181–183.
218. Prakasam HE, Shankar K, Paulose M, Varghese OK, Grimes CA. A New Benchmark for TiO₂ Nanotube Array Growth by Anodization. *The Journal of Physical Chemistry C*. 2007; 111(20): 7235–7241.
219. Paulose M, Prakasam HE, Varghese OK, Peng L, Popat KC, Mor GK, Desai TA, Grimes CA. TiO₂ Nanotube Arrays of 1000 μ m Length by Anodization of Titanium Foil: Phenol Red Diffusion. *The Journal of Physical Chemistry C*. 2007; 111(41):14992–14997.
220. Paulose M, Peng L, Popat KC, Varghese OK, LaTempa TJ, Bao N, Desai TA, Grimes CA. Fabrication of mechanically robust, large area, polycrystalline nanotubular/porous TiO₂ membranes. *Journal of Membrane Science*. 2008; 319(1-2):199–205.
221. Grimes, CA.; Mor, GK. *TiO₂ Nanotube Arrays - Synthesis, Properties, and Applications*. Springer; Dordrecht: 2009.
222. Ghicov A, Schmuki P. Self-ordering electrochemistry: a review on growth and functionality of TiO₂ nanotubes and other self-aligned MO_x structures. *Chemical Communications*. 2009; 20(1): 2791–2808. [PubMed: 19436878]
223. Rani S, Roy SC, Paulose M, Varghese OK, Mor GK, Kim S, Yoriya S, LaTempa TJ, Grimes CA. Synthesis and applications of electrochemically self-assembled titania nanotube arrays. *Physical Chemistry Chemical Physics*. 2010; 12(12):2780–2800. [PubMed: 20449368]
224. Roy P, Berger S, Schmuki P. TiO₂ Nanotubes: Synthesis and Applications. *Angew. Chem. Int. Ed*. 2011; 50(13):2904–2939.
225. Ainslie KM, Tao SL, Popat KC, Daniels H, Hardev V, Grimes CA, Desai TA. In vitro inflammatory response of nanostructured titania, silicon oxide, and polycaprolactone. *J. Biomed. Mater. Res*. 2009; 91A(3):647–655.
226. Albu SP, Ghicov A, Macak JM, Hahn R, Schmuki P. Self-Organized, Free-Standing TiO₂ Nanotube Membrane for Flow-through Photocatalytic Applications. *Nano Letters*. 2007; 7(5): 1286–1289. [PubMed: 17455983]
227. Albu SP, Ghicov A, Schmuki P. Lift Off Strategies for Self-Organized TiO₂ Nanotube Layers. *ECS Trans*. 2009; 16(52):195–202.
228. Wang J, Lin Z. Freestanding TiO₂ Nanotube Arrays with Ultrahigh Aspect Ratio via Electrochemical Anodization. *Chemistry of Materials*. 2008; 20(4):1257–1261.
229. Kant K, Losic D. A simple approach for synthesis of TiO₂ nanotubes with through-hole morphology. *Phys. Status Solidi RRL*. 2009; 3(5):139–141.
230. Li S, Zhang G. One-step realization of open-ended TiO₂ nanotube arrays by transition of the anodizing voltage. *Journal of the Ceramic Society of Japan*. 2010; 118(4):291–294.
231. Wang D, Liu L. Continuous Fabrication of Free-Standing TiO₂ Nanotube Array Membranes with Controllable Morphology for Depositing Interdigitated Heterojunctions. *Chemistry of Materials*. 2010; 22(24):6656–6664.
232. Wang D, Liu L, Zhang F, Tao K, Pippel E, Domen K. Spontaneous Phase and Morphology Transformations of Anodized Titania Nanotubes Induced by Water at Room Temperature. *Nano Letters*. 2011; 11(9):3649–3655. [PubMed: 21786788]
233. Lin J, Chen J, Chen X. Facile fabrication of free-standing TiO₂ nanotube membranes with both ends open via self-detaching anodization. *Electrochemistry Communications*. 2010; 12(8):1062–1065.

234. Li L-L, Chen Y-J, Wu H-P, Wang NS, Diau EW-G. Detachment and transfer of ordered TiO₂ nanotube arrays for front-illuminated dye-sensitized solar cells. *Energy & Environmental Science*. 2011; 4(9):3420–3425.
235. Albu SP, Ghicov A, Berger S, Jha H, Schmuki P. TiO₂ nanotube layers: Flexible and electrically active flow-through membranes. *Electrochemistry Communications*. 2010; 12(10):1352–1355.
236. Randall CL, Leong TG, Bassik N, Gracias DH. 3D lithographically fabricated nanoliter containers for drug delivery. *Advanced Drug Delivery Reviews*. 2007; 59(15):1547–1561. [PubMed: 17919768]
237. Randall CL, Gultepe E, Gracias DH. Self-folding devices and materials for biomedical applications. *Trends in Biotechnology*. 2012; 30(3):138–146. [PubMed: 21764161]
238. Gimi B, Leong T, Gu Z, Yang M, Artemov D, Bhujwala Z, Gracias D. Self-Assembled Three Dimensional Radio Frequency (RF) Shielded Containers for Cell Encapsulation. *Biomedical Microdevices*. 2005; 7(4):341–345. [PubMed: 16404512]
239. Leong TG, Lester PA, Koh TL, Call EK, Gracias DH. Surface Tension-Driven Self-Folding Polyhedra. *Langmuir*. 2007; 23(17):8747–8751. [PubMed: 17608507]
240. Cho J-H, Gracias DH. Self-Assembly of Lithographically Patterned Nanoparticles. *Nano Letters*. 2009; 9(12):4049–4052. [PubMed: 19681638]
241. Leong TG, Zarafshar AM, Gracias DH. Three-Dimensional Fabrication at Small Size Scales. *Small*. 2010; 6(7):792–806. [PubMed: 20349446]
242. Azam A, Laflin K, Jamal M, Fernandes R, Gracias D. Self-folding micropatterned polymeric containers. *Biomedical Microdevices*. 2011; 13(1):51–58. [PubMed: 20838901]
243. Gracias DH, Kavthekar V, Love JC, Paul KE, Whitesides GM. Fabrication of Micrometer-Scale, Patterned Polyhedra by Self-Assembly. *Adv. Mater.* 2002; 14(3):235–238.
244. Leong TG, Benson BR, Call EK, Gracias DH. Thin Film Stress Driven Self-Folding of Microstructured Containers. *Small*. 2008; 4(10):1605–1609. [PubMed: 18702125]
245. Randall CL, Kalinin YV, Jamal M, Manohar T, Gracias DH. Three-dimensional microwell arrays for cell culture. *Lab on a Chip*. 2011; 11(1):127–131. [PubMed: 21063585]
246. Randall CL, Kalinin YV, Jamal M, Shah A, Gracias DH. Self-folding immunoprotective cell encapsulation devices. *Nanomedicine: Nanotechnology, Biology and Medicine*. 2011; 7(6):686–689.

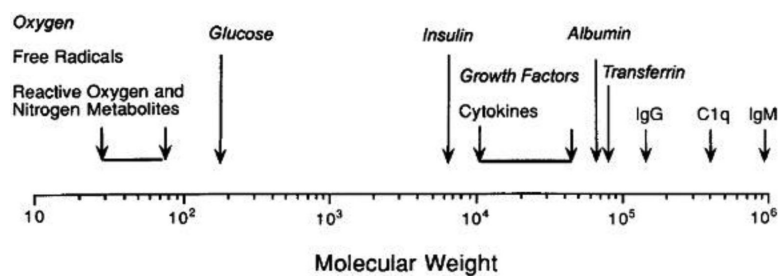


Figure 1. Molecular weight spectrum in immunoisolation: molecules that should pass the immunoisolation barrier are in italics, all other molecules may be deleterious to implanted tissue. Reproduced with permission from (56).

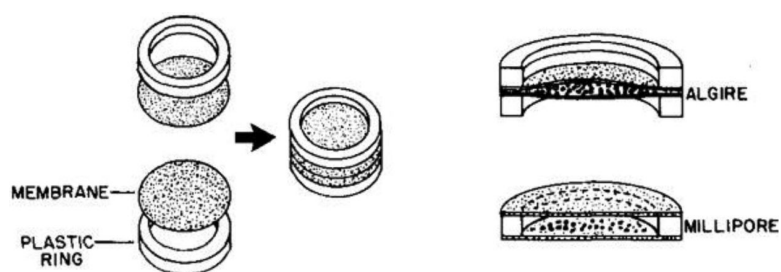


Figure 3: Schematic representation of different cellular encapsulation approaches. Algire and Millipore diffusion chambers for extravascular macroencapsulation. Reproduced with permission from (64).

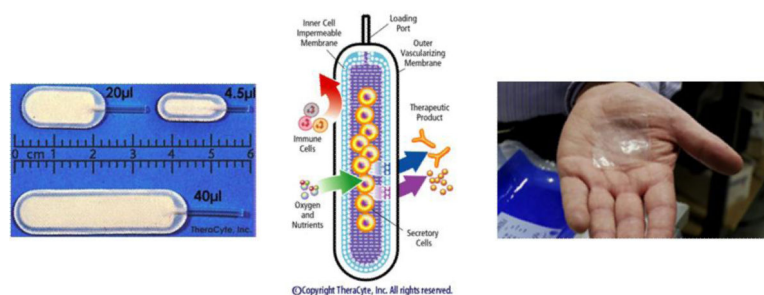


Figure 4.
Commercial macroencapsulation devices: TheraCyte (left and middle) and Islet Sheet (right).

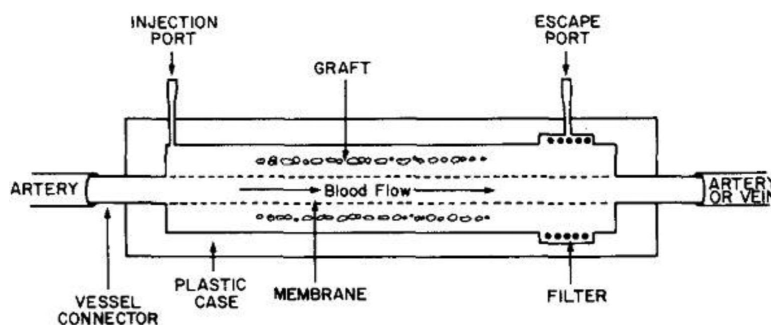


Figure 5.
Schematic representation of an intravascular diffusion chamber. Reproduced with permission from (64).

Figure 6.
Schematic
permission



Figure 7.

Two human pancreatic islets encapsulated in an alginate-based microcapsule (the red color is obtained after staining with dithizone that binds to zinc ions present in beta cells). Reproduced with permission from (149).

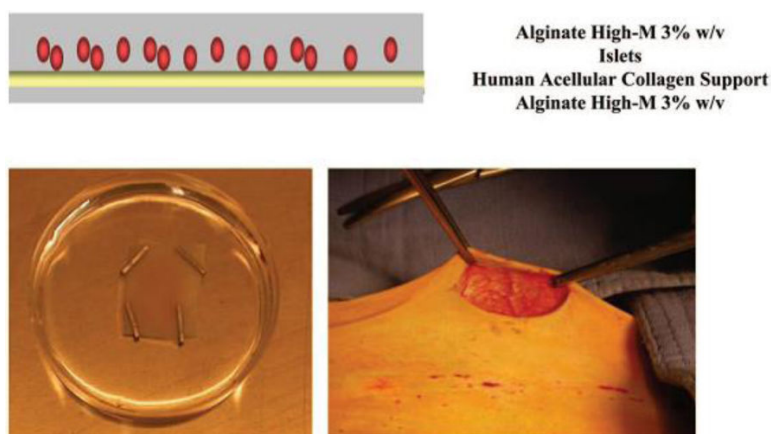


Figure 8.

Alginate and collagen macrocapsule containing a monolayer of pig islets, schematic representation (top) and picture (bottom, left) ; Implantation of the device into abdominal subcutaneous tissue of non-human primate (bottom, right). Reproduced with permission from (180).

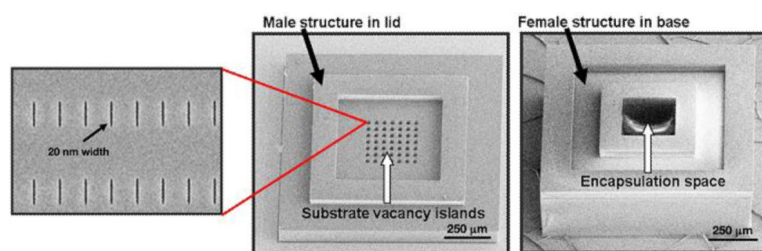
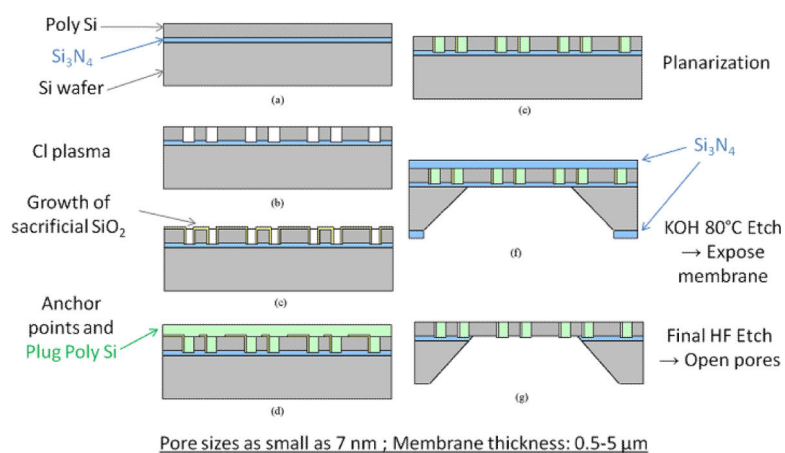


Figure 9.

SU-8 nanoporous microcapsule micrographs showing the lid, the base and a close-up of the nanoslots in the lid. Reproduced with permission from (184).

**Figure 10.**

Process scheme for the fabrication of Si nanoporous membranes. Reproduced with permission from (158).



Figure 11.

Picture of a Si nanoporous membrane showing the porous area surrounded by the support ridge (left), SEM micrographs: top view (middle) and cross-section showing the nanopores across the whole thickness of the membrane (right). Reproduced with permission from (191).

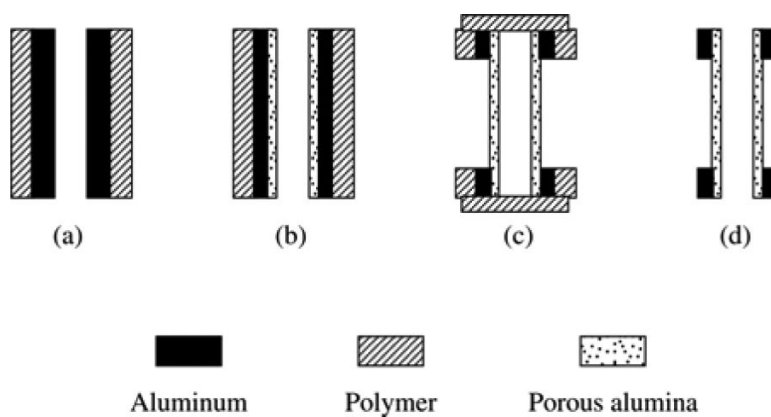


Figure 12.

Process scheme for the fabrication of Al_2O_3 nanoporous membranes embedded in an Al cylinder (side view). Reproduced with permission from (201).

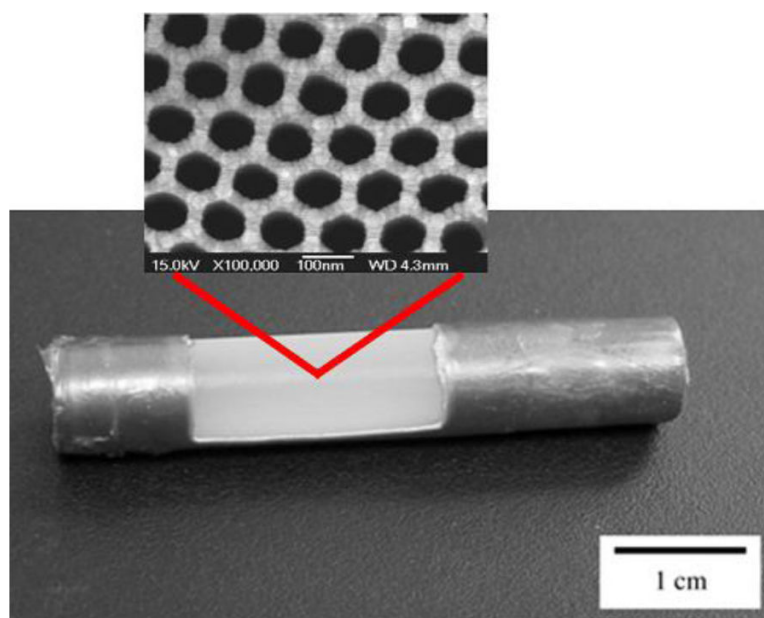


Figure 13. Cylindrical Al macrocapsule with Al_2O_3 nanoporous membrane windows, close-up: SEM micrograph of the top of the membrane. Reproduced with permission from (201, 205).

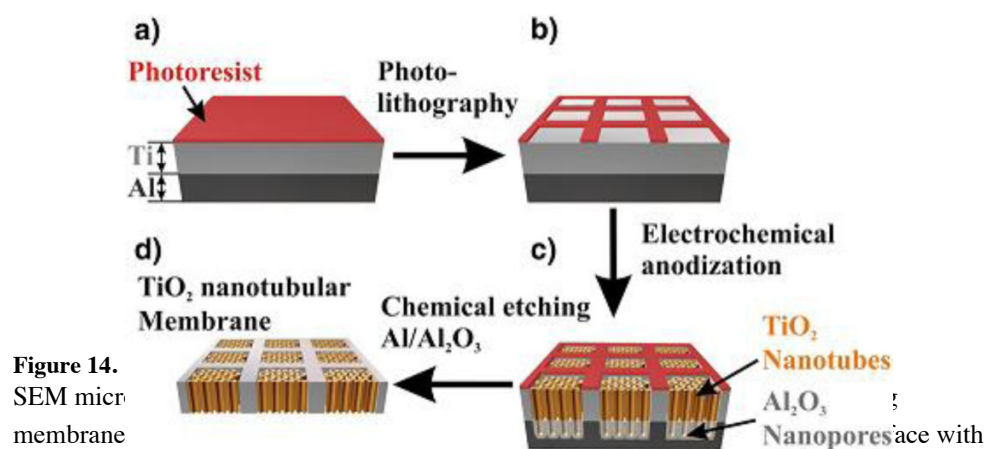


Figure 14.
SEM micrograph of a TiO_2 nanotubular membrane

inset showing high magnification (right). Reproduced with permission from (220).

Figure 15.

Process scheme for the fabrication of flexible TiO_2 nanotubular membranes. Reproduced with permission from (235).

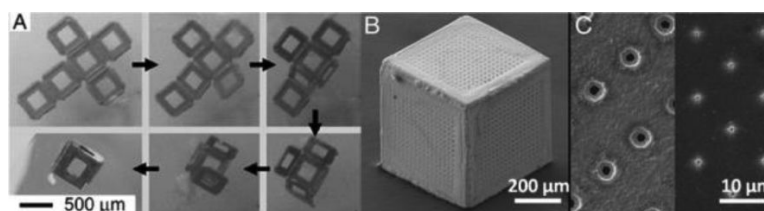


Figure 16.

Video snapshots showing the self-assembly of a lithographically fabricated template into a 3D hollow container (A) ; SEM micrograph of a 3D porous container (B) ; SEM micrograph of pores on the faces of containers of different pore sizes (C). Reproduced with permission from (236, 246).

References:

- (1) Atkinson, M. A.; Eisenbarth, G. S.; Michels, A. W. Type 1 Diabetes. *Lancet* **2014**, 383, 69–82.
- (2) Maria-Engler, S. S.; Mares-Guia, M.; Correa, M. L.; Oliveira, E. M.; Aita, C. A. M.; Krogh, K.; Genzini, T.; Miranda, M.; Ribeiro, M.; Vilela, L.; *et al.*
Microencapsulation and Tissue Engineering as an Alternative Treatment of Diabetes. *Braz. J. Med. Biol. Res.* **2001**, 34.
- (3) Avedisian, C. T.; Cavicchi, R. E.; McEuen, P. L.; Zhou, X. Nanoparticles for Cancer Treatment: Role of Heat Transfer. *Ann. N. Y. Acad. Sci.* **2009**, 1161, 62–73.
- (4) De Vos, P.; Spasojevic, M.; Faas, M. M. Treatment of Diabetes with Encapsulated Islets. *Adv. Exp. Med. Biol.* **2010**, 670, 38–53.
- (5) Orlando, G.; Gianello, P.; Salvatori, M.; Stratta, R. J.; Soker, S.; Ricordi, C.; Domínguez-Bendala, J. Cell Replacement Strategies Aimed at Reconstitution of the B-Cell Compartment in Type 1 Diabetes. *Diabetes* **2014**, 63, 1433–1444.
- (6) Scharp, D. W.; Marchetti, P. Encapsulated Islets for Diabetes Therapy: History, Current Progress, and Critical Issues Requiring Solution. *Adv. Drug Deliv. Rev.* **2014**, 67-68, 35–73.

- (7) Nyitray, C. E.; Chavez, M. G.; Desai, T. Compliant 3D Microenvironment Improves B-Cell Cluster Insulin Expression through Mechanosensing and B-Catenin Signaling. *Tissue Eng. Part A* **2014**, 1–34.
- (8) Roy, S.; Sala, R.; Cagliero, E.; Lorenzi, M. Overexpression of Fibronectin Induced by Diabetes or High Glucose: Phenomenon with a Memory. *Proc. Natl. Acad. Sci. U. S. A.* **1990**, 87, 404–408.
- (9) Serup, P.; Madsen, O. D.; Mandrup-poulsen, T. Islet and Stem Cell Transplantation for Treating Diabetes. **2010**, 29–32.
- (10) Barker, C. J.; Leibiger, I. B.; Berggren, P.-O. The Pancreatic Islet as a Signaling Hub. *Adv. Biol. Regul.* **2013**, 53, 156–163.
- (11) Bavamian, S.; Klee, P.; Britan, a; Populaire, C.; Caille, D.; Cancela, J.; Charollais, a; Meda, P. Islet-Cell-to-Cell Communication as Basis for Normal Insulin Secretion. *Diabetes. Obes. Metab.* **2007**, 9 Suppl 2, 118–132.
- (12) Egro, F. M. Why Is Type 1 Diabetes Increasing? *J. Mol. Endocrinol.* **2013**, 51.
- (13) Kallionpää, H.; Laajala, E.; Öling, V.; Härkönen, T.; Tillmann, V.; Dorshakova, N. V.; Ilonen, J.; Lähdesmäki, H.; Knip, M.; Lahesmaa, R. Standard of Hygiene and Immune Adaptation in Newborn Infants. *Clin. Immunol.* **2014**, 155, 136–147.
- (14) Zhang, L.; Chen, Y.; Li, C.; Lin, X.; Cheng, X.; Li, T. Protective Effects of Combined Intervention with Adenovirus Vector Mediated IL-10 and IGF-1

Genes on Endogenous Islet B Cells in Nonobese Diabetes Mice with Onset of Type 1 Diabetes Mellitus. *PLoS One* **2014**, 9, e92616.

- (15) Viera, S. M.; Pagovich, O. E.; Kriegel, M. A. Diet, Microbiota and Autoimmune Diseases. *Lupus*. **2014**, 23, 997–1003.
- (16) Mekonnen, D.; Gebre-Selassie, S.; Fantaw, S.; Hunegnaw, A.; Mihret, A. Prevalence of Hepatitis B Virus in Patients with Diabetes Mellitus: A Comparative Cross Sectional Study at Woldiya General Hospital, Ethiopia. *Pan Afr. Med. J.* **2014**, 17, 1–7.
- (17) Bodin, J.; Stene, L. C.; Nygaard, U. C. Can Exposure to Environmental Chemicals Increase the Risk of Diabetes Type 1 Development? *Biomed Res. Int.* **2015**, 2015, 1–19.
- (18) Andreoni, K. a; Brayman, K. L.; Guidinger, M. K.; Sommers, C. M.; Sung, R. S. Kidney and Pancreas Transplantation in the United States, 1996-2005. *Am. J. Transplant* **2007**, 7, 1359–1375.
- (19) Gummert, J. F.; Ikonen, T.; Morris, R. E. Newer Immunosuppressive Drugs: A Review. *J. Am. Soc. Nephrol.* **1999**, 10, 1366–1380.
- (20) Vaithilingam, V.; Tuch, B. E. Islet Transplantation and Encapsulation: An Update on Recent Developments. *Rev. Diabet. Stud.* **2011**, 8, 51–67.

- (21) Kahn, S. E.; Zraika, S.; Utzschneider, K. M.; Hull, R. L. The Beta Cell Lesion in Type 2 Diabetes: There Has to Be a Primary Functional Abnormality. *Diabetologia* **2009**, *52*, 1003–1012.
- (22) Kemp, C. B.; Knight, M. J.; Scharp, D. W.; Ballinger, W. F.; Lacy, P. E. Effect of Transplantation Site on the Results of Pancreatic Islet Isografts in Diabetic Rats. *Diabetologia* **1973**, *9*, 486–491.
- (23) Shapiro, A. M.; Lakey, J. R.; Ryan, E. A.; Korbitt, G. S.; Toth, E.; Warnock, G. L.; Kneteman, N. M.; Rajotte, R. V. Islet Transplantation in Seven Patients with Type 1 Diabetes Mellitus Using a Glucocorticoid-Free Immunosuppressive Regimen. *N. Engl. J. Med.* **2000**, *343*, 230–238.
- (24) Ryan, E. a; Paty, B. W.; Senior, P. a; Bigam, D.; Alfadhli, E.; Kneteman, N. M.; Lakey, J. R. T.; Shapiro, a M. J. Five-Year Follow-up after Clinical Islet Transplantation. *Diabetes* **2005**, *54*, 2060–2069.
- (25) Bonner-Weir, S.; Weir, G. C. New Sources of Pancreatic Beta-Cells. *Nat. Biotechnol.* **2005**, *23*, 857–861.
- (26) D'Amour, K. a; Bang, A. G.; Eliazar, S.; Kelly, O. G.; Agulnick, A. D.; Smart, N. G.; Moorman, M. a; Kroon, E.; Carpenter, M. K.; Baetge, E. E. Production of Pancreatic Hormone-Expressing Endocrine Cells from Human Embryonic Stem Cells. *Nat. Biotechnol.* **2006**, *24*, 1392–1401.

- (27) Matveyenko, A. V; Veldhuis, J. D.; Butler, P. C. Adaptations in Pulsatile Insulin Secretion , Hepatic Insulin Clearance , and β -Cell Mass to Age-Related Insulin Resistance in Rats. **2008**, *90095*, 832–841.
- (28) Butler, a E.; Cao-Minh, L.; Galasso, R.; Rizza, R. a; Corradin, a; Cobelli, C.; Butler, P. C. Adaptive Changes in Pancreatic Beta Cell Fractional Area and Beta Cell Turnover in Human Pregnancy. *Diabetologia* **2010**, *53*, 2167–2176.
- (29) Chen, S.; Borowiak, M.; Fox, J. L.; Maehr, R.; Osafune, K.; Davidow, L.; Lam, K.; Peng, L. F.; Schreiber, S. L.; Rubin, L. L.; *et al.* A Small Molecule That Directs Differentiation of Human ESCs into the Pancreatic Lineage. *Nat. Chem. Biol.* **2009**, *5*, 258–265.
- (30) Tang, C.; Zhao, X.; Han, J. Primary Culture of Porcine Pancreatic Acinar Cells. *Pancreas* **2002**, *25*, 68–70.
- (31) Aviv, V.; Meivar-Levy, I.; Rachmut, I. H.; Rubinek, T.; Mor, E.; Ferber, S. Exendin-4 Promotes Liver Cell Proliferation and Enhances the PDX-1-Induced Liver to Pancreas Transdifferentiation Process. *J. Biol. Chem.* **2009**, *284*, 33509–33520.
- (32) Nagaya, M.; Katsuta, H.; Kaneto, H.; Bonner-Weir, S.; Weir, G. C. Adult Mouse Intrahepatic Biliary Epithelial Cells Induced in Vitro to Become Insulin-Producing Cells. *J. Endocrinol.* **2009**, *201*, 37–47.

- (33) Zhou, Q.; Brown, J.; Kanarek, A.; Rajagopal, J.; Melton, D. a. In Vivo Reprogramming of Adult Pancreatic Exocrine Cells to Beta-Cells. *Nature* **2008**, *455*, 627–632.
- (34) De Vos, P.; Van Straaten, J. F.; Nieuwenhuizen, a G.; de Groot, M.; Ploeg, R. J.; De Haan, B. J.; Van Schilfgaarde, R. Why Do Microencapsulated Islet Grafts Fail in the Absence of Fibrotic Overgrowth? *Diabetes* **1999**, *48*, 1381–1388.
- (35) Gomez, E. W.; Chen, Q. K.; Gjorevski, N.; Nelson, C. M. Tissue Geometry Patterns Epithelial-Mesenchymal Transition via Intercellular Mechanotransduction. *Cell* **2011**, *110*, 44–51.
- (36) Gjorevski, N.; Nelson, C. M. Mapping of Mechanical Strains and Stresses around Quiescent Engineered Three-Dimensional Epithelial Tissues. *Biophys. J.* **2012**, *103*, 152–162.
- (37) Yang, X. D.; Michie, S. a; Tisch, R.; Karin, N.; Steinman, L.; McDevitt, H. O. A Predominant Role of Integrin Alpha 4 in the Spontaneous Development of Autoimmune Diabetes in Nonobese Diabetic Mice. *Proc. Natl. Acad. Sci. U. S. A.* **1994**, *91*, 12604–12608.
- (38) Zhao, Y.; Xu, J.; Wei, J.; Li, J.; Cai, J.; Miao, G. Preservation of Islet Survival by Upregulating $\alpha 3$ Integrin Signaling: The Importance of 3-Dimensional Islet Culture in Basement Membrane Extract. *Transplant. Proc.* **2010**, *42*, 4638–4642.

- (39) Krishnamurthy, M.; Li, J.; Fellows, G. F.; Rosenberg, L.; Goodyer, C. G.; Wang, R. Integrin α_3 , but Not β_1 , Regulates Islet Cell Survival and Function via PI3K/Akt Signaling Pathways. *Endocrinology* **2011**, *152*, 424–435.
- (40) Hammar, E.; Parnaud, G.; Bosco, D.; Perriraz, N.; Maedler, K.; Donath, M.; Rouiller, D. G.; Halban, P. a. Extracellular Matrix Protects Pancreatic Beta-Cells against Apoptosis: Role of Short- and Long-Term Signaling Pathways. *Diabetes* **2004**, *53*, 2034–2041.
- (41) Kaido, T.; Yebra, M.; Cirulli, V.; Rhodes, C.; Diaferia, G.; Montgomery, A. M. Impact of Defined Matrix Interactions on Insulin Production by Cultured Human Beta-Cells: Effect on Insulin Content, Secretion, and Gene Transcription. *Diabetes* **2006**, *55*, 2723–2729.
- (42) Krishnamurthy, M.; Li, J.; Al-Masri, M.; Wang, R. Expression and Function of $\alpha\beta_1$ Integrins in Pancretic Beta (INS-1) Cells. *J. Cell Commun. Signal.* **2008**, *2*, 67–79.
- (43) Nagata, N. A.; Inoue, K.; Tabata, Y. Co-Culture of Extracellular Matrix Suppresses the Cell Death of Rat Pancreatic Islets. *J. Biomater. Sci. Polym. Ed.* **2002**, *13*, 579–590.
- (44) Weber, L. M.; Hayda, K. N.; Anseth, K. S. Cell-Matrix Interactions Improve Beta-Cell Survival and Insulin Secretion in Three-Dimensional Culture. *Tissue Eng. Part A* **2008**, *14*, 1959–1968.

- (45) Hamelin, R.; Allagnat, F.; Haefliger, J.-A.; Meda, P. Connexins, Diabetes and the Metabolic Syndrome. *Curr. Protein Pept. Sci.* **2009**, *10*, 18–29.
- (46) Carvalho, C. P. F.; Barbosa, H. C. L.; Britan, a; Santos-Silva, J. C. R.; Boschero, a C.; Meda, P.; Collares-Buzato, C. B. Beta Cell Coupling and Connexin Expression Change during the Functional Maturation of Rat Pancreatic Islets. *Diabetologia* **2010**, *53*, 1428–1437.
- (47) Srinivas, M.; Rozental, R.; Kojima, T.; Dermietzel, R.; Mehler, M.; Condorelli, D. F.; Kessler, J. a; Spray, D. C. Functional Properties of Channels Formed by the Neuronal Gap Junction Protein connexin36. *J. Neurosci.* **1999**, *19*, 9848–9855.
- (48) Speier, S.; Gjinovci, A.; Charollais, A.; Meda, P.; Rupnik, M. Cx36-Mediated Coupling Reduces Beta-Cell Heterogeneity, Confines the Stimulating Glucose Concentration Range, and Affects Insulin Release Kinetics. *Diabetes* **2007**, *56*, 1078–1086.
- (49) Jain, R.; Lammert, E. Cell-Cell Interactions in the Endocrine Pancreas. *Diabetes. Obes. Metab.* **2009**, *11 Suppl 4*, 159–167.
- (50) Bavamian, S.; Klee, P.; Britan, a; Populaire, C.; Caille, D.; Cancela, J.; Charollais, a; Meda, P. Islet-Cell-to-Cell Communication as Basis for Normal Insulin Secretion. *Diabetes. Obes. Metab.* **2007**, *9 Suppl 2*, 118–132.

- (51) Van der Windt, D. J.; Bottino, R.; Casu, A.; Campanile, N.; Cooper, D. K. C. Rapid Loss of Intraportally Transplanted Islets: An Overview of Pathophysiology and Preventive Strategies. *Xenotransplantation* **2007**, *14*, 288–297.
- (52) Harlan, D. M.; Kenyon, N. S.; Korsgren, O.; Roep, B. O. Current Advances and Travails in Islet Transplantation. *Diabetes* **2009**, *58*, 2175–2184.
- (53) Ludwig, B.; Reichel, A.; Steffen, A.; Zimmerman, B.; Schally, A. V.; Block, N. L.; Colton, C. K.; Ludwig, S.; Kersting, S.; Bonifacio, E.; *et al.* Transplantation of Human Islets without Immunosuppression. *Proc. Natl. Acad. Sci. U. S. A.* **2013**, *110*, 19054–19058.
- (54) Stoyanova, V.; Petrova, S.; Tchorbadjieva, M.; Deliyska, B.; Vasilev, V.; Tsacheva, I. New Insight into the Autoimmunogenicity of the Complement Protein C1q. *Mol. Immunol.* **2011**, *48*, 678–682.
- (55) Martel, C.; Cointe, S.; Maurice, P.; Matar, S.; Ghitescu, M.; Thérroux, P.; Bonnefoy, A. Requirements for Membrane Attack Complex Formation and Anaphylatoxins Binding to Collagen-Activated Platelets. *PLoS One* **2011**, *6*, e18812.
- (56) Zhang, X.; He, H.; Yen, C.; Ho, W.; Lee, L. J. A Biodegradable, Immunoprotective, Dual Nanoporous Capsule for Cell-Based Therapies. *Biomaterials* **2008**, *29*, 4253–4259.

- (57) Mendelsohn, A.; Desai, T. Inorganic Nanoporous Membranes for Immunoisolated Cell-Based Drug Delivery. *Adv. Exp. Med. Biol.* **2010**, *670*, 104–125.
- (58) Hadjivassiliou, V.; Green, M. H.; Green, I. C. Immunomagnetic Purification of Beta-cells from Rat Islets of Langerhans. *Diabetologia* **2000**, *43*, 1170–1177.
- (59) Mairbäurl, H.; Weber, R. E. Oxygen Transport by Hemoglobin. *Compr. Physiol.* **2012**, *2*, 1463–1489.
- (60) Pedraza, E.; Coronel, M. M.; Fraker, C. a; Ricordi, C.; Stabler, C. L. Preventing Hypoxia-Induced Cell Death in Beta-cells and Islets via Hydrolytically Activated, Oxygen-Generating Biomaterials. *Proc. Natl. Acad. Sci. U. S. A.* **2012**, *109*, 4245–4250.
- (61) O’Sullivan, E. S.; Vegas, A.; Anderson, D. G.; Weir, G. C. Islets Transplanted in Immunoisolation Devices: A Review of the Progress and the Challenges That Remain. *Endocr. Rev.* **2011**, *32*, 827–844.
- (62) Mendelsohn, A. D.; Nyitray, C.; Sena, M.; Desai, T. a. Size-Controlled Insulin-Secreting Cell Clusters. *Acta Biomater.* **2012**, *8*, 4278–4284.
- (63) Tudies, S.; Vaithilingam, V.; Tuch, B. E. Islet Transplantation and Encapsulation : An Update on Recent Developments. **2011**.

- (64) Hofmann, D.; Entrialgo-Castaño, M.; Kratz, K.; Lendlein, A. Knowledge-Based Approach towards Hydrolytic Degradation of Polymer-Based Biomaterials. *Adv. Mater.* **2009**, *21*, 3237–3245.
- (65) Brauker, J. H.; Carr-Brendel, V. E.; Martinson, L. a; Crudele, J.; Johnston, W. D.; Johnson, R. C. Neovascularization of Synthetic Membranes Directed by Membrane Microarchitecture. *J. Biomed. Mater. Res.* **1995**, *29*, 1517–1524.
- (66) Sharkawy, a a; Klitzman, B.; Truskey, G. a; Reichert, W. M. Engineering the Tissue Which Encapsulates Subcutaneous Implants. I. Diffusion Properties. *J. Biomed. Mater. Res.* **1997**, *37*, 401–412.
- (67) Davila, J. C.; Lautsch, E. V; Palmer, T. E. Mechanical Behavior. 138–147.
- (68) Ward, W. K. A Review of the Foreign-Body Response to Subcutaneously-Implanted Devices: The Role of Macrophages and Cytokines in Biofouling and Fibrosis. *J. Diabetes Sci. Technol.* **2008**, *2*, 768–777.
- (69) Browning, H.; Resnik, P. Homologous and Heterologous Transplantation of Pancreatic Tissue in Normal and Diabetic Mice. **1951**.
- (70) Benson, J. L.; Niederkorn, J. Y. Immune Privilege in the Anterior Chamber of the Eye: Alloantigens and Tumour-Specific Antigens Presented into the Anterior Chamber Simultaneously Induce Suppression and Activation of Delayed Hypersensitivity to the Respective Antigens. *Immunology* **1992**, *77*, 189–195.

- (71) Niederkorn, J. Y. Mechanisms of Immune Privilege in the Eye and Hair Follicle. *J. Investig. Dermatology Symp. Proc.* **2003**, 8, 168–172.
- (72) Niederkorn, J. Y. Ocular Immune Privilege and Ocular Melanoma: Parallel Universes or Immunological Plagiarism? *Front. Immunol.* **2012**, 3, 1–10.
- (73) Barton, F. B.; Rickels, M. R.; Alejandro, R.; Hering, B. J.; Wease, S.; Naziruddin, B.; Oberholzer, J.; Odorico, J. S.; Garfinkel, M. R.; Levy, M.; *et al.* Improvement in Outcomes of Clinical Islet Transplantation: 1999-2010. *Diabetes Care* **2012**, 35, 1436–1445.
- (74) Stanekzai, J.; Isenovic, E. R.; Mousa, S. a. Treatment Options for Diabetes: Potential Role of Stem Cells. *Diabetes Res. Clin. Pract.* **2012**, 98, 361–368.
- (75) Kim, A.; Miller, K.; Jo, J.; Kilimnik, G.; Wojcik, P.; Hara, M. Islet Architecture: A Comparative Study. *Islets* **2009**, 1, 129–136.
- (76) Wang, R. N.; Paraskevas, S.; Rosenberg, L. Characterization of Integrin Expression in Islets Isolated from Hamster, Canine, Porcine, and Human Pancreas. *J. Histochem. Cytochem.* **1999**, 47, 499–506.
- (77) Zhao, Y.; Xu, J.; Wei, J.; Li, J.; Cai, J.; Miao, G. Preservation of Islet Survival by Upregulating $\alpha 3$ Integrin Signaling: The Importance of 3-Dimensional Islet Culture in Basement Membrane Extract. *Transplant. Proc.* **2010**, 42, 4638–4642.

- (78) Hauge-Evans, a C.; Squires, P. E.; Persaud, S. J.; Jones, P. M. Pancreatic Beta-Cell-to-Beta-Cell Interactions Are Required for Integrated Responses to Nutrient Stimuli: Enhanced Ca^{2+} and Insulin Secretory Responses of MIN6 Pseudoislets. *Diabetes* **1999**, *48*, 1402–1408.
- (79) Chowdhury, a; Dyachok, O.; Tengholm, a; Sandler, S.; Bergsten, P. Functional Differences between Aggregated and Dispersed Insulin-Producing Cells. *Diabetologia* **2013**, *56*, 1557–1568.
- (80) Maillard, E.; Sencier, M.-C.; Langlois, a; Bietiger, W.; Krafft, M.; Pinget, M.; Sigrist, S. Extracellular Matrix Proteins Involved in Pseudoislets Formation. *Islets* **2009**, *1*, 232–241.
- (81) Discher, D. E.; Janmey, P.; Wang, Y.-L. Tissue Cells Feel and Respond to the Stiffness of Their Substrate. *Science* **2005**, *310*, 1139–1143.
- (82) Butcher, D. T.; Alliston, T.; Weaver, V. M. A Tense Situation: Forcing Tumour Progression. *Nat. Rev. Cancer* **2009**, *9*, 108–122.
- (83) Rehfeldt, F.; Engler, A. J.; Eckhardt, A.; Ahmed, F.; Discher, D. E. Cell Responses to the Mechanochemical Microenvironment--Implications for Regenerative Medicine and Drug Delivery. *Adv. Drug Deliv. Rev.* **2007**, *59*, 1329–1339.
- (84) Kraning-rush, C. M.; Reinhart-king, C. A. Controlling Matrix Stiffness and Topography for the Study of Tumor Cell Migration. **2012**, *6*, 274–279.

- (85) Dahl, K. N.; Ribeiro, A. J. S.; Lammerding, J. Nuclear Shape, Mechanics, and Mechanotransduction. *Circ. Res.* **2008**, *102*, 1307–1318.
- (86) Kuehn, C.; Dubiel, E. a; Sabra, G.; Vermette, P. Culturing INS-1 Cells on CDPGYIGSR-, RGD- and Fibronectin Surfaces Improves Insulin Secretion and Cell Proliferation. *Acta Biomater.* **2012**, *8*, 619–626.
- (87) Merkwitz, C.; Blaschuk, O. W.; Schulz, A.; Lochhead, P.; Meister, J.; Ehrlich, A.; Ricken, A. M. The Ductal Origin of Structural and Functional Heterogeneity between Pancreatic Islets. *Prog. Histochem. Cytochem.* **2013**, *48*, 103–140.
- (88) Tomas, A.; Yermen, B.; Min, L.; Pessin, J. E.; Halban, P. a. Regulation of Pancreatic Beta-Cell Insulin Secretion by Actin Cytoskeleton Remodelling: Role of Gelsolin and Cooperation with the MAPK Signalling Pathway. *J. Cell Sci.* **2006**, *119*, 2156–2167.
- (89) Abiola, M.; Favier, M.; Christodoulou-Vafeiadou, E.; Pichard, A.-L.; Martelly, I.; Guillet-Deniau, I. Activation of Wnt/beta-Catenin Signaling Increases Insulin Sensitivity through a Reciprocal Regulation of Wnt10b and SREBP-1c in Skeletal Muscle Cells. *PLoS One* **2009**, *4*, e8509.
- (90) Zawadzka, M.; Dabrowski, M.; Gozdz, A.; Szadujkis, B.; Sliwa, M.; Lipko, M.; Kaminska, B. Early Steps of Microglial Activation Are Directly Affected by Neuroprotectant FK506 in Both in Vitro Inflammation and in Rat Model of Stroke. *J. Mol. Med. (Berl)*. **2012**, *90*, 1459–1471.

- (91) Riopel, M.; Krishnamurthy, M.; Li, J.; Liu, S.; Leask, a; Wang, R. Conditional β 1-Integrin-Deficient Mice Display Impaired Pancreatic B Cell Function. *J. Pathol.* **2011**, *224*, 45–55.
- (92) Rondas, D.; Tomas, A.; Soto-Ribeiro, M.; Wehrle-Haller, B.; Halban, P. a. Novel Mechanistic Link between Focal Adhesion Remodeling and Glucose-Stimulated Insulin Secretion. *J. Biol. Chem.* **2012**, *287*, 2423–2436.
- (93) Mitra, S. K.; Hanson, D. a; Schlaepfer, D. D. Focal Adhesion Kinase: In Command and Control of Cell Motility. *Nat. Rev. Mol. Cell Biol.* **2005**, *6*, 56–68.
- (94) Gautel, M. Cytoskeletal Protein Kinases: Titin and Its Relations in Mechanosensing. *Pflugers Arch.* **2011**, *462*, 119–134.
- (95) Vicente-Manzanares, M.; Ma, X.; Adelstein, R. S.; Horwitz, A. R. Non-Muscle Myosin II Takes Centre Stage in Cell Adhesion and Migration. *Nat. Rev. Mol. Cell Biol.* **2009**, *10*, 778–790.
- (96) Assoian, R. K.; Klein, E. a. Growth Control by Intracellular Tension and Extracellular Stiffness. *Trends Cell Biol.* **2008**, *18*, 347–352.
- (97) Yoon, J. C.; Ng, A.; Kim, B. H.; Bianco, A.; Xavier, R. J.; Elledge, S. J. Wnt Signaling Regulates Mitochondrial Physiology and Insulin Sensitivity. *Genes Dev.* **2010**, *24*, 1507–1518.

- (98) Almany, L.; Seliktar, D. Biosynthetic Hydrogel Scaffolds Made from Fibrinogen and Polyethylene Glycol for 3D Cell Cultures. *Biomaterials* **2005**, *26*, 2467–2477.
- (99) Guillame-Gentil, O.; Semenov, O.; Roca, A. S.; Groth, T.; Zahn, R.; Vörös, J.; Zenobi-Wong, M. Engineering the Extracellular Environment: Strategies for Building 2D and 3D Cellular Structures. *Adv. Mater.* **2010**, *22*, 5443–5462.
- (100) Huang, H.; Ding, Y.; Sun, X. S.; Nguyen, T. A. Peptide Hydrogelation and Cell Encapsulation for 3D Culture of MCF-7 Breast Cancer Cells. *PLoS One* **2013**, *8*.
- (101) Baker, B. M.; Chen, C. S. Deconstructing the Third Dimension: How 3D Culture Microenvironments Alter Cellular Cues. *J. Cell Sci.* **2012**, *125*, 3015–3024.
- (102) Raza, A.; Ki, C. S.; Lin, C.-C. The Influence of Matrix Properties on Growth and Morphogenesis of Human Pancreatic Ductal Epithelial Cells in 3D. *Biomaterials* **2013**, *34*, 5117–5127.
- (103) Wendt, D.; Riboldi, S. a; Cioffi, M.; Martin, I. Potential and Bottlenecks of Bioreactors in 3D Cell Culture and Tissue Manufacturing. *Adv. Mater.* **2009**, *21*, 3352–3367.
- (104) Bernard, A. B.; Lin, C.-C.; Anseth, K. S. A Microwell Cell Culture Platform for the Aggregation of Pancreatic B-Cells. *Tissue Eng. Part C. Methods* **2012**, *18*, 583–592.

- (105) Dutta, R. C.; Dutta, A. K. Comprehension of ECM-Cell Dynamics: A Prerequisite for Tissue Regeneration. *Biotechnol. Adv.* **2010**, *28*, 764–769.
- (106) Daoud, J.; Petropavlovskaja, M.; Rosenberg, L.; Tabrizian, M. The Effect of Extracellular Matrix Components on the Preservation of Human Islet Function in Vitro. *Biomaterials* **2010**, *31*, 1676–1682.
- (107) Thomas, C. H.; Collier, J. H.; Sfeir, C. S.; Healy, K. E. Engineering Gene Expression and Protein Synthesis by Modulation of Nuclear Shape. *Proc. Natl. Acad. Sci. U. S. A.* **2002**, *99*, 1972–1977.
- (108) Hohmeier, H. E.; Mulder, H.; Chen, G.; Henkel-Rieger, R.; Prentki, M.; Newgard, C. B. Isolation of INS-1-Derived Cell Lines with Robust ATP-Sensitive K⁺ Channel-Dependent and -Independent Glucose-Stimulated Insulin Secretion. *Diabetes* **2000**, *49*, 424–430.
- (109) Hatziavramidis, D. T.; Karatzas, T. M.; Chrousos, G. P. Pancreatic Islet Cell Transplantation: An Update. *Ann. Biomed. Eng.* **2013**, *41*, 469–476.
- (110) Shah, K. Encapsulated Stem Cells for Cancer Therapy. *Biomatter* **2013**, *3*, 1–7.
- (111) Song, K.; Yang, Y.; Li, S.; Wu, M.; Wu, Y.; Lim, M.; Liu, T. In Vitro Culture and Oxygen Consumption of NSCs in Size-Controlled Neurospheres of Calcium Alginate/gelatin Microbead. *Mater. Sci. Eng. C. Mater. Biol. Appl.* **2014**, *40*, 197–203.

- (112) De Faveri, S.; Maggiolini, E.; Miele, E.; De Angelis, F.; Cesca, F.; Benfenati, F.; Fadiga, L. Bio-Inspired Hybrid Microelectrodes: A Hybrid Solution to Improve Long-Term Performance of Chronic Intracortical Implants. *Front. Neuroeng.* **2014**, *7*, 7.
- (113) Robles, L.; Storrs, R.; Lamb, M.; Alexander, M.; Lakey, J. R. Current Status of Islet Encapsulation. *Cell Transplant.* **2013**.
- (114) Tomei, A. a; Manzoli, V.; Fraker, C. a; Giraldo, J.; Velluto, D.; Najjar, M.; Pileggi, A.; Molano, R. D.; Ricordi, C.; Stabler, C. L.; *et al.* Device Design and Materials Optimization of Conformal Coating for Islets of Langerhans. *Proc. Natl. Acad. Sci. U. S. A.* **2014**, *111*, 10514–10519.
- (115) Weir, G. C. Islet Encapsulation: Advances and Obstacles. *Diabetologia* **2013**, *56*, 1458–1461.
- (116) Buder, B.; Alexander, M.; Krishnan, R.; Chapman, D. W.; Lakey, J. R. Encapsulated Islet Transplantation: Strategies and Clinical Trials. *Immune Netw.* **2013**, *13*, 235–239.
- (117) Julien, S.; Nyitray, C.; Desai, T. A. Membranes to Achieve Immunoprotection of Transplanted Islets. *Frontiers Biosci. (Landmark Ed.)* **2014**, *19*, 49–76.
- (118) Cala, R.; Basta, G. Clinical Application of Microencapsulated Islets : Actual Prospectives on Progress and Challenges. **2014**, *68*, 84–92.

- (119) Cornolti, R.; Figliuzzi, M.; Remuzzi, A. Effect of Micro- and Macroencapsulation on Oxygen Consumption by Pancreatic Islets. *Cell* **2009**, *18*, 195–201.
- (120) Lathuilière, A.; Cosson, S.; Lutolf, M. P.; Schneider, B. L.; Aebischer, P. A High-Capacity Cell Macroencapsulation System Supporting the Long-Term Survival of Genetically Engineered Allogeneic Cells. *Biomaterials* **2014**, *35*, 779–791.
- (121) Ward, W. K.; Slobodzian, E. P.; Tiekotter, K. L.; Wood, M. D. The Effect of Microgeometry, Implant Thickness and Polyurethane Chemistry on the Foreign Body Response to Subcutaneous Implants. *Biomaterials* **2002**, *23*, 4185–4192.
- (122) Rentsch, B.; Bernhardt, R.; Scharnweber, D.; Schneiders, W.; Rammelt, S.; Rentsch, C. Embroidered and Surface Coated Polycaprolactone-Co-Lactide Scaffolds: A Potential Graft for Bone Tissue Engineering. *Biomatter* **2012**, *2*, 158–165.
- (123) Bernards, D. A.; Desai, T. A. Nanoscale Porosity in Polymer Films: Fabrication and Therapeutic Applications. *Soft Mater.* **2011**, *6*, 1621–1631.
- (124) Bernards, D. A.; Bhisitkul, R. B.; Wynn, P.; Steedman, M. R.; Lee, O.-T.; Wong, F.; Thoongsuwan, S.; Desai, T. A. Ocular Biocompatibility and Structural Integrity of Micro- and Nanostructured Poly(caprolactone) Films. *J. Ocul. Pharmacol. Ther.* **2013**, *29*, 249–257.

- (125) Bernards, D. A.; Desai, T. A. Nanotemplating of Biodegradable Polymer Membranes for Constant-Rate Drug Delivery. *Adv. Mater.* **2010**, *22*, 2358–2362.
- (126) Abedalwafa, M.; Wang, F.; Wang, L.; Li, C. Biodegradable Poly-Epsilon-Caprolactone (PCL) for Tissue Engineering Applications: A Review. *Rev. Adv. Mater. Sci* **2013**, *34*, 123–140.
- (127) Angius, D.; Wang, H.; Spinner, R. J.; Gutierrez-Cotto, Y.; Yaszemeski, M. J.; Windebank, A. J. A Systematic Review of Animal Models Used to Study Nerve Regeneration in Tissue-Engineered Scaffolds. *Biomaterials* **2013**, *33*, 8034–8039.
- (128) Bernards, D. A.; Lance, K. D.; Ciaccio, N. A.; Desai, T. A. Nanostructured Thin Film Polymer Devices for Constant-Rate Protein Delivery. *Nano Lett.* **2012**, *12*, 5355–5361.
- (129) Mendelsohn, A. D.; Bernards, D. a; Lowe, R. D.; Desai, T. a. Patterning of Mono- and Multilayered Pancreatic Beta-Cell Clusters. *Langmuir* **2010**, *26*, 9943–9949.
- (130) Lu, F.; Lei, L.; Shen, Y. Y.; Hou, J. W.; Chen, W. L.; Li, Y. G.; Guo, S. R. Effects of Amphiphilic PCL-PEG-PCL Copolymer Addition on 5-Fluorouracil Release from Biodegradable PCL Films for Stent Application. *Int. J. Pharm.* **2011**, *419*, 77–84.

- (131) Lin, W. J.; Lee, H. G. Design of a Microporous Controlled Delivery System for Theophylline Tablets. *J. Control. Release* **2003**, *89*, 179–187.
- (132) Rong, H. J.; Chen, W. L.; Guo, S. R.; Lei, L.; Shen, Y. Y. PCL Films Incorporated with paclitaxel/5-Fluorouracil: Effects of Formulation and Spatial Architecture on Drug Release. *Int. J. Pharm.* **2012**, *427*, 242–251.
- (133) Anzai, R.; Murakami, Y. Poly(ϵ -Caprolactone) (PCL)–polymeric Micelle Hybrid Sheets for the Incorporation and Release of Hydrophilic Proteins. *Colloids Surfaces B Biointerfaces* **2015**, *127*, 292–299.
- (134) Lei, L.; Liu, X.; Shen, Y. Y.; Liu, J. Y.; Tang, M. F.; Wang, Z. M.; Guo, S. R.; Cheng, L. Zero-Order Release of 5-Fluorouracil from PCL-Based Films Featuring Trilayered Structures for Stent Application. *Eur. J. Pharm. Biopharm.* **2011**, *78*, 49–57.
- (135) Online, V. A.; Ledeuil, J. B.; Uhart, A.; Allouche, J.; Dupin, J. C.; Martinez, H. New Insights into Micro / Nanoscale Combined. **2014**, 11130–11140.
- (136) Kim, Y.-J.; Kim, S.-S.; Park, J. B.; Sohn, B.-H.; Yi, G.-C. Controlled Growth of Inorganic Nanorod Arrays Using Graphene Nanodot Seed Layers. *Nanotechnology* **2014**, *25*, 135609.
- (137) Zhang, Z.; Yu, H.; Shao, X.; Han, M. Near-Room-Temperature Production of Diameter-Tunable ZnO Nanorod Arrays through Natural Oxidation of Zinc Metal. *Chemistry* **2005**, *11*, 3149–3154.

- (138) Martin, Y.; Vermette, P. Bioreactors for Tissue Mass Culture: Design, Characterization, and Recent Advances. *Biomaterials* **2005**, *26*, 7481–7503.
- (139) Tracey, K. J. The Inflammatory Reflex. **2002**, *420*, 853–859.
- (140) Bastiaens, P. When It Is Time to Die. **2009**, *459*.
- (141) Libert, C. A Nervous Connection. **2003**, *421*, 328–329.
- (142) Wang, L.; Du, F.; Wang, X. TNF-Alpha Induces Two Distinct Caspase-8 Activation Pathways. *Cell* **2008**, *133*, 693–703.
- (143) Fonseca, F. N.; Papanicolaou, G.; Lin, H.; Lau, C. B. S.; Kennelly, E. J.; Cassileth, B. R.; Cunningham-Rundles, S. Echinacea Purpurea (L.) Moench Modulates Human T-Cell Cytokine Response. *Int. Immunopharmacol.* **2014**.
- (144) Roff, S. R.; Noon-Song, E. N.; Yamamoto, J. K. The Significance of Interferon- Γ in HIV-1 Pathogenesis, Therapy, and Prophylaxis. *Front. Immunol.* **2014**, *4*, 498.
- (145) Yang, Y. H. C.; Vilin, Y. Y.; Roberge, M.; Kurata, H. T.; Johnson, J. D. Multi-Parameter Screening Reveals a Role for Na(+) Channels in Cytokine-Induced Beta-Cell Death. *Mol. Endocrinol.* **2014**, me20131257.
- (146) Miyazaki, J.; Araki, K.; Yamato, E.; Ikegami, H.; Yamamura, K. Establishment of a Pancreatic /Beta Cell Line That Retains Glucose-Inducible Insulin Secretion : Special Reference to Expression of Glucose Transporter Isoforms *. *Endocrinology* **1990**, *127*.

- (147) Szot, G. L.; Koudria, P.; Bluestone, J. a. Murine Pancreatic Islet Isolation. *J. Vis. Exp.* **2007**, 1640, 255.
- (148) Fowler, M.; Virostko, J.; Chen, Z.; Poffenberger, G.; Radhika, A.; Brissova, M.; Shiota, M.; Nicholson, W. E.; Shi, Y.; Hirshberg, B.; *et al.* Assessment of Pancreatic Islet Mass after Islet Transplantation Using in Vivo Bioluminescence Imaging. *Transplantation* **2005**, 79, 768–776.
- (149) Muschler, G. F.; Nakamoto, C.; Griffith, L. G. Engineering Principles of Clinical Cell-Based Tissue Engineering. *J. Bone Joint Surg. Am.* **2004**, 86-A, 1541–1558.
- (150) Dutta, R. C.; Dutta, A. K. Comprehension of ECM-Cell Dynamics: A Prerequisite for Tissue Regeneration. *Biotechnol. Adv.* **2010**, 28, 764–769.
- (151) Cotton, C. K. Engineering Challenges in Cell-Encapsulation Technology. *Trends Biotechnol.* **1996**, 14, 158–162.
- (152) Rafie, F.; Javadzadeh, Y.; Javadzadeh, A. R.; Ghavidel, L. A.; Jafari, B.; Moogooee, M.; Davaran, S. In Vivo Evaluation of Novel Nanoparticles Containing Dexamethasone for Ocular Drug Delivery on Rabbit Eye. *Curr. Eye Res.* **2010**, 35, 1081–1089.
- (153) Forier, K.; Raemdonck, K.; Smedt, S. C. De; Demeester, J.; Coenye, T.; Braeckmans, K. Lipid and Polymer Nanoparticles for Drug Delivery to Bacterial Biofilms. *J. Control. Release* **2014**, 190, 607–623.

- (154) Wang, Y.; Li, P.; Kong, L. Chitosan-Modified PLGA Nanoparticles with Versatile Surface for Improved Drug Delivery. *AAPS PharmSciTech* **2013**, *14*, 585–592.
- (155) Parboosing, R.; Maguire, G. E. M.; Govender, P.; Kruger, H. G. Nanotechnology and the Treatment of HIV Infection. *Viruses* **2012**, *4*, 488–520.
- (156) Karimi, Z.; Karimi, L.; Shokrollahi, H. Nano-Magnetic Particles Used in Biomedicine: Core and Coating Materials. *Mater. Sci. Eng. C. Mater. Biol. Appl.* **2013**, *33*, 2465–2475.
- (157) Chen, M.-C.; Sonaje, K.; Chen, K.-J.; Sung, H.-W. A Review of the Prospects for Polymeric Nanoparticle Platforms in Oral Insulin Delivery. *Biomaterials* **2011**, *32*, 9826–9838.
- (158) Stano, A.; Scott, E. a; Dane, K. Y.; Swartz, M. a; Hubbell, J. a. Tunable T Cell Immunity towards a Protein Antigen Using Polymersomes vs. Solid-Core Nanoparticles. *Biomaterials* **2013**, *34*, 4339–4346.
- (159) Thomas, S. N.; Vokali, E.; Lund, A. W.; Hubbell, J. a; Swartz, M. a. Targeting the Tumor-Draining Lymph Node with Adjuvanted Nanoparticles Reshapes the Anti-Tumor Immune Response. *Biomaterials* **2014**, *35*, 814–824.
- (160) Yu, S. S.; Lau, C. M.; Thomas, S. N.; Jerome, W. G.; Maron, D. J.; Dickerson, J. H.; Hubbell, J. A.; Giorgio, T. D. Size- and Charge-Dependent Non-Specific Uptake of PEGylated Nanoparticles by Macrophages. **2012**, 799–813.

- (161) Titta, A. De; Ballester, M.; Julier, Z.; Nembrini, C.; Jeanbart, L.; Vlies, A. J. Van Der. Nanoparticle Conjugation of CpG Enhances Adjuvancy for Cellular Immunity and Memory Recall at Low Dose. **2013**.
- (162) Daniel, M.-C.; Astruc, D. Gold Nanoparticles: Assembly, Supramolecular Chemistry, Quantum-Size-Related Properties, and Applications toward Biology, Catalysis, and Nanotechnology. *Chem. Rev.* **2004**, *104*, 293–346.
- (163) Burda, C.; Chen, X.; Narayanan, R.; El-Sayed, M. A. Chemistry and Properties of Nanocrystals of Different Shapes. *Chem. Rev.* **2005**, *105*, 1025–1102.
- (164) Caputo, F.; De Nicola, M.; Ghibelli, L. Pharmacological Potential of Bioactive Engineered Nanomaterials. *Biochem. Pharmacol.* **2014**.
- (165) Wang, L.; Liu, J.; Dai, Y.; Yang, Q.; Zhang, Y.; Yang, P.; Cheng, Z.; Lian, H.; Li, C.; Hou, Z.; *et al.* Efficient Gene Delivery and Multi-Modal Imaging by Lanthanide-Based Up-Conversion Nanoparticles. *Langmuir* **2014**.
- (166) Sun, T.; Zhang, Y. S.; Pang, B.; Hyun, D. C.; Yang, M.; Xia, Y. Engineered Nanoparticles for Drug Delivery in Cancer Therapy Angewandte. **2014**, 2–47.
- (167) Aditya, N. P.; Vathsala, P. G.; Vieira, V.; Murthy, R. S. R.; Souto, E. B. Advances in Nanomedicines for Malaria Treatment. *Adv. Colloid Interface Sci.* **2013**, *201-202*, 1–17.
- (168) Anselmo, A. C.; Mitragotri, S. An Overview of Clinical and Commercial Impact of Drug Delivery Systems. *J. Control. Release* **2014**, *190*, 15–28.

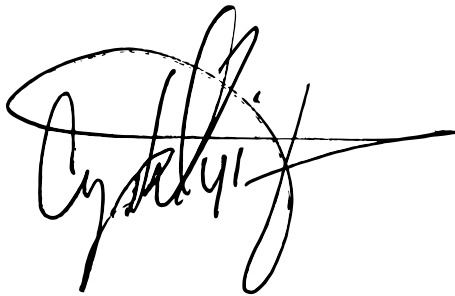
- (169) De Koker, S.; Lambrecht, B. N.; Willart, M. a; van Kooyk, Y.; Grooten, J.; Vervaet, C.; Remon, J. P.; De Geest, B. G. Designing Polymeric Particles for Antigen Delivery. *Chem. Soc. Rev.* **2011**, *40*, 320–339.
- (170) Anees, P.; Sreejith, S.; Ajayaghosh, A. Self-Assembled near-Infrared Dye Nanoparticles as a Selective Protein Sensor by Activation of a Dormant Fluorophore. *J. Am. Chem. Soc.* **2014**, *136*, 13233–13239.
- (171) Yen, S. K.; Padmanabhan, P.; Selvan, S. T. Multifunctional Iron Oxide Nanoparticles for Diagnostics, Therapy and Macromolecule Delivery. *Theranostics* **2013**, *3*, 986–1003.
- (172) Alharbi, K. K.; Al-Sheikh, Y. a. Role and Implications of Nanodiagnostics in the Changing Trends of Clinical Diagnosis. *Saudi J. Biol. Sci.* **2014**, *21*, 109–117.
- (173) Grillo, R.; Rosa, A. H.; Fraceto, L. F. Engineered Nanoparticles and Organic Matter: A Review of the State-of-the-Art. *Chemosphere* **2014**, *119C*, 608–619.
- (174) Norman, J. J.; Desai, T. a. Methods for Fabrication of Nanoscale Topography for Tissue Engineering Scaffolds. *Ann. Biomed. Eng.* **2006**, *34*, 89–101.
- (175) Ahamed, M. I. N.; Sankar, S.; Kashif, P. M.; Basha, S. K. H.; Sastry, T. P. Evaluation of Biomaterial Containing Regenerated Cellulose and Chitosan Incorporated with Silver Nanoparticles. *Int. J. Biol. Macromol.* **2014**, *72C*, 680–686.

- (176) Miller, D. L.; Spooner, G. J.; Williams, a R. Photodisruptive Laser Nucleation of Ultrasonic Cavitation for Biomedical Applications. *J. Biomed. Opt.* **2001**, 6, 351–358.
- (177) Review, H. Porphyrin Assemblies and Their Sca Ff Olds. **2014**.
- (178) Borisov, S. M.; Zenkl, G.; Klimant, I. Phosphorescent platinum(II) and palladium(II) Complexes with Azatetrabenzoporphyrins-New Red Laser Diode-Compatible Indicators for Optical Oxygen Sensing. *ACS Appl. Mater. Interfaces* **2010**, 2, 366–374.
- (179) Miyaura, N.; Suzuki, A. Palladium-Catalyzed Cross-Coupling Reactions. *Chemistry* **1995**, 95, 2457–2483.
- (180) Haghighi, B.; Bozorgzadeh, S. Enhanced Electrochemiluminescence from Luminol at Multi-Walled Carbon Nanotubes Decorated with Palladium Nanoparticles: A Novel Route for the Fabrication of an Oxygen Sensor and a Glucose Biosensor. *Anal. Chim. Acta* **2011**, 697, 90–97.
- (181) Stepinac, T. K.; Chamot, S. R.; Rungger-Brändle, E.; Ferrez, P.; Munoz, J.-L.; van den Bergh, H.; Riva, C. E.; Pournaras, C. J.; Wagnières, G. a. Light-Induced Retinal Vascular Damage by Pd-Porphyrin Luminescent Oxygen Probes. *Invest. Ophthalmol. Vis. Sci.* **2005**, 46, 956–966.

Publishing Agreement

It is the policy of the University to encourage the distribution of all theses, dissertations, and manuscripts. Copies of all UCSF theses, dissertations, and manuscripts will be routed to the library via the Graduate Division. The library will make all theses, dissertations, and manuscripts accessible to the public and will preserve these to the best of their abilities, in perpetuity.

I hereby grant permission to the Graduate Division of the University of California, San Francisco to release copies of my thesis, dissertation, or manuscript to the Campus Library to provide access and preservation, in whole or in part, in perpetuity.

A handwritten signature in black ink, appearing to read "C. Kelly", with a large, sweeping loop at the end.

5/28/2015

Author Signature Date